UNIVERSIDADE FEDERAL DO CEARÁ
CENTRO DE TECNOLOGIA
DEPARTAMENTO DE ENGENHARIA DE TRANSPORTES
PROGRAMA DE PÓS-GRADUAÇÃO EM ENGENHARIA DE TRANSPORTES

MATEUS DO NASCIMENTO LIRA

THE INFLUENCE OF LOAD INTENSITY ON STRUCTURAL RESPONSE OF AIRPORT PAVEMENTS ASSESSED BY NONDESTRUCTIVE EVALUATION METHODS

FORTALEZA
2023

MATEUS DO NASCIMENTO LIRA

THE INFLUENCE OF LOAD INTENSITY ON STRUCTURAL RESPONSE OF AIRPORT PAVEMENTS ASSESSED BY NONDESTRUCTIVE EVALUATION METHODS

Master Thesis presented to the Transportation Engineering Graduate Program from Federal University of Ceará as partial requisite for obtaining the master's degree in Transportation Engineering. Concentration area: Transportation Infrastructure.

Advisor: Dr. Francisco Heber Lacerda de Oliveira.
Co-advisor: Dr. Cláudia Azevedo Pereira.

FORTALEZA

2023

Dados Internacionais de Catalogação na Publicação
Universidade Federal do Ceará
Sistema de Bibliotecas
Gerada automaticamente pelo módulo Catalog, mediante os dados fornecidos pelo(a) autor(a)

L745t Lira, Mateus do Nascimento.
The influence of load intensity on structural response of airport pavements assessed by nondestructive evaluation methods / Mateus do Nascimento Lira. – 2023.
116 f. : il. color.

Dissertação (mestrado) – Universidade Federal do Ceará, Centro de Tecnologia, Programa de Pós-Graduação em Engenharia de Transportes, Fortaleza, 2023.
Orientação: Prof. Dr. Francisco Heber Lacerda de Oliveira.
Coorientação: Profa. Dra. Claudia Azevedo Pereira.

1. FWD. 2. HWD. 3. Airport Pavements. 4. Structural Evaluation. I. Título.

CDD 388

MATEUS DO NASCIMENTO LIRA

THE INFLUENCE OF LOAD INTENSITY ON STRUCTURAL RESPONSE OF AIRPORT PAVEMENTS ASSESSED BY NONDESTRUCTIVE EVALUATION METHODS

Master Thesis presented to the Transportation Engineering Graduate Program from Federal University of Ceará as partial requisite for obtaining the master's degree in Transportation Engineering. Concentration area: Transportation Infrastructure.

Approved on: ___/___/_____.

EXAMINING BOARD

_____
D. Sc. Francisco Heber Lacerda de Oliveira
Federal University of Ceará (UFC)

_____
D. Sc. Cláudia Azevedo Pereira
Technological Institute of Aeronautics (ITA)

_____
Ph.D. Suelly Helena de Araújo Barroso
Federal University of Ceará (UFC)

_____
D. Sc. Iuri Sidney Bessa
Federal University of Ceará (UFC)

_____
Ph.D. Kamilla Vasconcelos Savasini
Polytechnic School of the University of São Paulo (Poli/USP)

À minha mãe.

À minha irmã.

Às mulheres da minha vida.

ACKNOWLEDGMENTS

To the Brazilian Civil Aviation Authority, ANAC, by supporting this research with data and monetary financing.

To Mr. Heber Oliveira, for the amazing orientation. Heber has been patient since the undergraduate orientations, never giving up of advising me, and always counseling me and believing and trusting in my capacity of do all the things were proposed for me to do. Thank you very much, professor. Maybe you do not have the dimension of your importance, but you change the lives of your students. Thank you for your contributions to changing our society.

To Mrs. Claudia Azevedo, for all the contributions she gave for developing this research and supporting it to being a more and more mature study. Thank you for trusting in my capacity from the beginning to the end of this Master Thesis.

To Mrs. Suelly Barroso, for supporting my professional and human growth since the beginning of my career. A big thank you for giving me technical contribution and inspiration from my first monitory program to the last wrote line of this master thesis document, directly and indirectly impacting who I am, who I want to be, and who I will be. You are simply a wonderful person.

To the professors compounding the examining board, Mrs Kamilla Savasini, and Mr. Iuri Bessa, for their contributions to the improvement of this study.

To Mr. José Leomar, for his contributions to the improvement of this study in the qualification exam.

To my Family, especially my mother, my sister, and my boyfriend. Thank you for helping me to do not giving up of this project and for believing in my competence when even I have doubted of myself. I love you with all my heart.

To my friends, especially my journey brothers, the Heber's Sons Aldaianny Maia, Lucas Moreira, and Renata Sales, for supporting together the worries, the fears, the challenges, the achievements, the joys, and the gifts we sent to our advisor.

RESUMO

A condição estrutural dos pavimentos pode ser avaliada por meio da aplicação de dois métodos distintos: ensaios destrutivos e não-destrutivos (NDT). Existem variados NDT disponíveis para executar avaliações estruturais em pavimentos aeroportuários, porém os mais usados e recomendados são o *Falling Weight Deflectometer* (FWD) e o *Heavy Weight Deflectometer* (HWD). O FWD aplica cargas mais leves enquanto o HWD aplica cargas pesadas, sendo essa principal diferença entre os dois. Tal diferença de cargas leva à discussão sobre a adequabilidade de converter resultados obtidos pelo uso das cargas mais baixas do FWD para o das cargas mais pesadas do HWD devido à resposta estrutural dos pavimentos. Se essa resposta não for linear, podem ocorrer inconsistências na avaliação da estrutura que, em casos extremos, geram risco para as operações de pouso e decolagem. Visando auxiliar na resposta para a adequabilidade dessa conversão de resultados, o objetivo desta pesquisa foi avaliar a influência da intensidade da carga na resposta estrutural de pavimentos aeroportuários. Pavimentos flexíveis de três pistas de pouso e decolagem de regiões diferentes do Brasil foram avaliados com cargas variáveis de FWD e HWD. Índices/parâmetros obtidos a partir dessas avaliações foram estudados: as deflexões brutas e normalizadas, o Raio de Curvatura (RC), o *Impulse Stiffness Modulus* (ISM), e o Módulo de Resiliência (MR) retroanalisado. Esses índices, obtidos pela aplicação de cargas distintas, foram comparados para verificar se a mudança da carga implica em variações significativas nos seus valores. Testes estatísticos foram realizados para conferir confiabilidade ao estudo. Os resultados mostraram que as deflexões brutas apresentaram diferenças percentuais similares aos percentuais de diferença observados para a variação das cargas e que as deflexões normalizadas sofreram influência da carga aplicada. Os valores de RC diminuíram quando a carga amentou, em vez de terem apresentado o comportamento esperado de aumento sob maiores esforços. O ISM apresentou decréscimo quando a carga foi aumentada. Os resultados de MR diminuíram de valor quando a carga aumentou. O subleito apresentou-se como o mais impactado pela variação das cargas em comparação às demais camadas da estrutura. Concluiu-se que que a resposta estrutural dos pavimentos não é linear, e que as diferenças observadas não são elevadas o suficiente para prejudicar as avaliações estruturais de pavimentos aeroportuários. Contudo, se os resultados das avaliações forem empregados em processos sensíveis ao valor do módulo de resiliência das camadas, é recomendado o uso de cargas adequadas ao tráfego que solicita o pavimento.

Palavras-chave: FWD; HWD; pavimentos aeroportuários; avaliação estrutural.

ABSTRACT

The structural condition of pavements can be assessed by applying two distinct methodologies: destructive and nondestructive tests (NDT). There are many options of NDT available for use to structurally evaluate airfield pavements, but the most used and recommended are the Falling Weight Deflectometer (FWD) and the Heavy Weight Deflectometer (HWD). The two techniques apply impulse loads to generate deflection basins on the pavement and their main difference is that FWD imparts lighter loads while HWD applies heavier loads. This difference leads to a discussion about the suitability of converting the results obtained by using the lower loads of the FWD to the heavier loads the HWD can apply because of the structural response of the pavement. Misevaluations of the structure could happen if this response is not linear, and in extreme cases the landing and take-off operations can be exposed to risks. Aiming to support the conclusion about the suitability of this conversion, the research's objective was to evaluate the influence of the load intensity on the structural response of airport pavements. To investigate the influence of the load, the flexible pavement of three runways from distinct regions of Brazil were evaluated using different FWD and HWD loads. Indexes/parameters obtained from these evaluations were studied: raw and normalized deflections, the Radius of Curvature (RC), the Impulse Stiffness Modulus (ISM), and the back-calculated Resilient Modulus (RM). Each of these indexes, obtained by applying distinct loads, were compared to verify the hypothesis the load variation leads to significant variation in the indexes. Statistical tests were performed to support the reliability of the study. The results showed that raw deflections presented differences whose percentual values are similar to the percentual of difference between the loads, and that the normalized deflections (which would be equal if the structural response was linear) presented influence of the applied load. RC values decreased when the load increased, instead of presenting the expected behavior of decreasing under a heavier solicitation. ISM presented decrease when the load was increased. RM decreased when the applied load increased. The subgrade was identified as the most affected by the load variation in comparison to the other structural layers. It was concluded that the structural response of the pavement is not linear, and that the differences are not large enough to prejudice the structural analysis of the airport pavements. However, if the results would be used in processes sensitive to the layers' modulus variations, the use of loads suitable to the traffic demanding the pavement is recommended.

Keywords: FWD; HWD; airfield pavements; structural evaluation.

LIST OF FIGURES

LIST OF TABLES

LIST OF ABBREVIATIONS AND INITIALS

BB	Benkelman Beam
CoV	Coefficient of Variation
FWD	Falling Weight Deflectometer
GPR	Ground-Penetrating Radar
HWD	Heavy Weight Deflectometer
ISM	Impulse Stiffness Modulus
RDD	Rolling Dynamic Deflectometer
RC	Radius of Curvature
RM	Resilient Modulus

LIST OF SIMBOLS

cm	Centimeter
km/h	Kilometer per hour
kN	Kilonewton
m	Meter
mm	Milimeter
ms	Milisecond
µm	Micrometer
%	Percentage

TABLE OF CONTENTS

1 INTRODUCTION

This section discusses the scenario in which the research is inserted and presents the research structure. A contextualization is initially made by exposing the air transportation perspectives of the structural pavement evaluation and based on the context presented, the research problem is proposed. The objectives the research aims to achieve are listed next, and the document's structure is discussed at the end of the section.

1.1 Initial considerations

Some specific characteristics of airports' traffic make the structural condition of the airfield pavements one of the most important factors to be evaluated and monitored. The requirement of rapidly transporting a great number of people from one site to another, for business or tourism purposes, or even when concerning cargo transport (this latter on a smaller scale in comparison with the former), leads the airports to receive big numbers of operations of increasingly large aircraft.

Larger aircraft apply higher loads to the pavement, while the greater the movement at an airport, the greater the frequency of load application to its structure. The combination of the application of high loads to the pavement with the high frequency of these applications leads the pavement to reduce its fatigue life, which makes it necessary to be executed periodic surveys of the structural integrity along with the service life of the pavement (HACHIYA *et al.,* 2001).

The structural evaluation of the pavement turns possible, among other applications, for the air space control agencies to report the pavement structural bearing capacity for the airports they are responsible for. This information is important to prevent the premature deterioration of a structure by avoiding frequent operation of aircraft whose gross weight is incompatible with the load capacity the pavement presents.

In an extreme situation, the structural bearing capacity report of a pavement could avoid incidents like the occurred at the Surabaya Juanda International Airport, the third busiest airport in Indonesia, where an Airbus A320-200 carrying 151 passengers from Surabaya to Jakarta was unable to take off because its wheels sank on the pavement. When the aircraft moved to the runway to start the take-off, part of the pavement collapsed, immobilizing the airplane wheels.

The structural pavement condition can be assessed by applying two distinct methodologies: destructive and nondestructive tests. The names are intuitive indications of how

each of these methods works. The destructive methods require the demolition of a small portion of the pavement to evaluate the structure's composition, and to collect material (to be later tested in a laboratory). The nondestructive tests, on other hand, dispense demolishing the pavement. In the tests of this method type, the structural condition is evaluated by measuring the superficial response of the structure (in form of deflections) or capturing, at the surface, the answer of the pavement that permits the construction of images that enable its structural analysis. These two method types are different and possess distinct uses, advantages, and disadvantages.

The traditional destructive tests used to perform these surveys could be very disruptive to airport operations since they could involve numerous cores, borings, and excavation pits that remove all layers of the pavement. The repair of a test pit can be expensive and keep the test area closed for several days. This is the main disadvantage of the destructive methods. However, there are cases when it is needful to conduct this type of test. One common situation where destructive testing is necessary is in the case of needing to obtain layer material characteristics that only can be verified by testing it in a laboratory.

The Nondestructive Testing (NDT) equipment assesses the structure with no damage to the pavement. While NDT simulates the pass of a single wheel load, and measures pavement surface response (deflections), it makes it possible to quickly gather data at several locations without compromising the operationality of runways, taxiways, or aprons. This is the most important advantage of the NDT compared to the traditional destructive methods (FEDERAL AVIATION ADMINISTRATION, 2011).

There are many options of NDT equipment and techniques available for use to structurally evaluate airfield pavements. Some countries, such as Canada, Italy, and the United States regulate how structural surveys must be conducted on this type of pavement (FEDERAL AVIATION ADMINISTRATION, 2001, 2021; ENTE NAZIONALE PER L'AVIAZIONE CIVILE, 2015; TRANSPORT CANADA, 2004, 2016). Some countries, however, such as Brazil (AGÊNCIA NACIONAL DE AVIAÇÃO CIVIL, 2017), mention in their regulations that structural evaluation must be done, but do not specify in detail how it must be conducted (what equipment or techniques must be used, or what specifications must be adopted/respected).

It is important to structurally assess the pavement using loads that represents the real traffic that will solicit the structure. The National Civil Aviation Agency – Brazil (ANAC), in its alert emitted in 2021, comments about the inability of some NDT test devices to properly evaluate some airport pavements. The document recommends that the aerodrome operators perform analyses to select a test load compatible with the real traffic solicitation acting on the pavement (AGÊNCIA NACIONAL DE AVIAÇÃO CIVIL, 2021).

This proper load selection can prevent the repetition of incidents as previously mentioned, since the application of a load compatible with real solicitations is capable to mobilize the same portions of the structure that would be mobilized with the pass of an aircraft wheel. The use of an inappropriate load could generate a misevaluation of the structural bearing capacity of the pavement by not mobilizing all the same parts which would be mobilized with an aircraft pass, exposing the landing, taxing, and taking-off operations to one more risk.

In addition to this worry about using proper loads to structurally assess airport pavements with NDT devices, there is a technical discussion about the possibility of converting the pavement response of a light load to that of a heavier one. Considering that some pavement materials present a stress dependency on their stiffness modulus (OMAR, 1996), the structural response of the pavement could be nonlinear.

Trying to answer this question, some studies investigated the linearity of the pavement response. Road and airports pavement structures were tested using distinct loads of FWD and HWD but divergencies about the structural behavior were concluded. Some research concluded that there is some effect of the load on the pavement response, leading to changes in its stiffness and back-calculate moduli (GROGAN *et al.,* 1998; HOFFMAN; THOMPSON, 1981; KIM *et al.*, 1995;). For other studies, the conclusion was that the pavement response is the same regardless of the applied load (MCQUEEN; *et al*., 2001; ROCHA FILHO 1996).

1.2 Research's problem

Safety and costs are topics of chief importance in the airport operations environment. Concerning aircraft operations, all the available efforts must always be taken to minimize the risk they could be exposed to. Referring to the costs to maintain an airport patrimony, the operator seeks the lowest possible expenses.

Uncertainties about the structural pavement responses when submitted to distinct loads could lead to misevaluations of its structural integrity. If the structure has its bearing capacity underestimated, unnecessary outlays can be made to perform unnecessary maintenance; if this capacity is overestimated, a traffic heavier than the structure bears can be permitted leading to an accelerated degradation of the pavement. The damaged structure requires earlier, higher financial investments to be recovered and, in a more critical scenario, results a risk to the aircraft operations.

Considering the impacts a wrong structural assessment can present, the lack of knowledge about how the pavement behaves under different loads becomes a problem.

Investigations to achieve a better understanding of the issue are necessary and desirable aiming to contribute to the mitigation of the negative effects the mentioned problem can cause on airport operations.

1.3 Objectives

The main objective of the research is to verify the influence of load intensity on the structural response of flexible airport pavements. To achieve this goal, some specific objectives were defined:

a) To understand the behavior of responses the pavement presents when subjected to variable solicitations;
b) To verify the existence of linear structural response of the pavements studied;
c) To evaluate how the structural pavement response is evidenced in the results of raw deflections, normalized deflection, radius of curvature, Impulse Stiffness Modulus, and back-calculated resilient moduli.

1.4 Document structure

This document is composed of five chapters. Additionally, to this first, Chapter 2 presents a literature review with the most relevant studies related to the subjects and methods addressed in this research. Chapter 3 presents the methods used to develop the research, and Chapter 4 contains the results and discussions. Chapter 5 brings the conclusions and main limitations of the research. In the end it is presented the list of references.

2 LITERATURE REVIEW

As previously introduced, the integrity of the pavement structure can be assessed by using destructive and nondestructive methods, and there are advantages and disadvantages in adopting each of these options. The disruption the use of destructive methodologies could cause to the airport operations is probably the main factor discouraging the use of these methods, whilst the amount of data the nondestructive testing (NDT) can quickly collect without considerably affecting the airport traffic supported the NDT to be the preferred options to evaluate airport pavements.

NDT can collect and analyze data through different techniques and equipment. These data can be used to evaluate the pavement structurally and functionally. Some of the main utilities of NDT are the evaluation of the load-carrying capacity of existing pavements, the obtaining of material properties of in-situ pavement layers and subgrade, and the determination of the effective thickness of each layer of the structure (AMERICAN SOCIETY FOR TESTING AND MATERIALS, 2008; FEDERAL AVIATION ADMINISTRATION, 2011).

Regarding the in-situ properties of the materials, there may even be some differences in the representativity of the results the destructive and nondestructive methods produce. The pavement demolition destructive methods require collecting material to be laboratory tested can modify properties the structure presents in situ, such as compaction and moisture. If the original conditions are not properly reproduced in the laboratory, the results could not represent the real pavement behavior. When tested on the field by NDT evaluations, however, the structural response of the pavement as it works can be perceived, but the results can be mistakenly read.

Despite being disruptive to airport operations and of less use to routine structural pavement assessments, the destructive methods are fundamental in supporting suitable NDT results. This support consists in using the tests performed with the material collected by the destructive evaluations to compare it to the NDT results in the field to establish suitable, reliable laboratory-field relations. Determining the material properties in the laboratory is important to correctly read the NDT results and properly characterize the in-situ behavior of the pavement materials.

Once well-established these relations, the user has conditions to use the NDT techniques to assess and understand how the pavement works, avoiding misunderstandings. There are many options of equipment available to nondestructively assess the pavement. Technologies that use mechanic and electromagnetic waves emission, static and dynamic load

applications, and others. Some of the main techniques used to structurally evaluate the airport pavements will be following presented.

2.1 Nondestructive testing methods

A search in the regulations of the countries of chief importance in air transport of the International Civil Aviation Organization (ICAO) permits to understand how the structural evaluation of airport pavements is conducted around the world. Destructive tests are recommended, such as drilling and coring and the less invasive Dynamic Cone Penetrometer, but the NDT are the most mentioned.

Regulations and research addressing the structural evaluation of airfield pavements mention Infrared Thermography, Ground-Penetrating Radar, Dynaflect, Road Rater, Road Dynamic Deflectometer, Benkelman Beam, Falling Weight Deflectometer, and Heavy Weight Deflectometer as tools to perform the assessment of this type of structure. These methodologies will be briefly described in this subsection.

Infrared Thermography is an NDT that uses thermosensitive photographs. This device senses the infrared radiation emitted by the structure, detecting surface temperature differences. If there are distresses in the pavement structure, the heat transference is affected, leading to the surface temperature differences that are measured by infrared thermography. These differences are represented in images as heat maps, which permit the identification of defected areas. (MOROPOULOU *et al.*, 2000).

The measurements could be performed during both day and night-time hours. (MOROPOULOU *et al.*, 2001). Infrared thermography is used to identify delamination occurrence between Asphalt Concrete (AC) pavement layers (FEDERAL AVIATION ADMINISTRATION, 2011), and one advantage of this technique over other NDT is the evaluation of large areas by fast scanning. The measurement of areas is also an advantage because the reach is greater in comparison to most of the other methods which are point or line testing methods. The main limitation of the technique is that it does not make it possible to determine the depth and thickness of cracks and voids, which makes it desirable to perform infrared thermography combined with ground-penetrating radar (MOROPOULOU *et al.*, 2000, 2001).

Ground-Penetrating Radar (GPR) technology is an NDT that uses emitting and receiving short electromagnetic pulses to assess the pavement structure. The most common use of GPR is measuring pavement layer thickness, identifying large voids, detecting the presence

of excess water in the structure, locating underground utilities, and investigating significant delamination between pavement layers (FEDERAL AVIATION ADMINISTRATION, 2011). GPR is useful to determine the thickness of AC and thin Portland Cement Concrete (PCC) surface layers, but it is not useful when determining the thickness of thick PCC surface layers (PRIDDY *et al.*, 2015).

The NDT equipment that imparts loads to the structure measures the pavement surface response as deflections caused by the applied load (that simulates a moving wheel). There are different categories of deflection measuring equipment: static, steady state (vibratory, for example), and impulse load devices. Static tests, which measure deflections at one point under a nonmoving load, are slow and labor-intensive. NDT types of equipment that use dynamic loads create deflections by using vibratory or impulse loads, having faster data collection (FEDERAL AVIATION ADMINISTRATION, 2011).

According to the American Society for Testing and Materials (2020), two devices are the most common commercially available to test pavements using cyclic loading. They are the Dynaflect and the Road Rater.

Dynaflect, pictured in Figure 1, is an electromechanical device largely used in the United States for the measurement of dynamic deflections. When the equipment is stationed to measure, two rubber-coated steel wheels impart a 5.0kN peak-to-peak sinusoidal load at a fixed frequency of 8.0Hz. Advantages of Dynaflect include high reliability, low maintenance, and the ability to measure the deflection basin. Its main disadvantage is that the low dynamic applied load is so much smaller than the normal aircraft loads, which could produce inadequate deflections on heavy airport pavements. The use of this device is only recommended for light-load pavements serving aircraft less than 5,670kg (FEDERAL AVIATION ADMINISTRATION, 2011; PINTO; PREUSSLER, 2010).

Road Rater (Figure 2) is used to measure dynamic deflections also applying peak-to-peak sinusoidal loads to the pavement. Differences when comparing it to Dynaflect are that Road Rater generates the loads using the hydraulic acceleration of a steel mass achieving frequencies up to 60Hz and that the loads this equipment impart range from 2.0kN to 35.0kN. The measurements are done at the center of the load plate and in a radial distance using four- to seven-velocity transducers (AMERICAN SOCIETY FOR TESTING AND MATERIALS, 2020; FEDERAL AVIATION ADMINISTRATION, 2011). Despite being higher than the loads produced by the Dynaflect, the load range the Road Rater covers is even low to be used on heavy airport pavements (operating aircraft heavier than 5,670kg).

Figure 1 – Dynaflect trailer

Source: FEDERAL AVIATION ADMINISTRATION, 2011.

Figure 2 – Road Rater trailer

Source: FEDERAL AVIATION ADMINISTRATION, 2011.

According to Nam (2011), the Rolling Dynamic Deflectometer (RDD) is an NDT measurement device that uses dynamic sinusoidal loads generated by an electrohydraulic loading system. The equipment, mounted on a truck, imparts two types of forces to the pavement through a pair of loading rollers: simultaneously, a static hold-on force to keep the loading rollers in contact with the pavement, and a peak-to-peak dynamic force simulating the traffic are applied. For airport pavement assessment, the static force typically stays in a range of 44 to 71kN, and the peak-to-peak dynamic force achieves values from 44 to 62kN, at a typical operating frequency of 30Hz, capable to achieve from 20 to 50Hz.

RDD is employed when there is a requirement to measure deflection profiles continuously along airport pavements. The testing speed is about 1.60km/h and measurements are performed at the same time as the loan application by geophones installed on the geometrical center of three-wheel rolling carts positioned in a linear array under the truck and ahead of the loading rollers. Research that studied the use of RDD applied to airfield pavements deals with Jointed Concrete Pavements (JCP), verifying variations in deflection profile induced by variations in slab thickness, distance to joints, temperature, and testing speed. Considering the airport evaluation needs, RDD could not be so much used since it does not measure the moduli of pavement layers (NAM, 2011; NAM *et al.*, 2014).

Benkelman Beam (BB) is the most common static measurement device, and some other equipments were developed to automate its use, such as the Swedish La Croix Deflectograph, the British Transport, and Road Laboratory Pavement Deflection Data Logging – a modified La Croix Deflectograph, and Caltran's California Traveling Deflectometer (FEDERAL AVIATION ADMINISTRATION, 2011). This equipment consists of an interfixed lever with a tip test at the end of the longest arm, and a 10^{-2}mm-precision extensometer at the end of the smaller arm. The main advantage of the BB is its simplicity, with the deflections being measured by simply placing the tip test on the pavement between the dual rear tires of an 8.2t-loaded truck (used to impart the load to the structure) and moving the truck away from the beam. In another hand, the main disadvantages are that a long time is required to perform the tests, and that it is a procedure susceptible to operator interference (BRASIL, 2010; PINTO; PREUSSLER, 2010).

According to Ullidtz (1987, p. 257-282, *apud* ROCHA FILHO, 1996, p. 32), the major problem the BB results present is their lack of accuracy. The measurements' repeatability is greatly affected by environmental and operational factors and the dependency on load application conditions. The low loading speed impacts the AC layer viscoelastic response, and any variation in the loading time is significant to the layers' deformation, especially when testing on hot days.

Falling Weight Deflectometer (FWD) and Heavy Weight Deflectometer (HWD) are examples of impulse devices, which generate dynamic load by free-falling a mass onto a set of rubber springs. The magnitude of the impulse load can be varied by changing the mass and/or the drop height. Equipment can be classified as HWD when it can generate maximum dynamic loads greater than 150kN (FEDERAL AVIATION ADMINISTRATION, 2011). Figure 3 depictures an FWD device.

Figure 3 – Jils FWD

Source: FEDERAL AVIATION ADMINISTRATION, 2011.

The FWD and HWD equipment has different specifications depending on their manufacturer. In general, the equipment can impart forces of 7.0kN to 300kN generated by one- or two-mass generators, with load durations of 25 to 56ms and raising load time varying from 12ms to 28ms. The load plate could be rigid, segmented, or non-segmented, with a rubberized pad or split plate, varying its diameters in a range of 30cm to 45cm. (FEDERAL AVIATION ADMINISTRATION, 2011). The load magnitudes imparted by FWD make it generally to be used in representing truck and light aircraft traffic, while HWD better represents heavy aircraft loads (PRIDDY *et al.*, 2015). An HWD device is depictured in Figure 4.

Figure 4 – Dynatest HWD

Source: FEDERAL AVIATION ADMINISTRATION, 2011.

The deflections can be measured by 7 to 12 geophones or seismometers, positioned from 0.0cm to 250cm away from the load application point. Depending on the regulation agency, more than 12 geophones, and spacing up to 5.0m could be required. The deflection sensor's range is from 2.0mm to 5.0mm, resolution of 0.001mm, and accuracy of 2μm ± 2%. The test time required for an application of four loads stays between 20 and 35 seconds. All the equipment needs only a personal computer to support the test execution (BROUTIN; MOUNIER, 2016; FEDERAL AVIATION ADMINISTRATION, 2011).

Compared to other deflection-based methods (static as BB and steady-state as Road Rater), the impulse load equipment as FWD and HWD is the best in simulating the moving wheel load deflections. Other advantages are that FWD and HWD tests measure the extent of the deflection basin, having fast data acquisition, and requiring small preloads on the pavement surface. (FEDERAL AVIATION ADMINISTRATION, 2011; HOFFMAN; THOMPSON, 1981; LYTTON; SMITH, 1985; THOLEN *et al.*, 1985).

The deflections produced by FWD devices, differently from the results for BB, are not overestimated. For the same load magnitude, BB deflections are greater than FWD ones. It is observed because the instantaneous load application of FWD devices does not mobilize the time-dependent viscoelastic deformations of the layers (HOFFMAN; THOMPSON, 1981). The static load application of the test truck, on other hand, leads the BB to measure deflections containing elastic and time-dependent viscoelastic deformations, making the results to be greater than for FWD (BALBO, 2007). According to Pinto and Preussler (2010), BB deflections are 20% to 30% higher than FWD deflections.

Song *et al.* (2014) say that despite being the best device in generating a structural response that better correlates to the pavement response when subjected to a pass of a moving wheel load (not mobilizing so many time-dependent deformations as much as BB), FWD and HWD devices do not perceive elastic deformations only. Mult-Depth Deflectometers installed in an airport pavement, in depths varying from 36cm to 208cm, registered preload deformations that represent up to 76% of maximum deflections measured for 50kN HWD tests, and up to 50% for 160kN HWD tests. These deformations, which start to be registered 15 seconds after positioning the HWD equipment, are caused by the HWD device and towing vehicle weights.

The main information about the NDT used to structurally evaluate airport pavements were presented in this section. Table 1 summarizes the evaluation method and the advantages and disadvantages of each method discussed.

Table 1- Summary information about the main NDT used to assess airport pavements

Parameters	Data acquisition method	Result	Advantages	Disadvantages
Infrared Thermography	Thermosensitive photographs	Photographs of heat distribution	Evaluation of large areas	Incapable to determine depth and thickness of cracks and voids
Ground Penetrating Radar	Emitting and receiving electromagnetic pulses	Pulse reflection profile pictures	Fast data acquisition	Limitation in evaluating some materials and frequencies
Dynaflect	Application of sinusoidal loads	Deflection measurements	Low maintenance cost Ability to measure deflection basin	Applied loads are inadequate to evaluate airport pavements
Road Rater	Application of sinusoidal loads	Deflection measurements	Ability to measure deflection basin	Applied loads are inadequate to evaluate airport pavements
Rolling Dynamic Deflectometer	Application of sinusoidal loads	Deflection profile measurements	Ability to measure continuous profiles of pavement response	Not capable to measure moduli of pavement layers
Benkelman Beam	Application of static	Deflection measurements	Simplicity in performing the test	Long testing time Susceptible to operator interference
Falling Weight Deflectometer	Application of impulse load	Deflection basin measurements	Fast data acquisition Best device in simulating moving wheel loads	Expensive hiring and maintenance Expensive logistic of transportation
Heavy Weight Deflectometer	Application of impulse load	Deflection basin measurements	Fast data acquisition Best device in simulating moving wheel loads	Expensive hiring and maintenance Expensive logistic of transportation Few available devices Some maintenance services not available in Brazil

Source: THE AUTHOR.

2.2 Deflection basin characteristics and parameters

The main use of NDT deflections is associated with the in situ or effective pavement structural capacity. NDT deflection basin analysis is a technique for determining the most accurate estimates of the actual in situ layer properties. With the deflection values, deflection basin parameters can be calculated. These parameters are mainly used to check the structural integrity of in-service pavements, to relate the pavement response to critical threshold responses, and to calculate the in-situ layers' moduli (AMERICAN ASSOCIATION OF STATE HIGHWAY AND TRANSPORTATION OFFICIALS, 1993; OMAR, 1996).

The shape of the deflection basin obtained by FWD and HWD measurements relates to the influence of the distinct layers on the structural response of the pavement. The deflections closer to the point of load application are a general indicator of the pavement layer's structural response, and the more distant deflections are related to the subgrade response.

The deflection under the load plate indicates the performance of all structural layers with about 70% of subgrade contribution. The deflection basin from the point of loading the pavement to 200~300mm far from this point gives information about the surface and base layers' structural condition. From 300mm to 600mm far from the load plate, the deflection basin relates to the subbase stiffness. Deflections measured over 600mm away from the load plate mostly influence the subgrade structural response (Horak and Emery, 2006; FAA, 2011; Pigozzi *et al.*, 2014; White and Barbeler, 2018).

The maximum deflection has a long history of use because of old equipment like BB, but this parameter is not sufficient to perform a structural analysis. The same value of maximum deflection can be measured on two pavements with totally different deflection basins and structural response characteristics. Since the pavement deflects in a certain area as a result of a load application, parameters considering the entire deflection basin are more appropriate to perform structural analysis based on deflection results (HORAK, 1987; HORAK *et al.,* 2015). Table 2 summarizes the most common deflection basin parameters used to perform structural analyses of pavements.

Another spreadable used parameter is the Impulse Stiffness Modulus (ISM). ISM is a measure of the relative stiffness of the pavement at the location of the NDT, indicating the overall strength of the entire pavement structure. Pavement stiffness can be defined as the relation between the applied load and the pavement deflection at the point of the load application. This is the definition of the ISM, whose equation is presented in Equation 1 (FEDERAL AVIATION ADMINISTRATION, 2011).

Table 2- Summary presentation of the main deflection basin parameters

Parameters	Formulas	Structural indicator and association with pavement layer
Maximum deflection	D_0 as measured	All structural layers with about 70% of contribution by the subgrade
Radius of Curvature (RoC)	$RoC=\frac{L^2}{2D_0(D_0/D_{200})-1}$	Structural condition of surface and top of base layer
Base Layer Index (BLI) or Surface Curvature Index (SCI)	$SCI=BLI=D_0-D_{300}$	Base layer structural condition
Middle Layer Index (MLI) or Base Damage Index (BDI)	$MLI=BDI=D_{300}-D_{600}$	Subbase and selected layer structural condition
Lower Layer Index (LLI) or Base Curvature Index (BDI)	$LLI=BCI=D_{600}-D_{900}$	Lower structural layers and subgrade
Shape factors	$F_1=(D_0-D_{600})/D_{300}$ $F_2=(D_{300}-D_{900})/D_{600}$	Correlate to subgrade moduli
Additional shape factor	$F_3=(D_{600}-D_{1200})/D_{900}$	Lower layer condition or depth to a stiff layer
Area under pavement profile (AUPP)	$AUPP=\frac{5D_0-2D_{300}-2D_{600}-D_{900}}{2}$	Characterizing of pavement upper layers
Additional Areas	$A_2=\frac{6(D_0+2D_{450}+D_{600})}{D_0}$	Middle layer condition
	$A_3=\frac{6(D_{600}+2D_{900}+D_{1200})}{D_0}$	Lower layers condition
Area Indices	$AI_1=(D_0+D_{300})/2D_0$	Upper layer condition
	$AI_2=(D_{300}+D_{600})/2D_0$	Middle layer condition
	$AI_3=(D_{600}+D_{900})/2D_0$	Middle layer condition
	$AI_4=(D_{900}+D_{1200})/2D_0$	Lower layer condition

Source: HORAK (1987); HORAK; EMERY (2006); HORAK *et al.* (2015); adapted by the Author.

$$ISM=\frac{F}{D_0} \quad (1)$$

Where:

ISM = Impulse Stiffness Modulus (kN/mm);

F = applied load (kN);

D_0 = maximum deflection (mm).

The advantage of using ISM is its calculation simplicity. Regarding its application to airfield pavements, this parameter can be used in preliminary analyses of runways, taxiways, or aprons to identify structural homogeneous sections in the facilities. Increasing ISM values indicate increasing pavement strength (GROGAN *et al*., 1998; FEDERAL AVIATION ADMINISTRATION, 2011).

2.3 Corrections for deflections and backcalculated moduli

It is well known that, especially for AC pavements, deflections and pavement layer moduli are affected by temperature (AMERICAN ASSOCIATION OF STATE HIGHWAY AND TRANSPORTATION OFFICIALS, 1993; VAN GURP, 1995; KIM *et al.*, 1995; CHEN *et al.,* 2000; FEDERAL AVIATION ADMINISTRATION, 2011; BROUTIN; DUPREY, 2017). The resilient modulus of the asphalt material exponentially decreases with temperature increases (AKBARZADEH *et al.*, 2012).

Since deflection surveys are activities that can expend hours to execute, temperature variations, that naturally occur along the day and night, are often present in the results. To enable the proper use of these results in comparative analyses, it is necessary to correct the data to a reference temperature.

The American Association of State Highway and Transportation Officials (AASHTO), since its 1986's version of the Guide for Design of Pavement, recommends the use of linear curves to determine the correction temperature factor in the function of the AC mix temperature and total asphalt thickness. This method is also adopted by the most recent version of the Guide, correcting the deflections to 20°C and predicting the AC mix temperature using the pavement surface temperature and the average air temperature for the 5 days before the survey (AMERICAN ASSOCIATION OF STATE HIGHWAY AND TRANSPORTATION OFFICIALS, 1993).

The São Paulo's Highway Department (DER-SP) adopted the AASHTO correction method in its regulation, adjusting the reference temperature to the Brazilian reference of 25°C. The DER-SP method also uses an abacus to obtain the correction factor, but, differently of the AASHTO (AMERICAN ASSOCIATION OF STATE HIGHWAY AND TRANSPORTATION OFFICIALS; 1993) method, the DER-SP procedure measures only the pavement surface temperature, and just at the time of the FWD testing (DEPARTAMENTO DE ESTRADAS DE RODAGEM, 2006).

Problems were identified when applying the AASHTO temperature correction method to FWD deflections. The correction proposed by AASHTO (AMERICAN ASSOCIATION OF STATE HIGHWAY AND TRANSPORTATION OFFICIALS; 1993) is inaccurate, especially at temperatures over 38°C. The method, which was originally developed to correct BB deflections, returned considerable variance in the results of back-calculated pavement stiffness to FWD data (JOHNSON; BAUS, 1992; KIM *et al.*, 1995).

A detailed study of FWD deflections, conducted by Kim *et al.* (1995) to develop a new temperature correction procedure for FWD deflections and back-calculated AC moduli, showed that, in comparison to the linear AASHTO correction curves (Figure 5), a nonlinear function better represents the relationship between the measured deflections and the pavement temperature. The equation proposed by the authors to temperature correct maximum FWD deflections is following presented in Equation 2.

Figure 5 – AASHTO's adjustment to D_0 for AC mix temperature for pavement with granular or asphalt-treated base

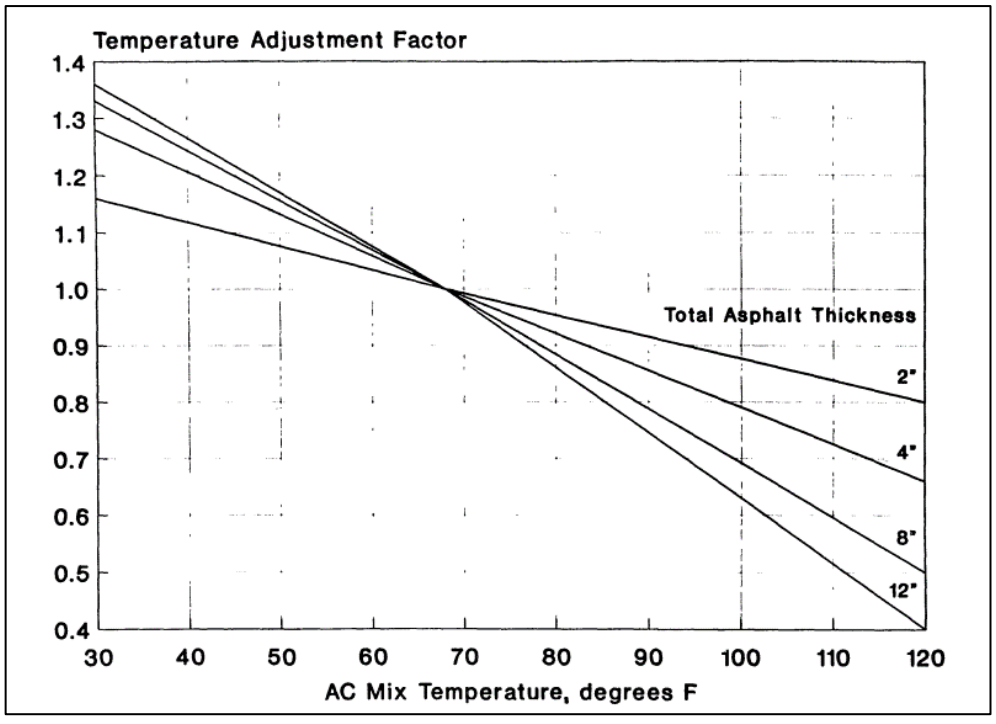

Source: AMERICAN ASSOCIATION OF STATE HIGHWAY AND TRANSPORTATION OFFICIALS; 1993

$$D_{0,20°C} = 10^{\alpha(68-T)} * D_{0,T} \quad (2)$$

Where:

$D_{0,20°C}$ = maximum deflection adjusted to the reference temperature of 20°C;

$D_{0,T}$ = maximum deflection measured at temperature T (°F);

T = AC layer mid-depth temperature (°F) at the time of FWD testing;

α = $3.67x10^{-4}t^{1.4635}$ for wheel path;
$3.65x10^{-4}t^{1.4241}$ for lane center;

t = thickness of the AC layer (in.).

Kim *et al.* (1995) hourly recorded the asphalt temperature, from 08:00 a.m. to 06:00 p.m., at different depths of a 140mm-thick AC layer in the Eastern USA. They also performed FWD tests on the same day and applied the AASHTO (AMERICAN ASSOCIATION OF STATE HIGHWAY AND TRANSPORTATION OFFICIALS, 1993) temperature correction to the deflections measured. The results demonstrated that the AASHTO method generates some inconsistent corrections because this procedure just uses the pavement temperature at its surface, which cannot account for differences in the pavement temperature gradient caused by the heating versus cooling cycle of a day. The authors found better correlations between measured deflections and the mid-depth temperature, so they implemented the mid-depth temperature in their temperature correction procedure for deflection adjustment (Equation 2).

The same study also developed a method to correct the back-calculated AC moduli. By plotting the ratio between back-calculated modulus at measured temperature versus temperature-corrected modulus in the function of the mid-depth temperature, the authors verified that the relationship is similar to all of the pavement sections studied, presenting discrepancies just for low temperatures (10°C or less). Because the modulus ratio curves are similar for all sections, the study derived the AC moduli temperature correction based on regression analysis, as presented in Equation 3 (KIM *et al.*, 1995).

$$E_{20°C} = 10^{0.0153(T-68)} E_T \quad (3)$$

Where:

$E_{20°C}$ = corrected AC modulus to the reference temperature of 20°C (ksi);

E_T = Back-calculated AC modulus from FWD testing at temperature T (ksi);

T = AC layer mid-depth temperature (°F) at the time of FWD testing.

Kim *et al.* (1995) developed Equation 3 using the modulus-temperature relationship obtained from laboratory testing and that is present in the MODULUS software (used to back-calculate the AC modulus). Because the AC stiffness is a strong function of temperature, the correction procedure produces meaningful results by specifying only the temperature corresponding to the testing time.

Chen *et al.* (2000) conducted a study about the correction of FWD measurements. Three road pavement structures from the Southern USA were continually tested for a 2- to 3-day period with 40kN FWD loads. The pavement temperature was collected using thermocouples installed within the AC layer. As result, the authors developed, for each pavement section, correction equations for the maximum deflection (D_0) and the following deflection (D_1) because they demonstrated that these deflections are significantly influenced by the pavement temperature. It was also developed a single equation for the back-calculated AC moduli correction.

The study of Chen *et al.* (2000) also proposed improvements to the Kim *et al.* (1995) correction equations. Using the data from the three sections studied, and collecting data from several ACs of different thicknesses, the authors tried to develop an equation that could be used to correct deflections from different structures, and that permits the users to adopt their reference temperature. The result is an adaptation for Kim *et al.*'s (1995) deflection temperature correction and is presented in Equation 4.

$$D_{0,Tr} = D_{0,T}\left(\frac{1.0823^{-0.0098t}}{0.8631}\, T_r^{0.8316} T^{-0.8419}\right) \quad (4)$$

Where:

$D_{0,Tr}$ = adjusted maximum deflection to the temperature T_r (mm);

$D_{0,T}$ = maximum deflection measured at temperature T (mm);

Tr = user defined reference temperature (°C);

T = AC layer mid-depth temperature (°C) at the time of FWD testing;

t = thickness of the AC layer (mm).

Although the studies were developed under different climatic conditions and pavement structures, Equations 2 and 4 generated correction factors that differ only 7.9% on average, with discrepancies observed just to temperatures under 14°C. For the AC moduli temperature correction, however, the variability was considerably high. Chen *et al.* (2000), comparing the correction factors generated using the Kim *et al.*'s (1995) equation (Equation 3), their equation, presented in Equation 5, and the equation used by the Texas Transportation Institute, presented in Equation 6, verified the existence of great variance between the three methods at temperatures higher than 33°C.

$$E_{Tr} = \frac{E_T}{(1.8T_r + 32)^{2.4462}(1.8T + 32)^{-2.4462}} \quad (5)$$

$$E_{25°C} = \frac{E_T T^{2.81}}{185000} \quad (6)$$

Where:

E_{Tr} = adjusted AC modulus to the temperature T_r (MPa);

$E_{25°C}$ = adjusted AC modulus to the reference temperature of 25°C (MPa);

E_T = backcalculated AC modulus to the temperature T (MPa);

T_r = user defined reference temperature (°C);

T = AC layer mid-depth temperature at the time of FWD testing (°C for Equation 5; °F for Equation 6);

Since Equation 3 only adjust the AC moduli to the 20°C temperature, and Equation 6 only adjusts to 25°C, the comparison between these two methods is not adequate. Equation 5, in turn, can adjust the moduli to any defined temperature, and can be compared to both the other equations. The correction factors for Equations 5 and 6 presented a close agreement for the two correcting temperatures (20°C and 25°C), but the results for Equation 3 reached almost double the values calculated using Equation 5 (CHEN *et al.*, 2000).

Another effect the temperature has on the pavement is the variation of the load effectively applied to the structure. Temperature changes the viscosity of bituminous binders, leading the AC pavement to present more or less stiffness. As stiffer the structure is, the higher is the load effectively transmitted to the pavement. A surface pavement temperature increase of 10°C leads to a reduction of 5% in the load applied to a flexible airport pavement (ROCHA FILHO, 1996).

The influence of temperature on the testing equipment also impacts the effectively applied load. Rocha Filho (1996) affirms that the stiffness of the FWD buffers during compression of the falling weights is affected by the temperature when testing in hot climates, leading to variations in the load transmitted to the pavement.

Testing flexible road and airport pavements, Rocha Filho (1996) also verified that the changes in pavement stiffness induced by the temperature variation change the deflection values. Higher temperatures cause a reduction in the pavement stiffness, leading it to present higher deflections. This effect is stronger for the maximum deflections (D_0), being the deflections farther from the load application point practically unchanged, demonstrating that the surface coat is the most temperature-affected layer of the pavement. In addition, to the AC pavements, as thicker the surface coat is, the higher will be the measured D_0 deflection.

To turn the deflections comparable, despite being obtained by the application of different loads, and the variations in the loading induced by the equipment itself and due to temperature changes, it is of consensus the need for normalizing the D_0 data. FAA (FEDERAL AVIATION ADMINISTRATION, 2011) proposes a method to correct maximum deflections, as presented in Equation 7.

$$D_{0,N} = \left(\frac{L_{norm}}{L_{applied}}\right) * D_0 \tag{7}$$

Where:

$D_{0,N}$ = adjusted deflection (10^{-2}mm);
D_0 = measured maximum deflection (10^{-2}mm);
L_{norm} = normalized load (kN);
$L_{applied}$ = effectively applied load (kN).

2.4 Load influence on pavements structural evaluation

Given the complexity of pavement materials and the uncertainties of many parameters of design, it is normally assumed the linear elasticity of materials when performing structural analysis of the pavements. However, some pavement materials such as soils and non-treated granular materials present nonlinear behavior, i.e., its stiffness modulus depend on the material's tension state. (ANTUNES, 1993; OMAR, 1996). Some research addressing results that evidence this non-linearity of the pavement structures will be following presented.

The study of Hoffman and Thompson (1981), comparing deflection measurements produced by BB, Road Rater, and FWD on pavements from AASHO Test Road facilities identified the tendency of the structure's stiffness to be reduced with the increase of the test load. For FWD tests, the variation of the applied load from 15kN to 75kN produced a decrease in the pavement stiffness in 82% of the test sections. The results for the Road Rater tests presented the same tendency. According to the authors, the deflection values increased faster than the load, presenting a non-linear response.

Studying the overlay design of road pavements, Lytton and Smith (1985) compared deflection measurements from different devices. Results from static, steady-state, and impulse deflection devices were compared. According to the authors, when an NDT device produces loads lesser than the design loads, measured deflections and material properties obtained for the light load must be correlated to those produced by the design load. However, it could produce questionable results because of the stress sensitivity the pavement and subgrade could present.

A study conducted on road pavements from the Eastern USA varied the FWD drop force, imparting 27kN, 40kN, 49kN, and 77kN to the pavement structure. The authors find that the back-calculated AC moduli were relatively the same, regardless of the FWD load level. The moduli of the aggregate base course increased as the FWD load increased, and the subgrade modulus presented different trends of influence on the FWD load level, depending on its material type (KIM *et al.*, 1995).

The granular base course, and subgrades of sandy granular material (A-3 in the Highway Research Board Classification – HRB soil classification) increased its moduli by increasing the FWD load because of the effect of the confining pressure on the modulus of granular materials. Lime-stabilized subgrade decreased its modulus with increasing FWD load level. Subgrades of highly plastic clayey materials (A-6 or A-7 in HRB soil classification)

presented a decrease in their moduli when the FWD load increased, because of the effect of the deviator stress on the modulus of fine-grained soils (KIM *et al.*, 1995).

The observed variation in the granular materials' properties identified in the study could be an effect of the complexity this type of material presents, especially depending on the solution employed in each structure using granular layers. The type of material, the compaction and moisture used to construct the layers, and others. But the assumption these variations also could be an effect of the load influence cannot be discarded, since this is another condition imposed on the granular materials that when combined with the other mentioned variables can lead the pavement structure to present distinct behaviors.

McQueen *et al.* (2001) studied the influence of varying the load intensity of FWD and HWD tests on flexible pavements at the Federal Aviation Administration (FAA) National Airport Pavement Test Facility (NAPTF). The tested pavement sections were constructed on low (CBR of 4%), medium (CBR of 8%), and high-strength (CBR of 25%) subgrades. They concluded that there is no need to perform heavy load NDT tests, such as HWD, on evaluating airport pavement structures since was identified that pavement stiffness and back-calculated subgrade moduli are independent of FWD or HWD force amplitudes. This conclusion, according to the authors, is also applied to rigid pavements.

This result is the quite opposite of the conclusion Grogan *et al.* (1998) found in their study that also tested airfield pavements varying the applied loads. The 1998's study concluded that the pavement response is not linear for flexible pavements. This divergence between the conclusions may have been caused by some limitations the study of McQueen *et al.* (2001) presented, compared to the research of Grogan *et al.* (1998). While the latter studied 12 different pavements from 6 distinct airports and adopted loads of 44kN, 67kN. 110kN, and 220kN, the former used loads of 40kN, 60kN, 82kN, and 115kN, and just studied pavements from the NAPTF.

When assessing a pavement using FWD, the increase in applied load magnitude considerably increases the measured deflections. White and Barbeler (2018) obtained this result through a study that compared FWD surveys performed with drop forces of 50 and 100kN. The increase in deflection is an expected result since the same point of the structure is being submitted to a higher force. To turns it possible to compare the effect of increasing load magnitude on the measured deflections, a normalization of deflections should be done as proposed by FAA (FEDERAL AVIATION ADMINISTRATION, 2011), presented in Equation 7.

The effect of increasing load magnitude is more clearly noted in the results of the ISM. The average values obtained show that by increasing the drop force from 50kN to 100kN, the back-calculated ISM for granular materials (base and subbase layers) increases from 6.8% to 36.8%. The coefficient of variation (CoV) obtained is also considerably higher with higher drop forces (WHITE; BARBELER, 2018).

The study of Rocha Filho (1996) submitted the same points of flexible and rigid road pavement, and flexible airport pavement to different loads. The different loads were applied by varying the drop height in the FWD. The results demonstrated that the effectively applied load increases with the increase in pavement stiffness. This effect has more impact on lower loads. To the rigid pavement, the increase in the effectively applied load was 31% to lower loads, whilst the application of higher loads resulted in a maximum increase of 3%.

The same study verified the effect of load level variation on the back-calculated moduli for airport pavements. To the range of loads adopted, 27.60kN to 91.30kN, it was noted that the structure is linear in all the pavement layers. The observed differences in back-calculated moduli for the different loads stay inside the error tolerance associated with the own back-calculation process imprecision (ROCHA FILHO, 1996).

The studies presented did not achieve an agreement in their conclusions about the linearity of the pavements, and they do not present arguments trying to explain what could influence in these divergent conclusions. Table 3 presents the main results and conclusions the studies presented have obtained.

Table 3- Summary presentation of the main conclusion of the studies addressing the structural response of pavements subjected to variable loading

Study	Methodology	Main conclusion
Hoffman and Thompson (1981)	Comparison of deflection measurements of Benkelman Beam, Road Rater, and FWD	Pavement response is not linear
Lytton and Smith (1985)	Comparison of layer moduli and deflection measurements of Benkelman Beam, Dynaflect, Road Rater, and FWD	To correlate measured deflection and material properties obtained for different loads could produce questionable results
Kim *et al.* (1995)	Comparison of back-calculated layer moduli obtained for variable FWD loads	Back-calculated moduli for AC is relatively the same; Granular material's moduli increased with increasing FWD loads; Stabilezed and plastic subgrades' moduli decrased with increasing FWD loads.
Rocha Filho (1996)	Comparison of back-calculated moduli obtained for variable FWD loads	Pavement response is linear
Grogan *et al*. (1998)	Comparison of ISM and back-calculated moduli obtained for variable FWD and HWD loads	Pavement response is not linear for flexible pavements
McQueen *et al.* (2001)	Comparison of ISM and back-calculated moduli obtained for variable FWD loads	ISM and back-calculated moduli do not depend on the applied load for flexible and rigid pavements
White and Barbeler (2018)	Comparison of ISM obtained for variable FWD loads	ISM for granular materials increase with increasing the load

Source: The Author.

3 METHODS

The development of the research consisted in collecting, correcting, organizing, calculating parameters, and statistically testing the data obtained. This sequence of steps was established to make it possible to take some conclusions about the existence of the load intensity influence on the linearity of the structural response of the pavement. The following subsections present each of the steps of the method in detail.

3.1 Data collection

Three runway pavements at different sites were tested with both Falling Weight Deflectometer (FWD) and Heavy Weight Deflectometer (HWD) loads. The airports located in northeastern Brazil and in southeastern Brazil were evaluated in their full extension. The airports studied (here called A, B, and C) are civil aviation airports that operate civil aviation, military aviation, and cargo aircraft in operation for more than 40 years.

Airport A has a 2,500m-length and 45m-width runway, with a flexible structure of three layers, as presented in Figure 6. The surface course presents thicknesses varying from 30.0cm to 38.0cm of Asphalt Concrete (AC). The base and subbase layers are 28.0cm-thick and constructed with macadam and gravel soil. The structure is seated on a sandy soil subgrade which presents CBR values up to 24%. The layer thickness was obtained by coring for the surface and by using Benkelman Beam data for the others (DIRENG, 1991; AGÊNCIA NACIONAL DE AVIAÇÃO CIVIL, 2020).

Airport B's runway, which is 3,000m long and 45m wide, has a flexible structure of three layers. The surface course presents thicknesses varying from 22.0cm to 26.0cm of AC. The pavement presents two distinct sections referring to the base and subbase materials. Section 1, which is 2,000m long, presents an asphaltic base with thicknesses varying from 31.0cm to 33.0cm, and a white sand subbase of 73.0cm to 74.0cm. The 900m of section 2 has a 29.0cm-thick hydraulic macadam base, a 50.0cm-thick red clayey sand, and a 13.0cm-thick subgrade reinforcement constructed with white sand. The structures are seated on a subgrade with CBRs varying from 16% to 60%. The layer thicknesses were obtained by coring and drilling (AGÊNCIA NACIONAL DE AVIAÇÃO CIVIL, 2018). Figure 7 depictures a scheme of the structure of the Airport B runway.

Figure 6 – Airport A runway's pavement structure

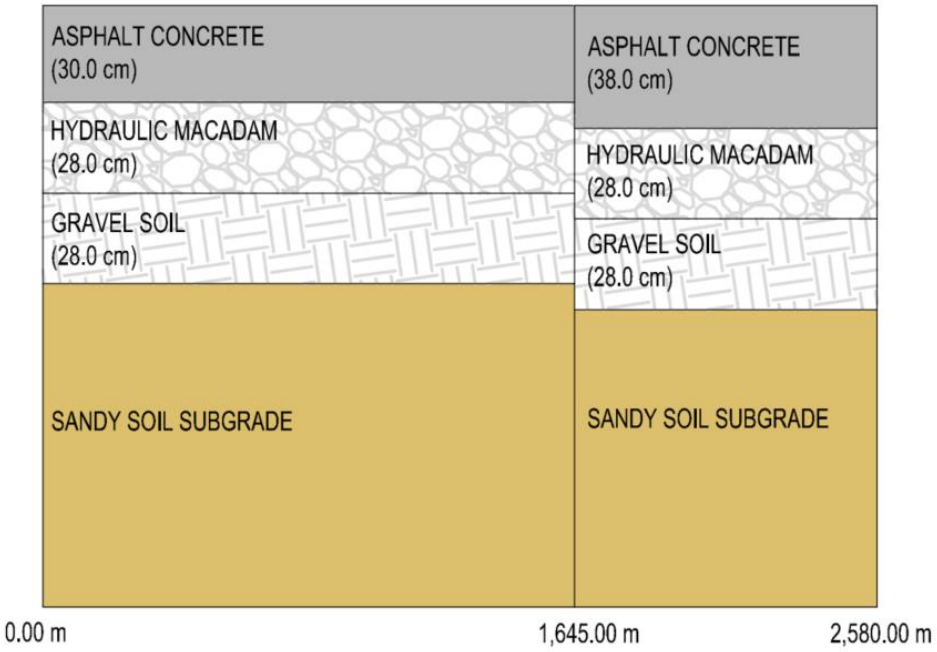

Source: THE AUTHOR.

Figure 7 – Airport B runway's pavement structure

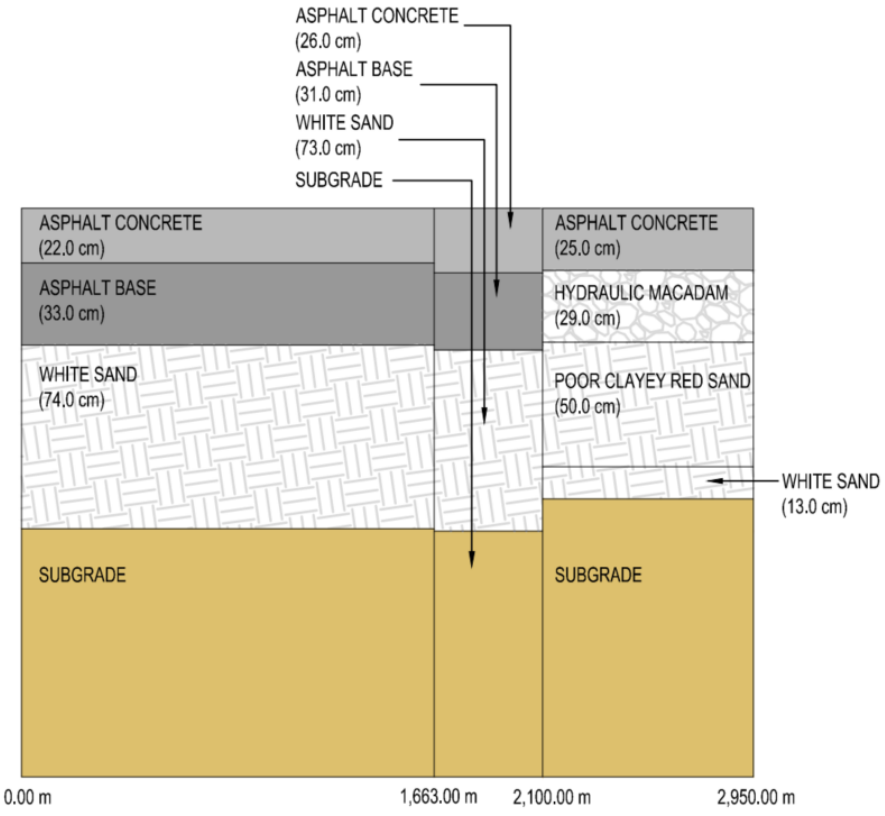

Source: THE AUTHOR.

The runway of Airport C has 2,680m in length and 45m in width. The structural layers are compounded of 8.0cm of AC to the wearing course, 20.0cm of macadam to the base, and 25.0cm of yellow sandy clay to the sub-base. The structure is constructed on a subgrade which presents 24% of CBR. Figure 8 schematizes the Airport C runway's structure. The layer thicknesses were obtained by coring and drilling.

Figure 8 – Airport C runway's pavement structure

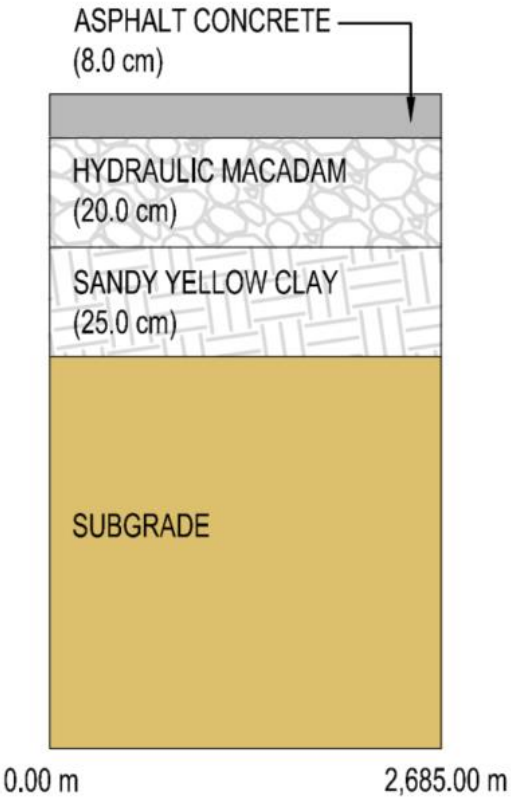

Source: THE AUTHOR.

For the FWD and HWD tests, the structures were evaluated by adopting target loads of 80kN, 200kN, and 280kN applied using a 45cm-diameter load plate. The tests were performed in the offsets +3.0m, -3.0m, +6.0m, and -6.0m distant from the runway's axis, with the additional survey of the runway axis line for airports A and C. These values of applied load and offsets are conventional values used in this type of evaluation, representing the characteristics of the majority of aircraft models operating in airports nowadays. The deflections generated were captured by 9 geophones that can be positioned at distances of 0mm, 200mm, 300mm, 450mm, 600mm, 900mm, 1200mm, 1500mm, 1800mm, and 2100mm far from the center of the load plate. Table 4 presents the combination of the geophones spacing

for the three airports studied. The time pulse simulated was equal to 0.25ms. Figure 9 and Figure 10 depicture the FWD and HWD devices.

Figure 9 – The system of load application of FWD and HWD devices

Source: THE AUTHOR.

Figure 10 – Sensors used to measure the deflection basin and the plate load of FWD and HWD devices

Source: THE AUTHOR.

Table 4 – Test configuration for the airports studied

Variable		Airport A	Airport B	Airport C
Number of drops	80kN	1	1	2
	200kN	2	3	2
	280kN	2	0	1
Sensors' spacings (mm)	D_0	0	0	0
	D_1	200	200	300
	D_2	300	300	450
	D_3	450	450	600
	D_4	600	600	900
	D_5	900	900	1200
	D_6	1200	1200	1500
	D_7	1500	1500	1800
	D_8	1800	1800	2100
Surveyed offsets		±3.0m; ±6.0m; axis	±3.0m; ±6.0m	±3.0m; ±6.0m; axis

Source: THE AUTHOR.

The data were collected by a single device adaptable to impart both FWD and HWD loads with the test points spaced from 10m to 25m. The device was positioned once on each point, and the different loads were imparted quickly and without moving the equipment to guarantee that the same points were being evaluated with the different load magnitudes. All the tests were performed during the nighttime. Table 4 summarizes the test configuration for each airport studied. The differences in the sensor's spacing observed for Airport C are caused by the configuration of the device available for testing.

3.2 Data correction

Due to the variation in the loads effectively applied during the deflection measurement process, the deflections must be corrected to a normal load. Considering the tire pressure and tire contact area of the main commercial and cargo aircraft of the studied airports studied' mixes (five models are responsible for 80% of the annual departures, approximately), the 200kN wheel load was defined as the normal load to be used in the deflection normalization. This normalization must be performed just in case of analysis comparing deflection values.

In the case of calculating the resilient modulus of the materials, the deflections should not be corrected before the back-calculating process. To resilient modulus, just a temperature correction must be performed, adopting the method proposed by Chen *et al.* (2000), whose model is presented in Equation 6

$$E_{25°C} = \frac{E_T T^{2.81}}{185000} \quad (6)$$

The deflections, when used in analyses of maximum deflection (D_0) or Impulse Stiffness Modulus (ISM), must be temperature-corrected too. This correction must be performed by using the model presented in Equation 4, proposed by Chen *et al.* (2000). All the corrections, of D_0 deflections and back-calculated moduli, must be performed considering the standard temperature of 25°C. The used correction relations were selected because of their ability to adjust the temperatures to the standard 25°C.

$$D_{0,Tr} = D_{0,T}\left(\frac{1.0823^{-0.0098t}}{0.8631}\, T_r^{0.8316} T^{-0.8419}\right) \quad (4)$$

3.3 Data organization

The organization of the data consisted in identifying and removing outliers of D_0 and measurements that produced a deflection basin with anomalies. This organization process was conducted separately for the data set of each surveyed offset. In the case of identifying a D_0 outlier value, the entire deflection basins (all the 9 deflectometers' measurements in the corresponding point), for all the different drop forces applied in the point, were removed from the data set of that line being evaluated. The same must be done when a deflection basin with an anomaly is identified.

To classify a datum as an outlier the definition presented by Devore (2005) was used. It specifies as an upper limit to accept a value the sum between the third quartile plus the interquartile fraction (interquartile fraction is the difference between the third quartile minus the first quartile). As lower limit is defined the difference between the first quartile minus the interquartile fraction. Values out of this interval are outliers and must not be considered in the analysis. The following relation represents the interval of usable data, which are not outliers.

$$Q_1 - 1{,}5FI \geq usable\ data \geq Q_3 + 1{,}5FI$$

Where:

Q_1 = first quartile;

Q_3 = third quartile;

FI = interquartile fraction.

Anomalies in deflection basins were identified using automated spreadsheets to apply the errors' definitions established by FAA (FEDERAL AVIATION ADMINISTRATION, 2011). Among the three types of errors that are defined, errors type one and three were chosen to be removed from the data sets. Error type two was not investigated since its definition is not presented in detail in the reference document. The three types of anomalous deflection basins are following described.

- Type 1 anomalous deflection basin: basins presenting any of the deflections greater than the deflection under the load plate;
- Type 2 anomalous deflection basin: basins presenting unusually large decrease in deflection between two adjacent sensors;
- Type 3 anomalous deflection basin: basins presenting the deflection of an outermost sensor of two adjacent sensors greater than the deflection at the sensor that is closer to the load plate.

Outlier data were not removed simultaneously for all analysis performed. The observation of an outlier can occur due to failures in the testing device or to structural deficiency at the tested point. For investigations comparing deflections, the presence of outliers could prejudice the analyzes so all deflection basins containing D_0 outliers were removed in case of analyzing deflections, radius of curvature, and impulse stiffness modulus.

The D_0 outlier combined with the rest of the deflections of the deflection basin, in the moduli's back-calculation process, can be useful in understanding and considering the effect the load variation can present on the structural response of structurally damaged points. Considering this, the basins with D_0 outliers were not removed in the back-calculation process.

3.4 Parameter's calculation

Among the existent parameters that can be obtained by using deflection values, the ISM and the RoC were the chosen index to be used in the analysis of the present research. ISM should be calculated for each point and each drop of each applied load. This calculation must proceed as indicated in the following equations (FEDERAL AVIATION ADMINISTRATION, 2011; HORAK; EMERY, 2006).

$$ISM=\frac{F}{D_0}$$

$$RoC=\frac{L^2}{2D_0(D_0/D_{200})-1}$$

In the ISM calculation process, the D_0 deflection must be previously corrected because of the temperature variations. This correction must follow the instructions presented in section 3.2. The ISM calculation occurs after the data organizing step; hence the results will already be free of outliers. The process of removing anomalous values does not need to be executed.

3.5 Moduli calculation

The properties of the material layers were obtained by the back-calculation process. The FAA's software BAKFAA 3.3.0 was employed in calculating the resilient modulus of each layer material. This process requires the definition of seed values from which the software begins the iterative process of calculating the moduli. Seed values were defined for all layers because in the processes of back-calculation all the layers were free to have their moduli changed (including the subgrade). To represent the material encountered in the structure of the three airports studied the values suggested by the software to the type of material present in each case were adopted. The values are presented in Table 5.

Table 5 - Seed values of resilient moduli to starting back-calculating process

In situ material	Equivalent software material	Seed value (MPa)
Asphalt concrete	P-401-P-403 Surface	1,375
Asphaltic base material	P-401/P-403 Base	2,755
Macadam Hydraulic Macadam	P-208	515
Gravel soil Clayey sand Sandy clay	P-154	275
Subgrade soil	High Strength Subgrade	140

Source: FEDERAL AVIATION ADMINISTRATION, 2011. Adapted by the Author.

The information presented in Table 5 is conventionally used in the practice of structural evaluation, and the values were defined considering the United States' available

materials. Despite being commonly used in Brazil, these values do not accurately represent the characteristics of some construction materials used in Brazilian pavement structures. This is a limitation of the structural evaluation processes adopted to assess Brazilian airport pavements.

Since the FWD and HWD tests are performed under variable conditions of temperature, the modulus obtained for the asphaltic layers must be corrected for a reference temperature. In the case of Brazilian pavements, the standard temperature used is 25°C. To perform this correction, the correction model presented in Equation 6 must be employed.

Because the data used to back-calculate the moduli are free of anomalous basins only, an examination for identifying outliers must be performed. The adopted criteria to consider a datum an outlier must be the same as presented in section 3.3, where is described the process of removing D_0 outlier values.

3.6 Statistic tests

Aiming to obtain reliable conclusions from the data analysis, statistical tests were performed. Two tests were selected, according to the characteristics the data presents. It was necessary to analyze the data by its variance to verify if it is aleatory or if it presents a pattern. Aleatory variance indicates no influence of the analyzed variable on the results, but if any pattern is identified, there is a dependence on the results. In the case of existing dependence, another test should be applied to quantify this influence.

There are two premises these types of tests require so that they can be properly applied to a data set. They are related to the normality in the data distribution and the data pairing. A test for this type of data distribution must be used if the data studied do not follow a normal distribution. And about data pairing, since the results studied were obtained by applying different loads at the same points of the pavement, there is a pairing between deflections measured at the same point.

The statistic tests were performed using the software RStudio v.4.2.1, a free statistical analysis software that works using the R computer programming language. All the following described tests and their respective p-values are respected for their use in the RStudio. The statistical tests that will be described are hypothesis tests. All the tests performed adopted the 5% of significance or confidence of 95%.

In the data analysis process, the results generated by two distinct loads are compared by subtraction. As a standard process, the result of a higher load is subtracted from the results of a lighter load (lighter load's D_0 minus higher load's D_0, lighter load's ISM minus higher

load's ISM, lighter load's moduli minus higher load's moduli). Thus, negative variation values indicate values larger for higher applied loads.

The normal distribution of the data was verified by the application of the Shapiro-Wilk test. In the cases of airports evaluated with three different loads, the Shapiro-Wilk Test verified the normality in the distribution of the data referred to each load. In the cases of being compared to the results generated by the application of only two loads, the Shapiro-Wilk Test verified the normality of the distribution of the differences obtained by the subtraction between the results of these two loads.

The null hypothesis of the Shapiro-Wilk Test is the existence of normal distribution in the analyzed data, whilst the alternative hypothesis says that the data do not follow a normal distribution. The null hypothesis is not rejected when the p-value of the Shapiro-Wilk Test is higher than 0.05. If the p-value is equal to or less than 0.05, the null hypothesis is rejected, meaning that the data do not follow a normal distribution.

If the data studied do not follow a normal distribution, non-parametric tests must be used in the analyses. In the cases of three loads applied in the data collection, the Friedman Test must be used. Its null hypothesis admits the equality of the median for the different loads of each data set compared, whilst the alternative hypothesis says the medians are different. The null hypothesis is rejected when the p-value of the test is equal to or less than 0.05.

If the null hypothesis is rejected, it means that there is at least one pair of data sets whose medians are different from each other. In these cases, a post hoc test should be performed to verify the groups presenting differences. The Dunn Test with the adjustment of the p-value by using the Bonferroni Method (called Dunn-Bonferroni) should be the test performed in this verification. The adjusted p-value equal to or less than 0.05 is indicative that there is some difference between the two tested groups.

For airports A and C, which have data of three distinct loads, initially was applied the Friedman Test and in the cases the null hypothesis was rejected the Dunn-Bonferroni post-hot was performed. For Airport B, which presents data of two loads only, just the Dunn-Bonferroni Test was applied.

3.7 Data analyzes

The process of analyzing the data was conducted in the way to turning possible to be identified the existence of the influence of the applied load on the structural behavior of the pavement, as well as of quantifying this influence on the pavement response, in case it exists.

Four distinct analyzes were performed, all of them being comparative analyzes of the values of raw deflections, normalized deflections, radius of curvature, ISM, and back-calculated material moduli.

The first analysis used the normalized D_0 deflections. For each test point, the D_0 deflection obtained by the application of the different loads was compared after the process of normalization. The distinct loads were combined in pairs for comparison, and the variations between the results of each of these pairs were registered. As an exemplification, for the airports tested with three loads, the pairs for comparison were 80kN-200kN, 80kN-280kN, and 200kN-280kN.

Each test point has a value of variation respecting each load pair. These values were grouped (i) by load, (ii) by surveyed offset, (iii) by type of structure composition, and (iii) by the airport studied, and the comparisons were performed after these aggregations. After the aggregation of the data, statistical tests were performed so that the existence of the influence of each variable on the results can be reliably confirmed or refuted.

The second analysis was conducted using ISM values, aiming to support any conclusion the D_0 analysis had generated, confirming it or denying it, by verifying the stiffness of the structures. The ISM analyses were performed by aggregating the ISM values by the same aggregative variables adopted in the D_0 analyses, and the statistical tests used were also the same.

The third analysis was conducted using the same methodology adopted in the two formers, changing the parameter studied by the use of the back-calculated layer material moduli. This analysis is a little bit different from the two previously performed investigations because since the material moduli was obtained particularly for each layer, the load influence on the pavement response can be verified by the change in moduli values of each layer.

The fourth and last analysis was conducted by comparing ISM and back-calculated moduli. The same methodology of the previous three analyses was adopted. This last analysis aims to validate the ISM results' behavior by comparing the behavior of the material moduli for the same pavement section studied.

4 RESULTS AND DISCUSSION

The results were obtained by using information from 1692 test points. Information was collected from 1826 test points, but the data from 134 of these points were suppressed because of the presence of outliers. These numbers refer to the sum of the total points, tested and effectively used in the analysis, for the three airports studied.

After data organization, the first step in the statistical analysis was conducted, which was the verification of the distribution the data present. The Shapiro-Wilk Tests constated that the deflection data, and all the other data obtained from using the deflections, do not follow a normal distribution. Because that, the non-parametric statistical tests were performed. The lack of normality in the data distribution was also the reason for using median in most of the analyzes presented instead of using the average. It was because the median is the parameter that better represents the central tendency of the data sets. Thus, when generalizations about the behavior of the parameter/structure are presented, they are related to the analysis of the median values observed.

Considering the existence of different parameters that can reflect the structural pavement response, this section will present the results and discuss the findings by analyzing four parameters: deflections, Radius of Curvature (RC), Impulse Stiffness Modulus (ISM), and Resilient Modulus (RM). For the airports presenting more than one structural pavement section, the analyzes of the parameters were performed considering the entire runways' data, without using separately the parameters calculated for distinct structural section.

4.1 Effects of repeatedly loading pavements

Considering the methods the present study adopted for evaluating the pavement structures, with a successive application of loads at the same point, the verification of how the structures behave under this type of solicitation is important as a tool to identify some possible influence of the method on the results. Airport A has the application of two consecutive loads of 80kN followed by two other consecutive loadings with 200kN. Airport B has three consecutive 200kN-loadings, and Airport C has three consecutive applications of 80kN-loads.

The main trend observed when the results for consecutive loadings are compared is the reduction in the measured deflections. For the data of all three airports, reduction in the deflections measured by all the sensors were verified in 57.8% of cases. To avoid the influence the variation in effectively applied load has on the raw deflection, normalized deflections were

compared. Individually for each airport, Airport A, Airport B, and Airport C presented a reduction in normalized deflections of consecutive applications of repeated loads in 45.1%, 69.4%, and 66.0% of cases, respectively.

A hypothesis that possibly could explain these observations is that some material of the structure suffers a transient stiffening with the prior loadings. The lack of time between one load application and the next one (that is just a few seconds) could not be sufficient to permit the structure to returns to its normal state, leading the latter load applications to produce smaller deflections. The amount of normalized deflections that present a decrease between two consecutive applications of repeated loads is depictured in Figure 11 for help to understand how the distinct layers behave under these loading repetitions.

Figure 11 – Percentage of normalized deflections decreasing between two consecutive applications of repeated loads (All airports)

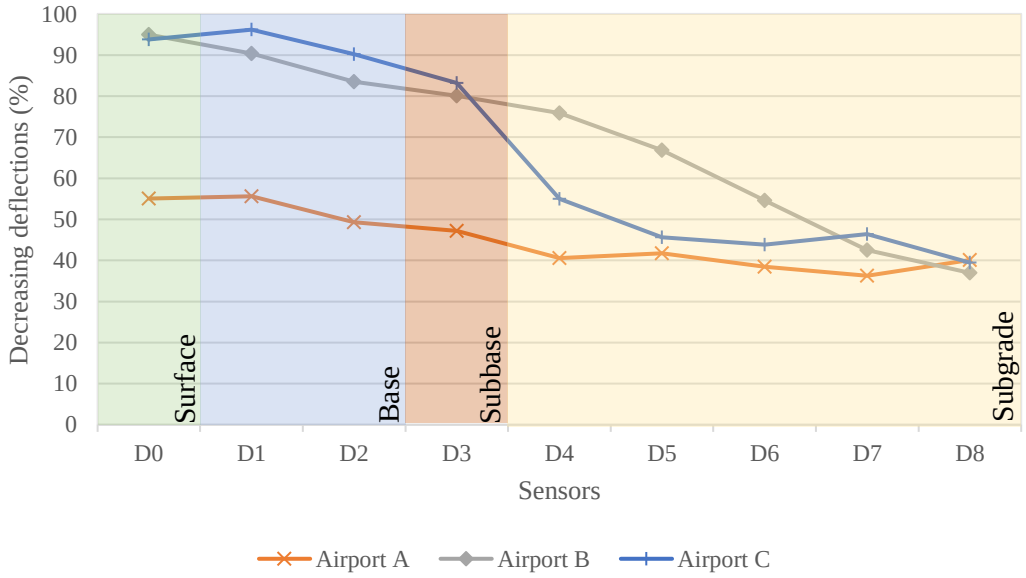

Source: THE AUTHOR.

The shape of the curves presented in Figure 11 for the three airports suggests the three upper layers of the structures are those most affected by the repetition of loadings. In the graph, the amount of deflections decreasing between two consecutive loads is remarkable from D_0 to D_3, with the percentages gradually decreasing from one sensor to another. From D_4 to D_8 the percentages keep gradually decreasing, but in a softer trend. For Airport A, the percentages presented have a considerably different behavior for the first sensors. It could be due to specific structural conditions for this airport when compared to the other two airports studied in terms of upper layers' thicknesses and materials.

This behavior could be an indicative that the shallower a layer is, the stronger is the effect of the consecutive loadings in stiffening the materials. The load dissipation grows up when the depth increases so that at deeper points the load mobilizing the structure is lower which leads to a smaller stiffening of the layer material. This explains the higher percentages observed for those sensors measuring the contribution of the upper layers.

For Airport C, three consecutive loads of 80kN were applied. The results turn possible to verify how the effect of transient stiffening occurs as new repetitions of loading are performed. Figure 12 depictures the percentages of normalized deflections that present lower values from the first to a second application of an 80kN-load, and also the amount of deflections that present a reduction in the normalized deflection values from the second to the third 80kN-load application.

Figure 12 – Percentage of normalized deflections decreasing between two consecutive applications of 80kN-loads (Airport C)

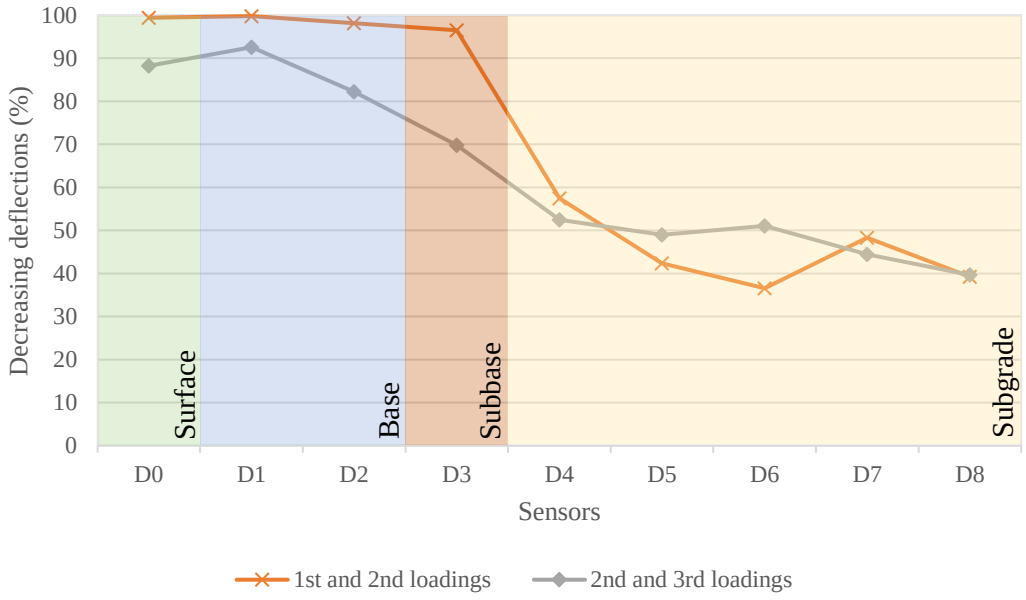

Source: THE AUTHOR.

The shapes of the curves presented in Figure 12 are naturally similar to those of Figure 11, with the highest percentages for the sensors D_0 to D_3. But it is possible to verify that there is a difference between the behavior of the stiffening from the first to the second load applications (first comparison) and that presented by the second to the third loadings (second comparison). In that zone of the structure more susceptible to the transient stiffening effect (the upper layers), the first comparison generates more decreasing deflections than the second comparison.

This could be due to the fact the structure has no stiffening at the first loading, so the deflection will be higher than if any consolidation existed, as the case of the second loading. From the second to the third loadings a considerable effect of stiffening is already present in the structure, so the deflections not necessarily will reduce. Depending on the structural condition at the tested point, from the second to the third loadings the behavior of the deflection could varies, reason why the lesser percentage is noticed for the second comparison. Similar behavior is verified when heavier loads are applied. Airport B had three consecutive applications of 200kN-loads. For this structure the same trend was observed, as can be verified in Figure 13.

Figure 13 – Percentage of normalized deflections decreasing between two consecutive applications of 200kN-loads (Airport B)

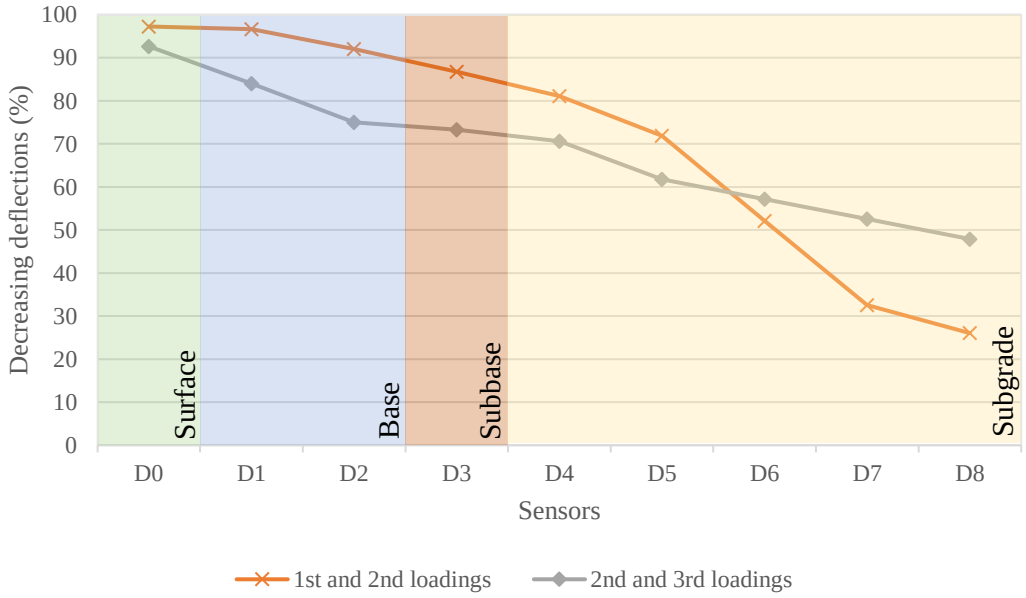

Source: THE AUTHOR.

The comparison of the graphs of Figure 12 ad Figure 13 could produce some understanding of how the distinct loads intensity influences the stiffening of the pavement structure, but effects directly linked to the structural arrangement of the pavements could lead to wrong interpretations. The analysis of the results for Airport A could be suitable to perform this analysis. Airport A had the consecutive application of two 80kN-loads followed by two loadings with 200kN-loads. Figure 14 depictures the graphs of the normalized deflections for each of these cases of load application.

Figure 14 – Percentage of normalized deflections decreasing between two consecutive applications of repeated 80kN- and 200kN-loads (Airport A)

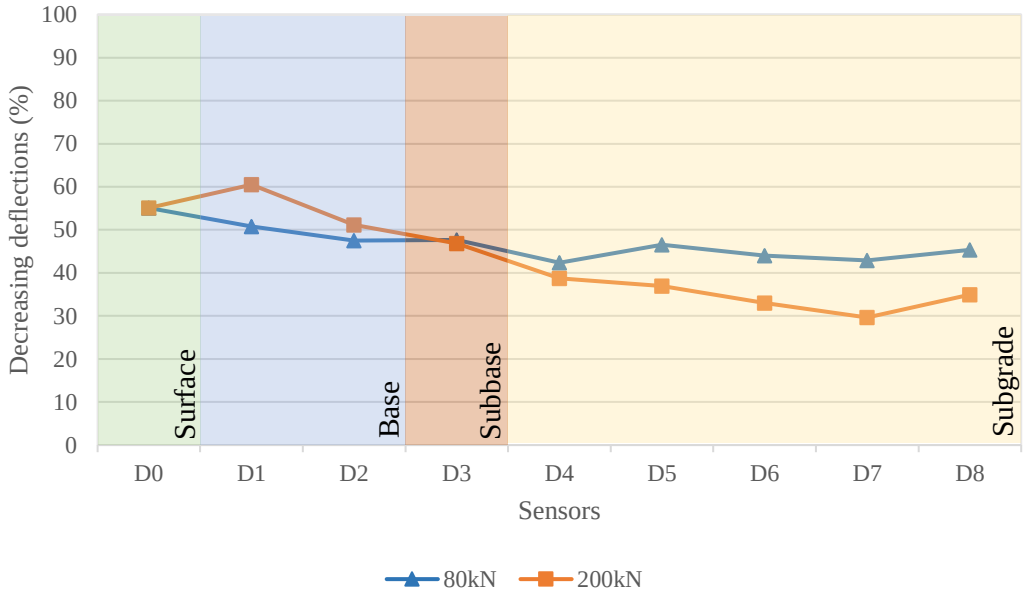

Source: THE AUTHOR.

The lines of the graph in Figure 14 show the percentages for the 200kN-load are higher than those for the 80kN-load for the initial sensors (D_0 to D_3) but without considerable differences. This behavior could be explained by the fact the structure subjected to a load higher than the initial ones presents incremental stiffening, suffering the same previously presented effects on the deflections for new loadings. A higher load mobilizes the structure, a higher deflection is measured, and the structure presents more stiffening. When a second application of this higher load is performed the structure is already stiffened for that load level, and the measured deflection is lower.

This effect, however, does not seem to occur for the subgrade material, where the number of deflections decreasing when comparing two consecutive applications of the 200kN-loads is lower than for the loadings with 80kN. The soil of the subgrade, which has different behavior compared to the asphalt and granular materials of the other layers, could not have the capability of present considerable incremental stiffening for new applications of higher loads, so that the behavior of the new measured deflections could vary instead of following the trend of decrease.

4.2 Deflections

The influence of the load on deflection results is intuitive and well-known. The expected behavior of the pavement deflection is that its values increase by increasing the applied load. In practice, it is exactly what happens. From the data studied, the deflection increased with the load in all the tested points.

For Airport A, when the applied load increased from 80kN to 200kN (a 150% increase), the measured deflections increased 175%, whilst when increasing from 80kN to 280kN (corresponding to a 293% increase in the applied load), the deflections were 249% larger. An increase of 40% in the load (200kN to 280kN) leads to an increase of 43% in the deflection values. Figure 15 depictures the behavior of all the deflections along the bowl when different loads are applied for Airport A.

Airport B has just one variation of load, from 80kN to 200kN. The median value of the increase in the deflection for this airport is 148%. The graph of Figure 16 depictures the deflection basin constructed with the median values of deflection for each sensor.

Airport C presented the same behavior, but with some divergence in the percentual values of variation, possibly observed because of the influence of the different composition of the structures that Airport A and Airport C have. When the applied load increased from 80kN to 200kN, the measured deflections increased 138% for Airport C. When increasing from 80kN to 280kN (293% load increase), the deflections were 234% larger. An increase of 40% in the load (200kN to 280kN) leads to an increase of 40% in the deflection values. Figure 17 depictures the behavior of all the deflections along the bowl when different loads are applied for Airport C.

Figure 15 – Increase in the deflection by increasing applied load (Airport A)

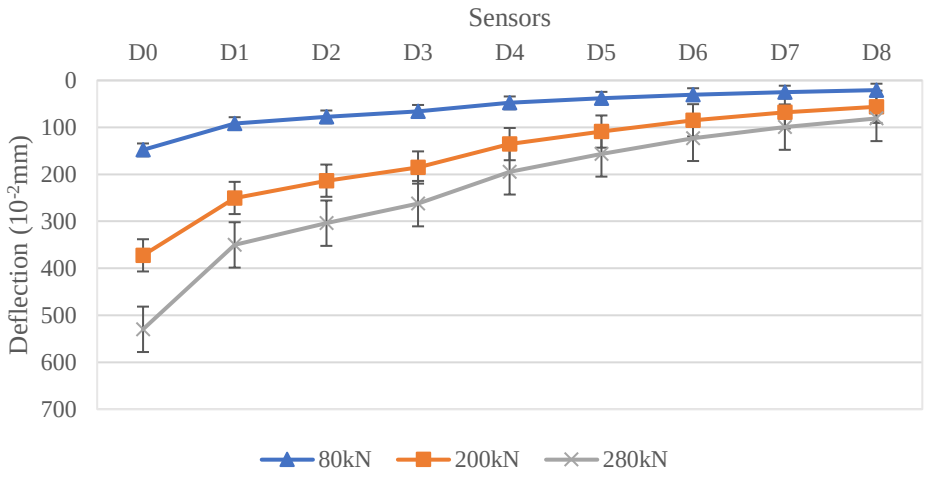

Source: THE AUTHOR.

Figure 16 – Increase in the deflection by increasing applied load (Airport B)

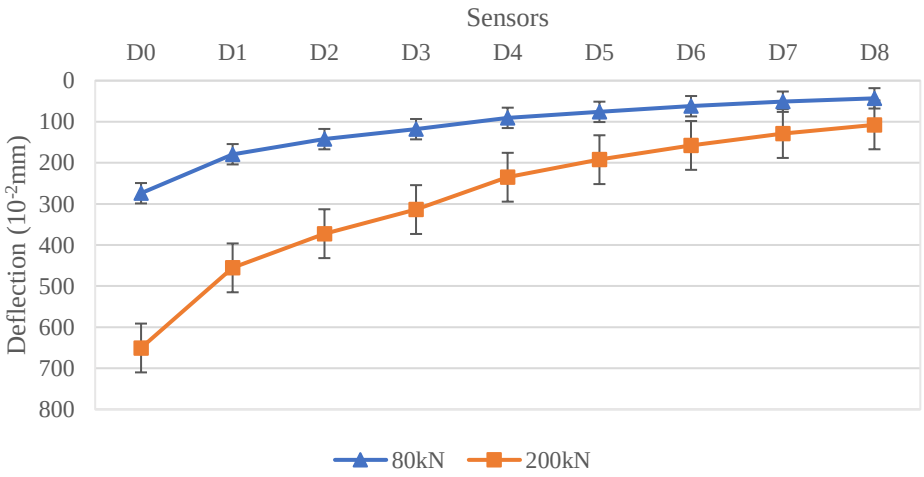

Source: THE AUTHOR.

Figure 17 – Increase in the deflection by increasing applied load (Airport C)

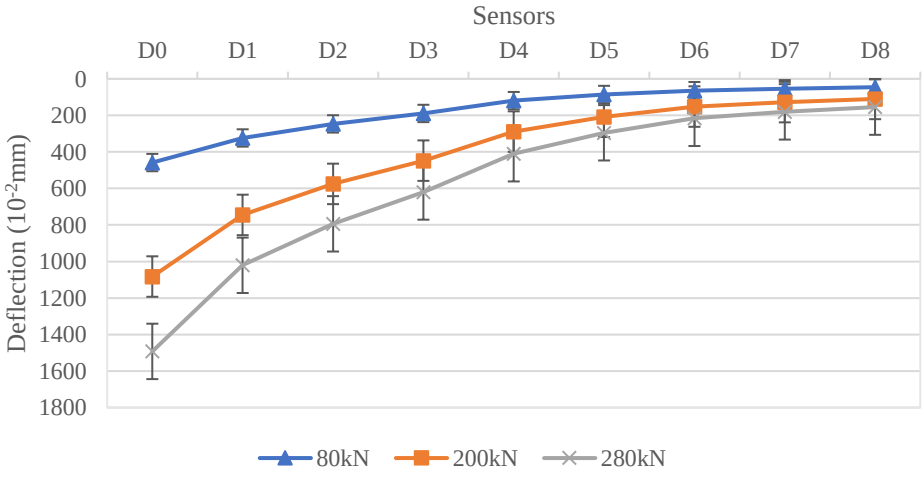

Source: THE AUTHOR.

Referring to the maximum deflection, D_0, it would be expected to be the deflection most significantly influenced by the changes in the applied load since it is the sensor positioned under the load application point, which measures the load impact with the minimum effect of load distribution. Comparing the deflection values (Figure 18), however, it is possible to verify that the number of points in which D_0 was the sensor presenting the lowest percentual variation (the least influenced sensor) in deflections measured for different loads is 45% bigger than the number of times in which D_0 was the most affected.

Figure 18 – Sensors' measurements being rated as most and least affected by load variation (all airports)

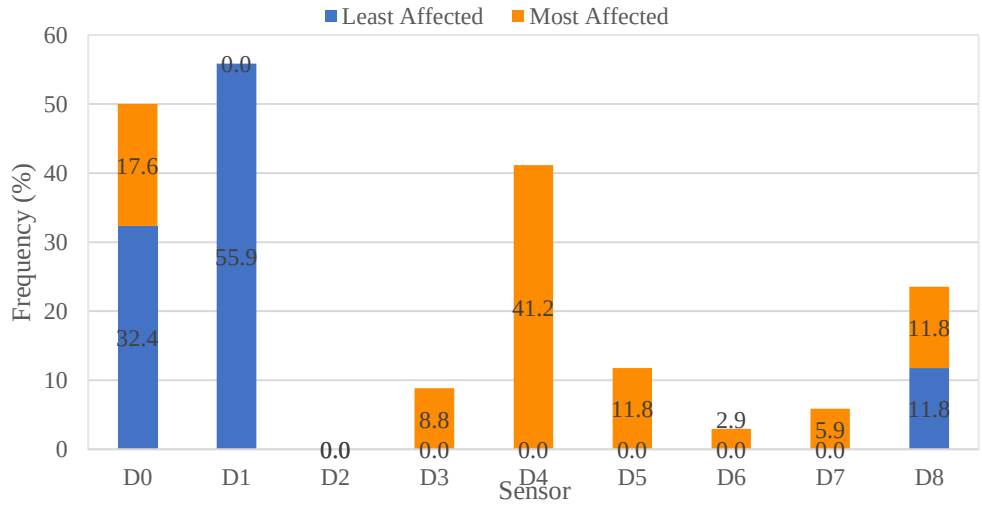

Source: THE AUTHOR.

To build the graph presented in Figure 18, each deflection bowl had its sensors' measurements ranked from the least to the most affected by the load variation; 9 sensors, 9 positions in the rank. Figure 18 suppresses the intermediate ranks and shows only the extreme positions: most and least influenced sensor/deflection. It is possible to see that the two first sensors tend towards being less affected by the load. The analysis of the intermediate ranks confirms (Table 6) this behavior. The rates 5 to 9 for the sensors D_3 to D_9 represents more than 50% of the evaluations. The 1-9 scale rates the sensor by its susceptibility in changing its measurement when the applied load varies, so 1 is the least affected (lowest susceptibility) and 9 is the most affected (highest susceptibility) sensor in the same deflection bowl.

Table 6 – Classification of sensor's measurements according to susceptibility to load variation – percentual frequency (all airports)

Rank	D_0 (%)	D_1 (%)	D_2 (%)	D_3 (%)	D_4 (%)	D_5 (%)	D_6 (%)	D_7 (%)	D_8 (%)
1	32.4	55.9	0.0	0.0	0.0	0.0	0.0	0.0	11.8
2	8.8	23.5	44.1	0.0	0.0	0.0	0.0	14.7	8.8
3	20.6	2.9	20.6	14.7	0.0	0.0	17.6	11.8	11.8
4	5.9	11.8	11.8	26.5	11.8	0.0	5.9	14.7	11.8
5	0.0	5.9	8.8	26.5	2.9	5.9	14.7	20.6	14.7
6	8.8	0.0	5.9	8.8	2.9	23.5	23.5	23.5	2.9
7	2.9	0.0	8.8	5.9	5.9	32.4	32.4	0.0	11.8
8	2.9	0.0	0.0	8.8	35.3	26.5	2.9	8.8	14.7
9	17.6	0.0	0.0	8.8	41.2	11.8	2.9	5.9	11.8

Source: THE AUTHOR.

The farther the position of a sensor, the deeper the layer contributes to the deflection this sensor is measuring. Thus, if the farther sensors are the most influenced by the load variation, a first interpretation about how the layers are affected by the load variation can be made: the variation in the applied load has more influence in deeper layers of the pavement structure. This discussion will be further developed later.

The raw deflection results, as shown, can be used to conduct some investigations about the response of the pavement layers. In the case of trying to analyze the linearity in the pavement structural response, however, the observed patterns in deflections generated by different loads do not turn possible to take any conclusion about the matter. The use of results generated by different loads to accomplish this goal requires an equalization between the deflections so that a reasonable comparison can be performed. This equalization could be done by normalizing the deflections to the same load value for all the measurements performed.

If the structure's response to the applied load is linear, deflections obtained by different loads would be equal when linearly converted to the same load value. If it does not occur, the linearity of the structural response becomes to be questionable. To verify this behavior, all the deflections measured were normalized to a 200kN-load. Figure 19, Figure 20, and Figure 21 allow to compare the same deflections presented in Figure 15, Figure 16, and Figure 17, respectively, after the process of normalization.

Figure 19 – Comparison among normalized deflections (Airport A)

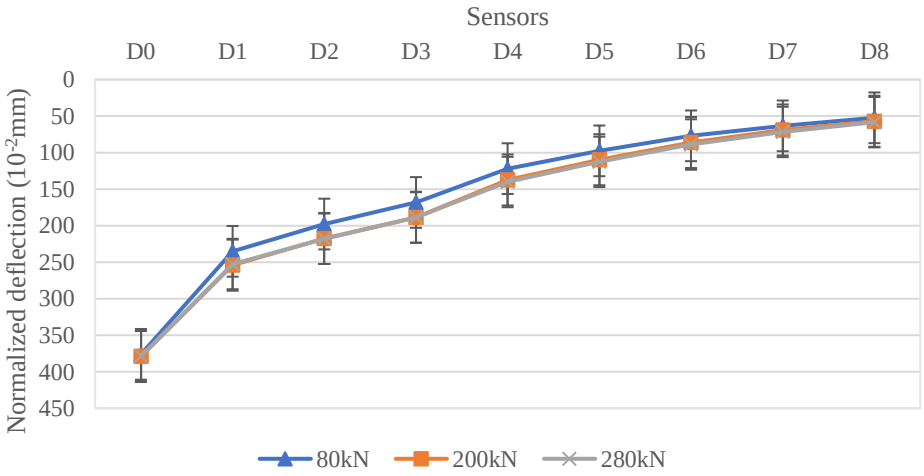

Source: THE AUTHOR.

Figure 20 – Comparison among normalized deflections (Airport B)

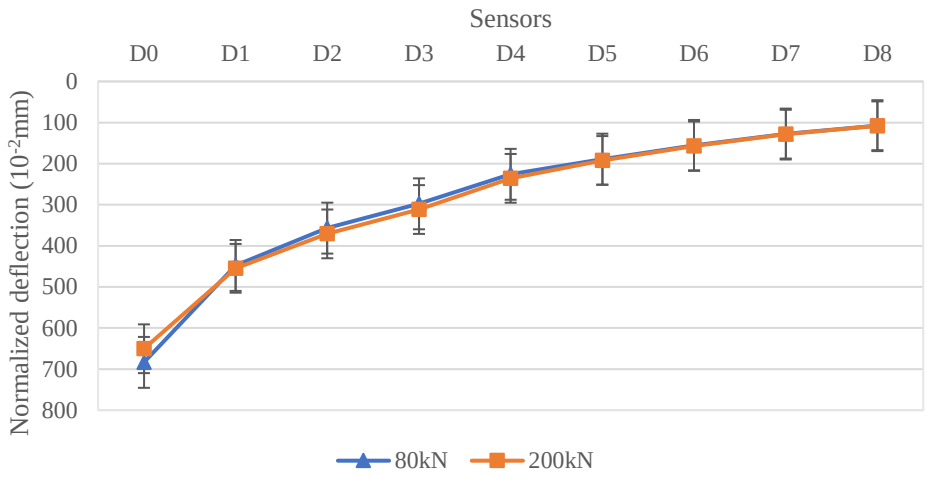

Source: THE AUTHOR.

Figure 21 – Comparison among normalized deflections (Airport C)

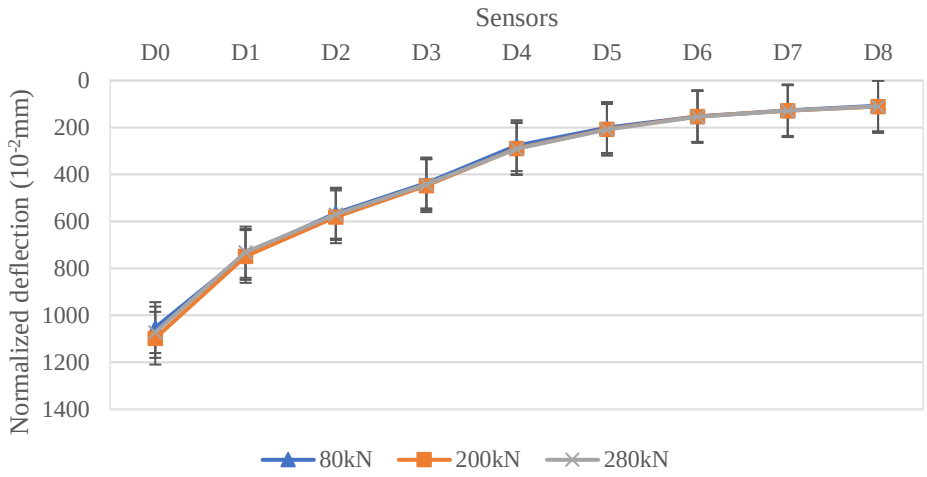

Source: THE AUTHOR.

Differently from the observed for the raw deflections, the distribution of the deflections in Figure 19, Figure 20, and Figure 21 are similar for all three loads. The lines of the graphs are overlapping, indicating that after normalization the deflections became quasi equal indicating the linear response of the structure. Only Airport A presented a noticeable difference between the 80kN-line and the other lines of the graph in Figure 19. Aiming to verify the significance of this difference and check the existence of load influence for the other airports not noticeable by the graphs the deflections measured by all the sensors for the three distinct

applied loads were compared and statistically tested, and the existence of difference among the results for different loads was confirmed.

Despite the normalization, all the combinations between deflections of different loads present statistically significant differences. Comparing the 80kN's deflections to the 200kN's, the median differences stay about 9.3% for Airport A, -1.5% for Airport B, and 3.3% for Airport C. Notice that for Airport B the value is negative. The normal load defined is 200kN, and Airport B has the application of just 80kN and 200kN loads. In the process of load application there are inaccuracies in the effectively applied load

When this comparison is performed between the 80kN's and 280kN's, this difference is about 10.8% for Airport B, and 3.4% for Airport C. Analyzing the graph pictured in Figure 19, it seems like the 200kN's and 280kN's normalized deflections do not present differences, but there is a statistically significant difference of about 1.2% for Airport A. For Airport C this value was 0.0%.

The values of these differences are small and could be considered induced by errors in the surveys or even by variability in the structure. Regarding to the repeatedly application of the same load in the surveys, the variability was high. For Airport A the Coefficient of Variation (CoV) for the difference observed between two consecutive 80kN-load applications was 590%, and 3.472% for the 200kN-load consecutive applications. For Airport B, the CoV for 200kN-load was 1.310%, and for Airport B, a CoV of 100% was observed for the 80kN-load consecutive applications. White and Beehag (2022) consider high variation for applied loads of FWD or HWD when CoV bigger than 30% is observed, which is a value lesser than the obtained for the two analyzed airports.

The hypothesis the small differences between normalized deflections are an initial indication of the non-linear structural response of the pavement cannot be disregarded since the statistical tests found a relation between load variation and results variation. Table 7 presents a summary of the statistics results obtained for the normalized deflections' analyses.

The numbers show that the difference in the results exists when using distinct loads, with the influence being greater as the load increases. It can also be noted that for heavier solicitations the influence is similar. When a light (80kN) and a heavy (200kN) are compared, the 120kN difference in the solicitation force leads to a 9.3% of variation in the results of Airport A, but when two heavy loads (200kN and 280kN) are used, the 80kN difference between the applied loads leads the deflections to change 1.2%. For Airport C, the variation

Table 7 – Summary statistic results for normalized deflections (all airports)

Loads compared		Airport A	Airport B	Airport C
80kN × 200kN	Median difference (%)	9.3	-1.5	3.3
	Average difference (%)	9.4	-1.3	3.9
	Standard deviation (%)	7.9	6.4	6.6
80kN × 280kN	Median difference (%)	10.8	-	3.4
	Average difference (%)	10.7	-	4.1
	Standard deviation (%)	11.7	-	8.4
200kN × 280kN	Median difference (%)	1.2	-	0.0
	Average difference (%)	1.6	-	0.0
	Standard deviation (%)	6.0	-	4.5

Source: THE AUTHOR.

reduces differences are reduced from 3.3% to 0.0%. The variability measured by the standard deviation also presents a reduction.

To illustrate the variation of the results, Figure 22, Figure 23, and Figure 24 present the distribution of the normalized deflections some classes of percentual difference. These differences are those observed when the deflections generated by different loads for respective sensors are compared. In the graphs, the amplitude of the classes was defined in such a way as to represent the maximum amount of data.

Figure 22 – Percentual changes in normalized deflection when load is varied (Airport A)

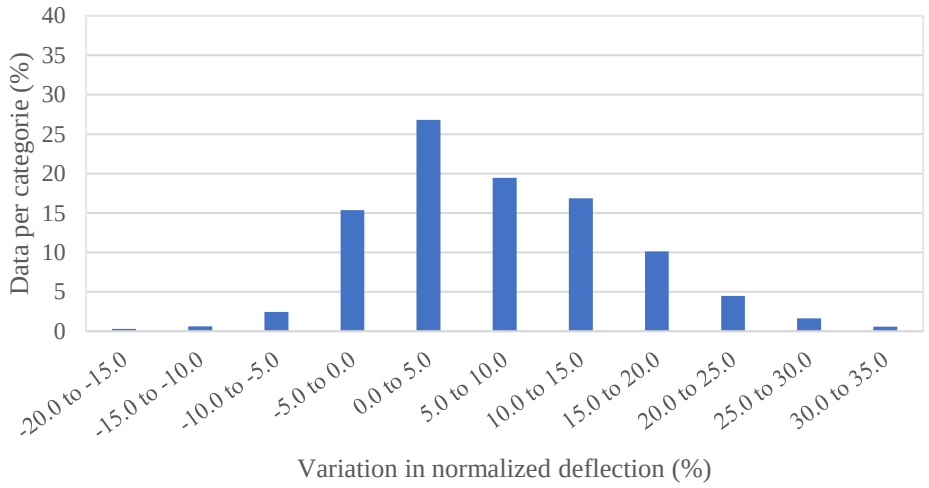

Source: THE AUTHOR.

Figure 23 – Percentual changes in normalized deflection when load is varied (Airport B)

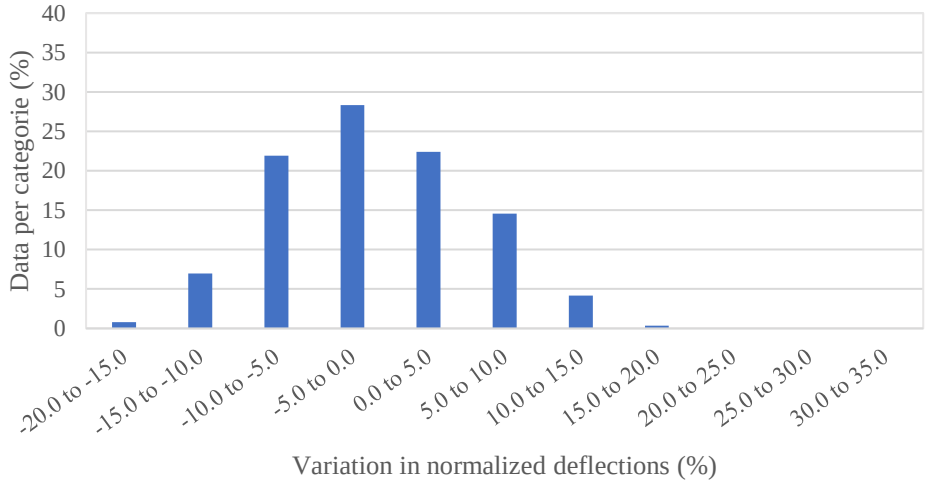

Source: THE AUTHOR.

Figure 24 – Percentual changes in normalized deflection when load is varied (Airport C)

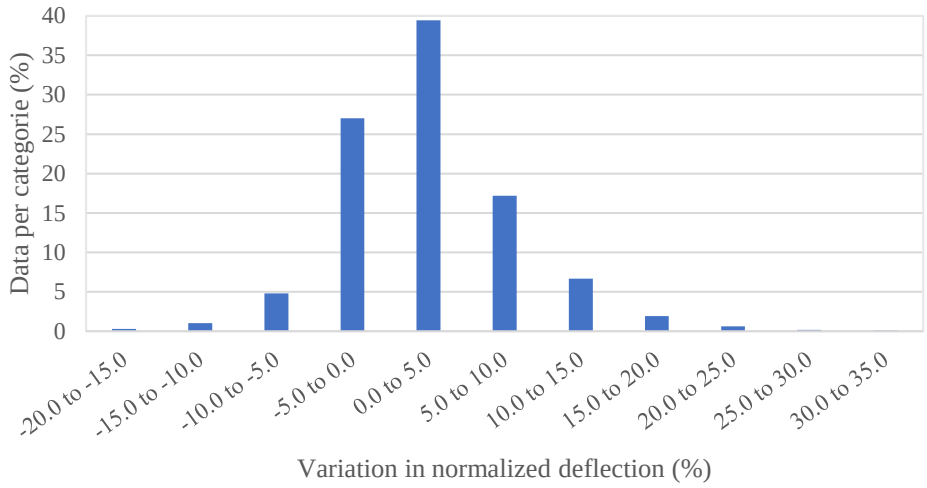

Source: THE AUTHOR.

The variability illustrated in Figure 22, Figure 23, and Figure 24 can be observed mainly due to the conditions that cannot be controlled. Aspects related to the load application and to the structure as its integrity, age, use, construction conditions, presence of distresses, maintenance interventions, layer's materials, and thicknesses, etc.

To visualize how the uncontrolled conditions influences the variability of the deflections, analyze at the bars of the graph from Figure 25, Figure 26, and Figure 27. In the graph, the differences among normalized deflections are presented for each sensor. Comparing the graphs for the three airports, they follow the same behavior, despite presenting considerable changes in their values of percentual difference.

Figure 25 shows that the biggest differences are observed for the intermediate sensors. The maximum deflection, D_0, is impacted differently depending on the airport and it can be mainly due to the dependency of the deflections on the structural materials and layer thicknesses, which differs from one structure studied to another. The structural conditions also lead deflections to be bigger (or smaller) when submitted to heavier or lighter loads, which causes bigger or smaller differences between two loads and makes the graph from Figure 25 to be different for each airport.

Figure 25 – Median percentual changes in normalized deflection by sensor (Airport A)

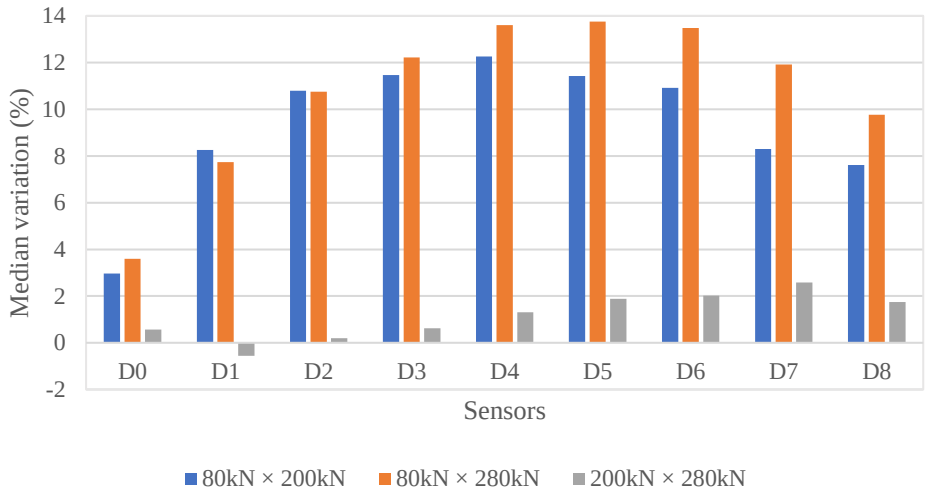

Source: THE AUTHOR.

Figure 26 – Median percentual changes in normalized deflection by sensor (Airport B)

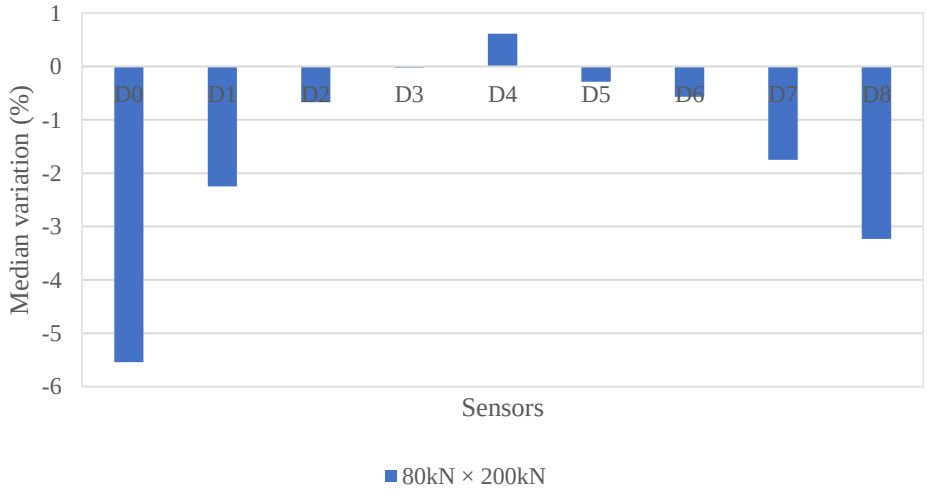

Source: THE AUTHOR.

Figure 27 – Median percentual changes in normalized deflection by sensor (Airport C)

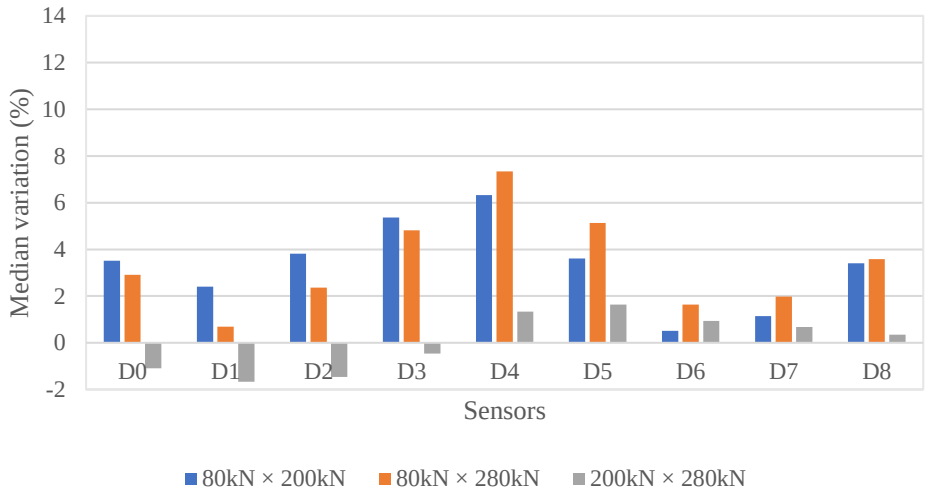

Source: THE AUTHOR.

Some sensors for Airport B and Airport C present a singular behavior. As shown in Figure 25 and in Figure 27, the bars of some sensors are in the negative part of the graph, which means negative differences. For negative difference, the deflection when applied to a heavier load must be smaller than that measured when applied to a lighter load. This behavior is not intuitive and could be due to some momentaneous/transient stiffening the materials suffer after being subjected to the first loadings. This effect was previously discussed.

Studying the percentual differences by comparing the loads, an interesting behavior can be observed. In general, the farther the sensor is from the load application point, the higher the difference between the deflections read by the sensor when different loads are applied. Figure 28, Figure 29, and Figure 30 present the comparison among normalized deflections generated by distinct loads.

Figure 28 – Measure of the difference between normalized deflections of different loads in each sensor (Airport A)

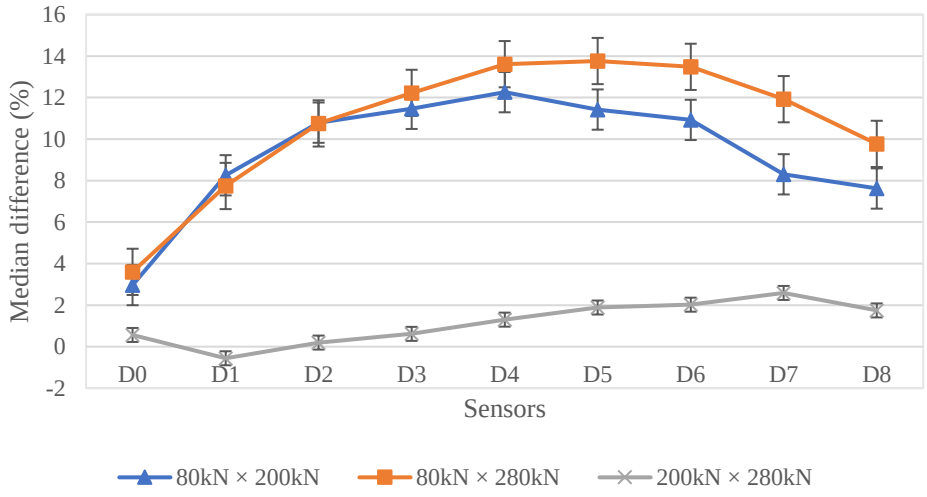

Source: THE AUTHOR.

Figure 29 – Measure of the difference between normalized deflections of different loads in each sensor (Airport B)

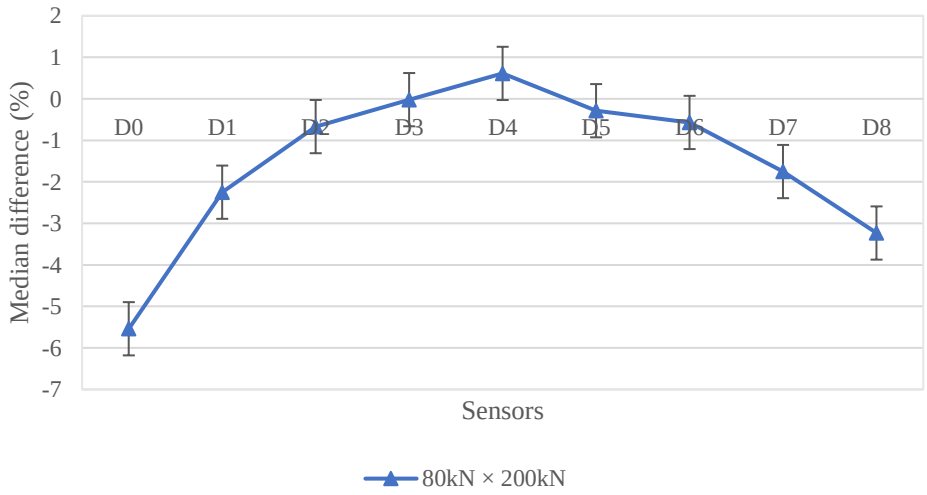

Source: THE AUTHOR.

Figure 30 – Measure of the difference between normalized deflections of different loads in each sensor (Airport C)

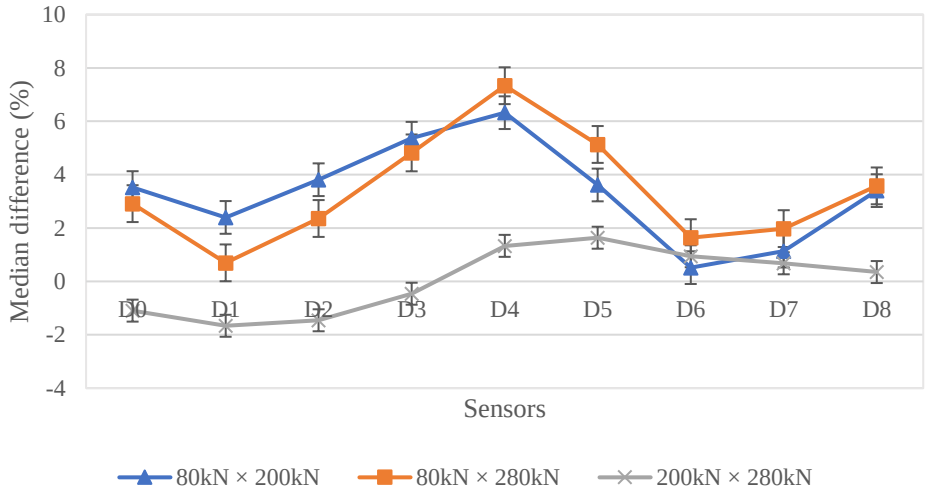

Source: THE AUTHOR.

The shape of the curves presented in Figure 28, Figure 29, and Figure 30 indicates an increase in the differences according to the sensors become further of the load application point, with maximum differences in the intermediate sensors. This behavior could be firstly explained by the depth the different loads mobilize the structural layers. Since there is the application of different loads in the same pavement structure, higher loads will perform a bigger mobilization of the structure until deeper depths on the pavement when compared to lower loads because of the size of the pressure bulbs created, and because of the load dissipation that occurs as the depth increases.

The pressure bulb created by the 80kN-load is smaller and reaches a swallower depth compared to those created by the 200kN- and 280kN-load when applied in the same structure. This way, as the sensors become more distant from the load application point, the structural response of deeper points of the structure is measured, and the mobilization of the deeper structural layers for the 80kN-load becomes less significant compared to the 200kN- and the 280kN-load, leading to the increases in the differences and in the ascendant shape of the graphs.

Evidence of this behavior can be seen when are analyzed the curves in Figure 28, Figure 29, and Figure 30 and is verified that the highest differences are observed in the comparison between the FWD 80kN-load and the HWD 280kN-load (which represents the biggest gap between applied loads), and the lowest differences are observed to the smallest gap of applied loads, represented by the comparison between the HWD loads of 200kN and 280kN.

From sensor D_4, the curves drop, which means a reduction in the differences between the results for different loads. These sensors correspond to those that measure the contribution of deeper layers' contribution, with great influence of subgrade. A drop in this part of the graphs could suggest some specific behavior related to the subgrade material, concerning its susceptibility to the applied load, when compared to the base and subbase materials.

The growth observed for the furthest sensor, D_8, can be related to the spreadability of the loads. When the depth increases, the spreadability increases as well, with higher loads presenting a more considerable effect than lower loads at the same distance from the load application point.

4.3 Radius of Curvature

Since the effect of the load variation on the deflections was verified, as presented in the previous subsection, the indexes that are calculated using these deflections should also suffer some influence. This subsection aims to understand how the change in the deflection values caused by the variation in the applied load leads to changes in the Radius of Curvature (RC), one of these indexes calculated using deflection information.

The way RC is calculated makes it to be inversely proportional to the used deflections (D_0 and D_1). So, if the deflection increases RC decreases, and vice versa. This fact is a first attention point to use RC in an analysis where the applied load varies. If the load varies, the raw deflections also will vary and, consequently, the RC values will change.

The worse the pavement condition, the higher the deflections so the smaller the RC calculated. The attention in varying the applied load in this type of analysis is that if the load increases the RC decreases. This decrease can be interpreted as indicative of worse conditions of the structure if RC values of distinct loads are compared.

Analyzing the RC results presenting statistically significative differences when different loads are applied, in addition to the effect of decreasing these index's values when the loads are increased was identified the tendency of the RC to present increase in its values. This unexpected behavior can be visualized in Figure 31 and Figure 32 for Airports A and C, respectively. RC was not calculated for Airport B because the second sensor for the measurements in this airport is positioned at 300mm far from the load application point. To calculate RC this distance must be equal to 200mm (HORAK AND EMERY, 2006).

Figure 31 – RC data categorized by presenting increasing and decreasing behavior (Airport A)

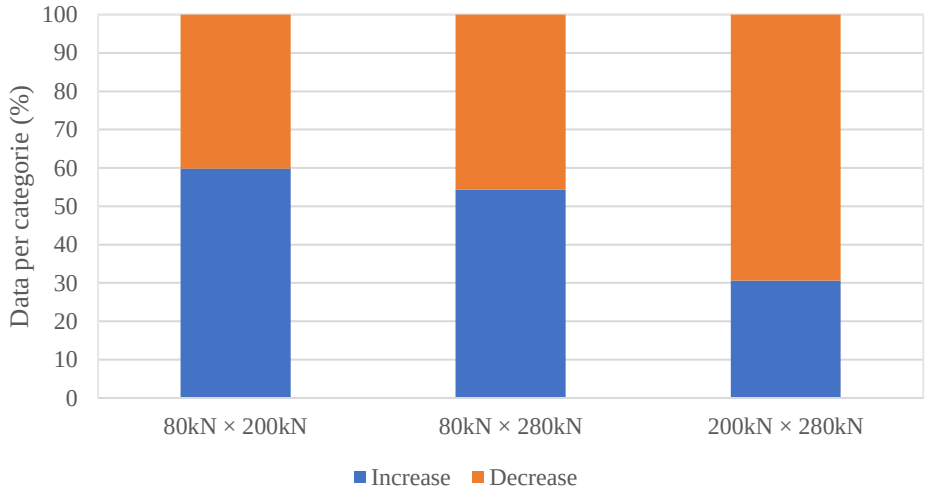

Source: THE AUTHOR.

Figure 32 – RC data categorized by presenting increasing and decreasing behavior (Airport C)

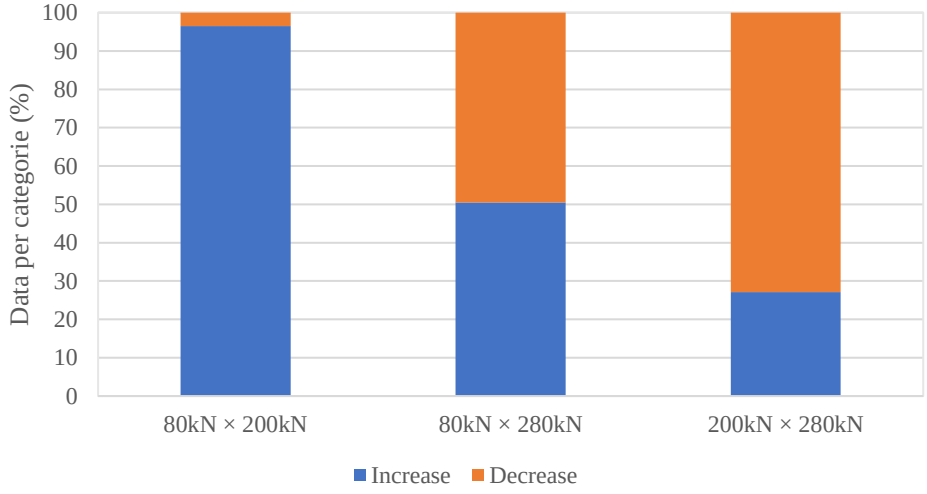

Source: THE AUTHOR.

The data represented in Figure 31 and Figure 32 suggest that this unexpected variation in RC values occurs for lighter loads. In the graphs, as the load increases the amount of increasing RC drops. Maybe there is a solicitation threshold under which the response of the structure subjected to a load application is its stiffening.

The higher the RC value, the stiffer the pavement should be. The smaller the difference between D_0 and D_1 (the deflections used in the calculus), the bigger the RC value. It is like the structure warps more uniformly, as a more rigid and solid group. This behavior is depictured in Figure 33.

Figure 33 – Example of deflection bowls that results in decreasing RCs

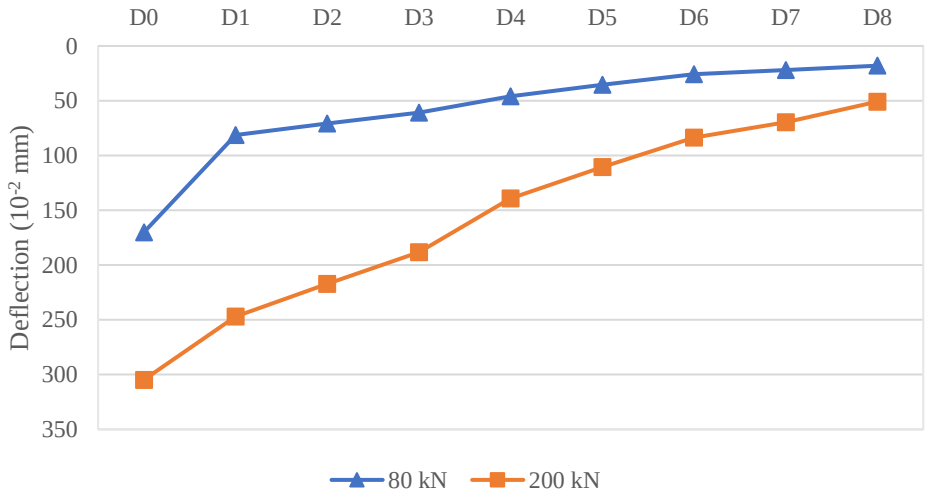

Source: THE AUTHOR.

This pattern could be observed due to an effect that is perceived when a single load intensity is repeatedly applied at the same point, with consecutive applications. The deflection in these cases is smaller for the last load applications. In the data of Airports A and C, the measurement for D_0 was lower for the second than for the first application of a 80kN-load in 55.0% and 91.5% of the cases, respectively. It appears the structure is subjected to an instant stiffening, leading the subsequent load application to produce a smaller deflection.

Comparing the application of two distinct loads generating increasing RCs, the first load generates a bowl with a pointed D_0 that deviates from the soft basin formed by the other sensors' deflections (as the blue line of the graph of Figure 33) and also could produce a transient stiffening in the structure in a manner that when applied the second load, the momentaneous stiffed structure produces a less pointed D_0 creating a softer deflection bowl (as the orange line in Figure 33). This way the increasing RC is observed in the comparison between the results of two distinct applied loads.

4.4 Impulse Stiffness Modulus (ISM)

Since the analysis of the normalized deflection gave an indication of the non-linearity of the structure, confirming that exist differences in the results obtained when applying distinct loads, the analysis of the Impulse Stiffness Modulus (ISM) is expected to also reflect this non-linearity behavior because the ISM calculation uses these deflections. As

conducted in the previous analyses, the ISM also performed statistical tests with 95% of confidence to confirm or deny the existence of the influence of the load intensity on the results.

The tests indicated there are statistically significant differences among the ISM calculated when the load intensity is varied. These differences, however, are small. The average values calculated to these differences stay around 2.0%. Figure 34 presents the behavior of the variation of the ISM values. In the graph, the bar referring to 280kN-load is not being presented for Airport B because this airport just had the application of the 80kN and 200kN loads. The distinct nature of the values of ISM in the graph represents the stiffness each structure presents. Higher ISM indicates a stiffer structure and vice versa.

Figure 34 – Variation in the ISM (all airports)

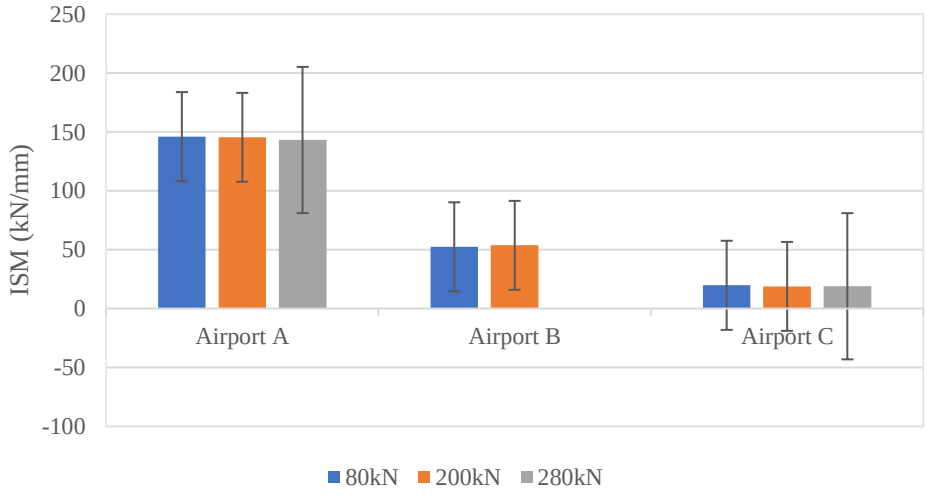

Source: THE AUTHOR.

As commented, the changes the ISM presents when varying the applied load are few expressive as observed for normalized deflection variations. Considering the use of the ISM in structural analyses of pavement, the variation in the values caused by the variation of the load is not high enough to produce significant impacts on the results of the structural evaluation.

ISM is commonly used to create a distribution graph along the extension of the pavement studied in such a way as to visualize variations in the graph's line which indicate the existence of a homogeneous section in the structure. Using the ISM values generated by 80kN or by 280kN loads, which produce the highest differences between ISM values, will not produce a distribution line with variation sufficient to influence the decision-maker to divide the pavement into more or less homogeneous sections.

It is pertinent to highlight the behavior of the ISM under the load variation. The analysis of the graph in Figure 34 shows what happens when load increases: the ISM values drop. This is the general behavior, confirmed by analyzing all the data sets for all the airports. Since the ISM can be understood as a relative stiffness of the structure, it is possible to affirm that the pavement reacts presenting less rigidity when subjected to heavier solicitations. From the data statistically significant, 64.3% of the total presented decrease with increasing load. Figure 35, Figure 36, and Figure 37 depicture the ISM behavior under load variation.

Figure 35 – Amount of increasing and decreasing ISM data (Airport A)

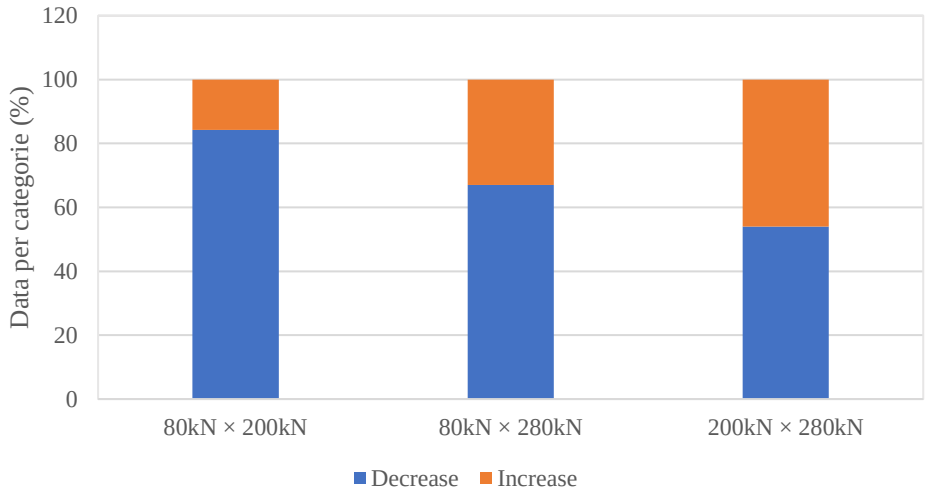

Source: THE AUTHOR.

Figure 36 – Amount of increasing and decreasing ISM data (Airport B)

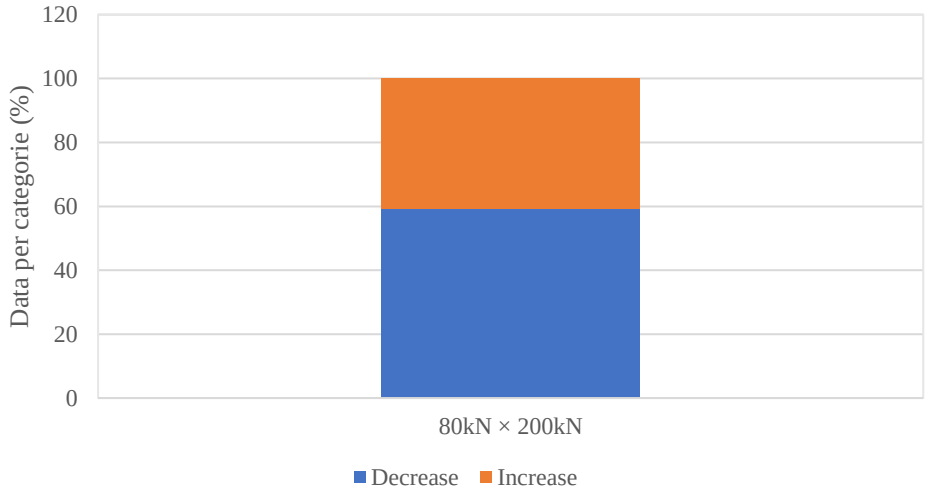

Source: THE AUTHOR.

Figure 37 – Amount of increasing and decreasing ISM data (Airport C)

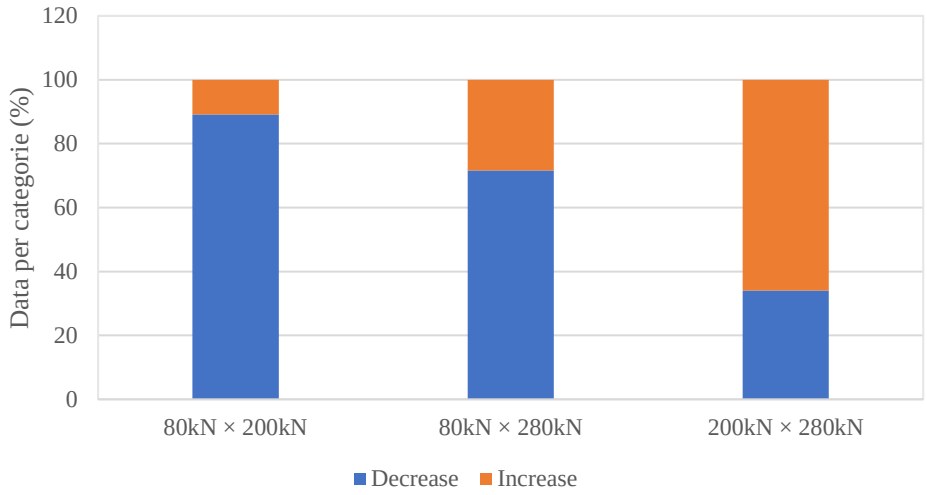

Source: THE AUTHOR.

As observed for normalized deflection and for the radius of curvature, ISM also presents a specific trend under increasing the load. As the applied load grows the number of points presenting a decrease in the ISM drops. It means that, despite the majority of the cases with load increasing presents ISM decrease, when the loads compared becomes higher the number of increases in ISM also increases, meaning the structure behaves stiffer. Since the ISM is a relative measure of the structure's stiffness this trend suggests the structure behaves stiffer under higher loads.

4.5 Back-calculated Resilient Modulus

The last parameter to be studied is the Resilient Modulus (RM). Compared to the discussed parameters, the RM is the worldwide most used parameter to perform structural analysis in airport pavements and is also the least intuitive about the load intensity influence on its results. Different from the other parameters studied, the process of back-calculation that generates the results gives the RM by layer so that the investigation of the load variation effect per layer becomes viable.

For the RM the generalization of the conclusions became more difficult to perform. From the tests conducted, there were statistically significant results for the influence of the load in the RM values of just 29% of the total considering the tests performed for the three airports. For the normalized deflections and the ISM, this number of significant results for the statistical

tests reached 95%. A result is considered statistically significant when the statistic test confirms that the variation of the load leads to a difference in the results.

This low rate of significant results can be caused by uncertainties in the inputs of the back-calculation process. The layer thicknesses are key information for a proper RM result. The stratigraphy of the structures studied was not obtained by drilling and coring the pavements, which would be the most reliable method to collect this information. In addition, the construction process can generate variations in the layer thicknesses along the extension of the constructed structure, leading to more uncertainties in the inputs leading to RM results that could not properly represent the in-situ conditions.

The low rate of significant tests, however, is not a confirmation of the inexistence of the influence of the load variation on the RM results. It can be due to the use of loads insufficiently heavy to lead the structures studied to respond differently, for example. But although it is not possible to affirm the behavior the RM results must present when the load is varied, some interesting tendencies should be presented from the part of the data that presented a real variation caused by the change in the applied loads.

The impacts of the load intensity in a specific part of the pavement is evidenced when the influence of the load variation in the RM results by layer is analyzed. The graph in Figure 38 shows the remarkable impacts in the subgrade compared to the other layers of the structures. From the tests with statistically significant differences between RM values obtained by two distinct loads, which are plotted on the graph, 50% of the total refers to the subgrade.

Figure 38 – Distribution of statistically significant differences of RM (all airports)

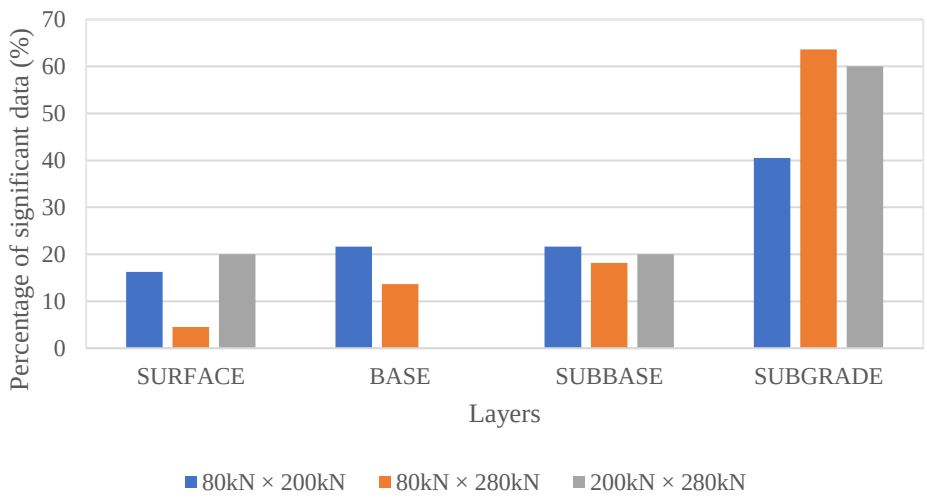

Source: THE AUTHOR.

Classifying the other pavement layers by their tests with significant differences, the sub-base is the second most influenced layer (20% of the total), the base is the third (17%), and the surface is the least impacted by the changes in the applied load (13% of the total statistically significant data). This distribution of the impacts suggests that the deeper a layer is, the higher the impact suffered in the back-calculated RM under a load variation.

This behavior of the influence increasing with the depth in the pavement structure could be related to the effect the spreadability of the loads could have on the results. Higher loads will perform a bigger mobilization of the structure until deeper depths on the structure when compared to lower loads because of the size of the pressure bulbs created, and because of the load dissipation that occurs as the depth increases. As can be verified in Figure 38, the use of the higher gap of loads (80kN and 280kN) produced a higher amount of significant data for the subgrade (the deeper layer) while for the other layers this pair of loads produced has lesser significance.

Considering airports A and C, whose evaluation used three distinct applied loads (80kN, 200kN, and 280kN), the effects previously discussed and presented in Figure 38 are easily visualized, and other impacts can be perceived. Figure 39 and Figure 40 present the percentual distribution of the significant differences in the load variation caused for Airports A and C, respectively. The percentages in these graphs, different from the graph of Figure 38 that just used the number of significant tests, were calculated by comparing the significant results to the total of performed tests. In both figures the highest influence in the subgrade is markedly notable.

Figure 39 – Distribution of statistically significant differences of RM for Airport A.

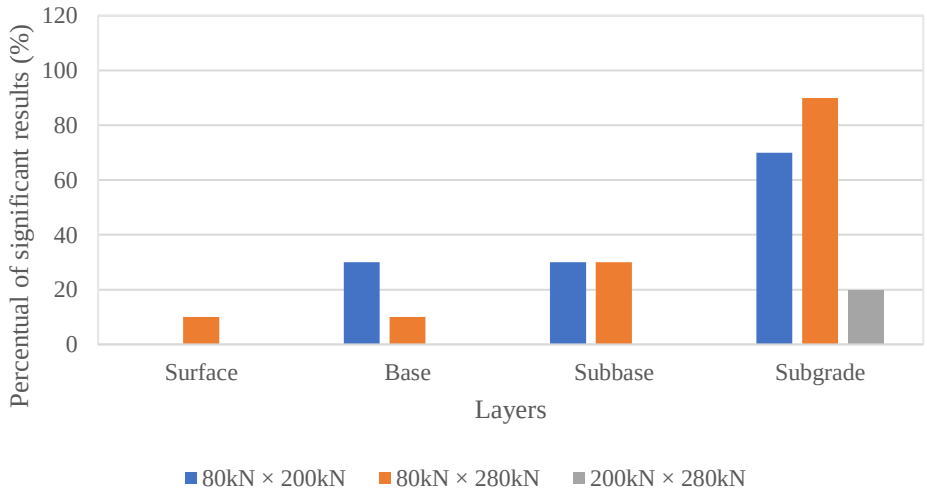

Source: THE AUTHOR.

Figure 40 – Distribution of statistically significant differences of RM for Airport C.

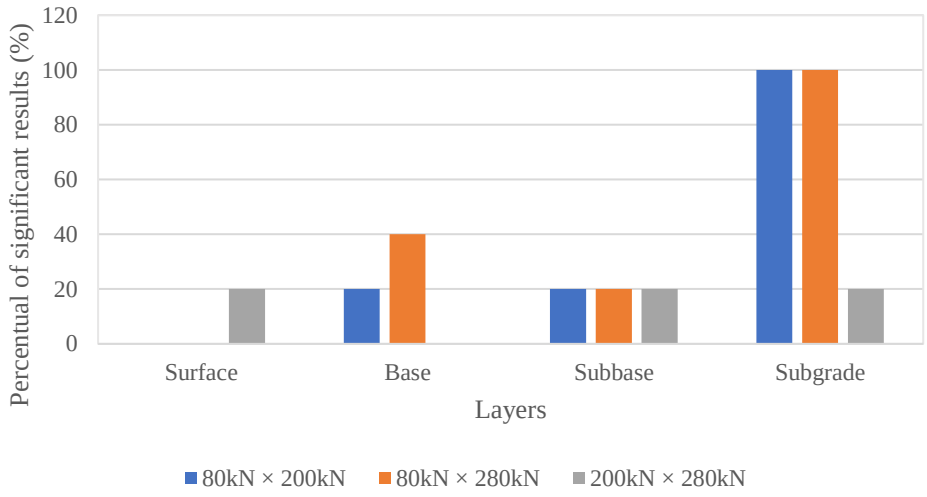

Source: THE AUTHOR.

This behavior of the influence increasing with the depth in the pavement structure seems to be related to the effect discussed for the normalized deflections, when the influence in the results is stronger accordingly the sensors are sensors more distant from the load application point, whose measure the contribution of the deeper layers to the deflection. The impacts of the spreadability of the loads could be more relevant at deeper points, where lighter loads may not mobilize some parts of the structure a heavier load could do, leading to distinct results of deflection and, consequently, of back-calculated RM.

Another remarkable effect Figure 39 and Figure 40 present is related to the number of significant differences in the variation of the load from 200kN to 280kN leads on the subgrade. While the variation from the lighter load of 80kN to the heavier loads of 200kN and 280kN led to significant differences in almost all the tests performed, the variation between the two heavy loads just led to significant differences in the RM results in 20% of the cases to each airport.

Besides this, the variation between heavy loads leads to the smallest number of significant differences in the other layers (surface, base, and subbase) if compared to changing the load from a lighter to a heavier one. It can be indicative that there is a limit beyond which increasing the applied load does not lead to significant changes in the structural response of some pavement structures.

Regarding the answer of the RM values to the loads' change, the findings corroborate a previously discussed behavior. It is relevant to remember that from the total of

performed tests to RM data, just 29% presented significant results. Despite being a low rate, this set of significant data behaves similarly, which permits the construction of a reliable interpretation and discussion about the identified patterns. The following analyzes and discussions are based on these 29% of significant data.

A first analysis of the part of the RM data set that presents statistically significant differences in its results permits to conclude that the RM values decrease when the load increases. From the significant data, 63.4% presents a decrease in the RM values. This behavior is the same presented by the ISM (for ISM this percentage is 64.3%) and confirms that it is not only the relative stiffness of the pavement but also the structure's rigidity that decreases under an increase in the applied load.

This decrease, however, does not occur in all cases of load variation. The data suggest that when two heavy loads are applied the RM value can increase or decrease following the same proportion. When the variation is between a light and a heavy load application, the effect of reduction in the RM is remarkable, as can be checked in Figure 41. 63.1% of cases of variation from 80kN to 200kN present a decrease in the values, whilst this number grows to 66.8% if the loads 80kN and 280kN are applied. When the two heavy loads (200kN and 280kN) are applied, 72.5% of the comparisons return a decrease in the RM values.

Figure 41 – Significant results of RM (all airports).

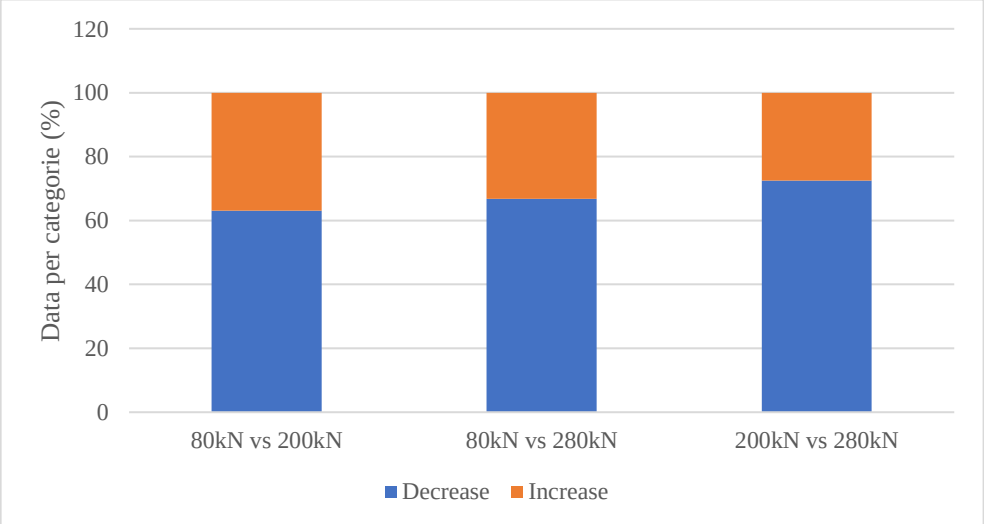

Source: THE AUTHOR.

Some distinct trends can be noticed if the amount of decreasing data is presented by airport. Figure 42, Figure 43, and Figure 44 present the percentage of data with a decrease

in RM values by the airport. In the figures, information on some load pairs is not present because were not obtained statistically significant results for these missing data sets.

The variability in the amount of data that presents decrease when the load increases is a remarkable difference among the airports studied. The uniformity presented for Airport A, where the amount of decreasing data in Figure 42 is approximately the same for all layers and load pairs, is not observed for Airport B in Figure 43, and for Airport C (Figure 44) this uniformity does not exist. A factor that could impact these variations in addition to the dependency of RM behavior of decreasing or increasing is the variability in the inputs to the back-calculation process.

Figure 42 – RM decreasing data by layer (Airport A)

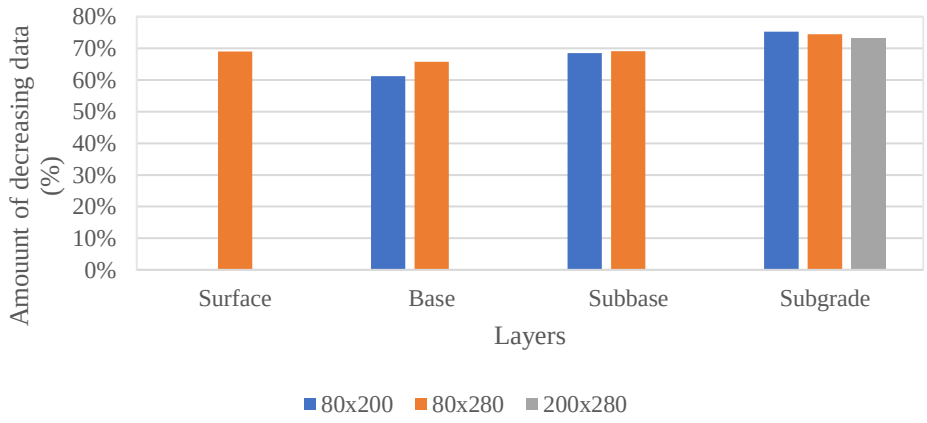

Source: THE AUTHOR.

Figure 43 – RM decreasing data by layer (Airport B)

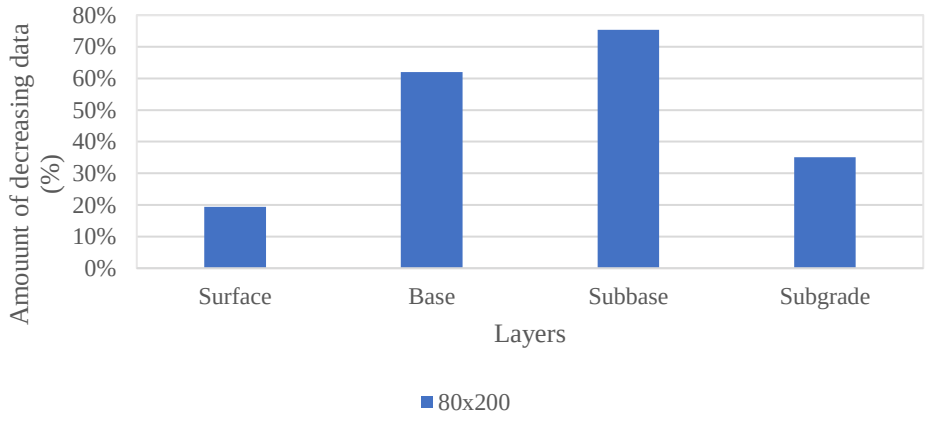

Source: THE AUTHOR.

Figure 44 – RM decreasing data by layer (Airport C)

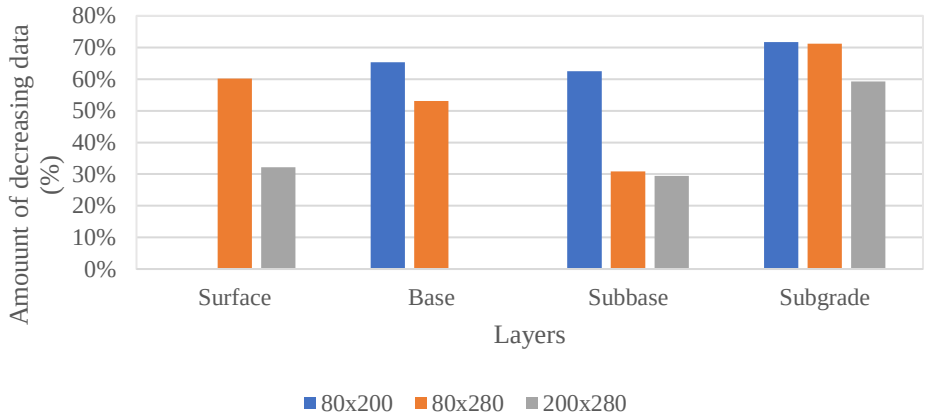

Source: THE AUTHOR.

Layer thickness is an important input impacting considerably on the obtained results of back-calculated RM. For the airports studied there is the possibility for the structural stratigraphy of presenting variation along the full extension of the pavements which could not be perceived in the tests performed to collect the layer thicknesses. The presence of inaccurate inputs in the back-calculation could have generated sets of data with results which not exactly correspond to the real characteristics of the runways' structures.

The magnitude of the decreases cannot be generalized because the data present variations linked to the analyzed airport. Airport A presented the highest decreases that are three times bigger than those for Airport C, which presented the lowest reduction in its structural rigidity. Table 8 presents the percentual average decreases for the three airports studied.

Table 8 – Average decrease values of RM by airport

Loads compared		Airport A	Airport B	Airport C
80kN × 200kN	Median decrease (%)	21.4	17.0	6.6
	Average decrease (%)	31.4	24.2	13.0
	Standard deviation (%)	121.0	109.1	82.4
80kN × 280kN	Median decrease (%)	22.5	-	9.7
	Average decrease (%)	15.3	-	17.4
	Standard deviation (%)	121.7	-	89.0
200kN × 280kN	Median decrease (%)	11.7	-	6.3
	Average decrease (%)	15.3	-	15.1
	Standard deviation (%)	108.9	-	75.8

Source: THE AUTHOR.

Data presented in Table 8 support the conclusion that the bigger the gap between the applied loads, the bigger the reduction in the RM values. The data also show that the results depend on the structure evaluated, which is intuitive since distinct structural conditions such as construction materials and pavement integrity impact the rigidity of the structure.

Considering the distinct effect the load variation presents on the layers of the pavement, being identified as a suggestion of a bigger influence on deeper parts of the structure, some results of the RM variation by layer will be following presented. These results use the 29% statistically significant data previously mentioned.

4.5.1 Impacts of load variation in back-calculated Resilient Modulus for surface layer

The surface layer presents the biggest variations of the RM in MPa measurements. It is expected since this layer has the highest values of back-calculated RM. Because of the high variability in the data, the representation of the differences will be represented in histograms with classes of variation of RM. Figure 45, Figure 46, and Figure 47 presents the information for the three airports.

Airports B and C present a similar trend in the distribution of the differences in RM. In Figure 45 the data are considerably dispersed in the classes, in such a way that it is not

possible to generalize one single class and define an average value for the changes in RM values. In Figure 46 and Figure 47, the differences have a bigger occurrence in the classes around the zero of the distribution. These values of variation average 12.0% of median decrease for Airport A, 6.1% of decrease for Airport B, and 18.0% for Airport C.

The variations stay in disagreement with the results presented by Kim *et al.* (1995), that affirmed the asphalt concrete back-calculated moduli were relatively the same when Falling Weight Deflectometer (FWD) loads are increased. When compared to the higher loads (200kN and 280kN), however, the behavior is of increasing the surface back-calculated moduli for Airport C, presenting a median increase of 23.3%.

The amount of significative data is the lowest for the surface layer compared to the other layers of the pavement. For Airport A, B and C the number of observations in the significant data sets are 42, 191, and 167, respectively. From these numbers, the amount of cases the surface RM presents decreases when the load increases is more expressive for airports A and C. In Figure 45 and Figure 47 the majority of the data stays in the negative part of the graphs. This behavior agrees with the previously discussed effect the load increase has on RM values.

Figure 45 – Variation of RM for surface layer (Airport A)

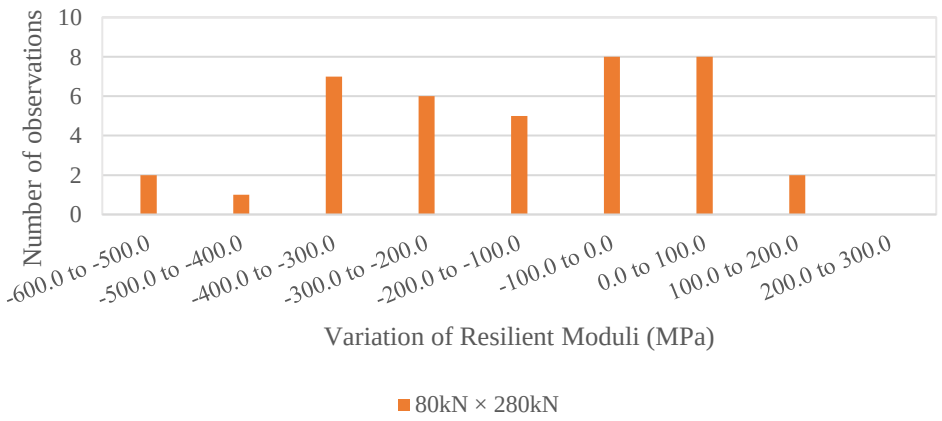

Source: THE AUTHOR.

Figure 46 – Variation of RM for surface layer (Airport B)

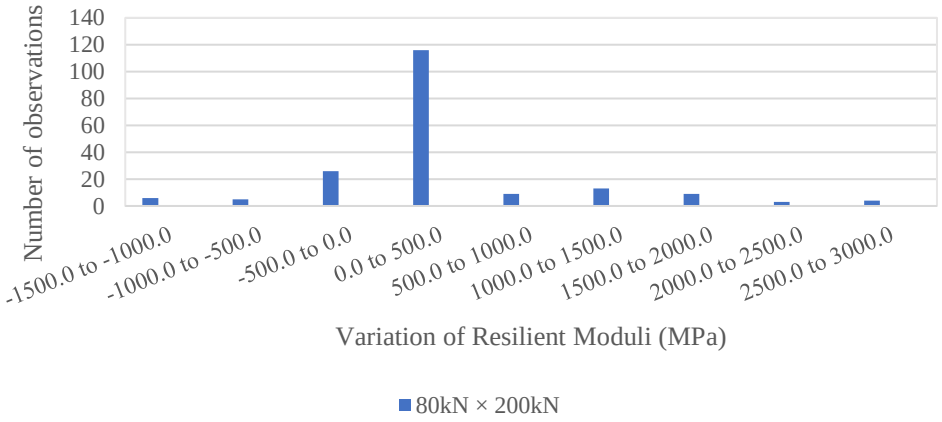

Source: THE AUTHOR.

Figure 47 – Variation of RM for surface layer (Airport C)

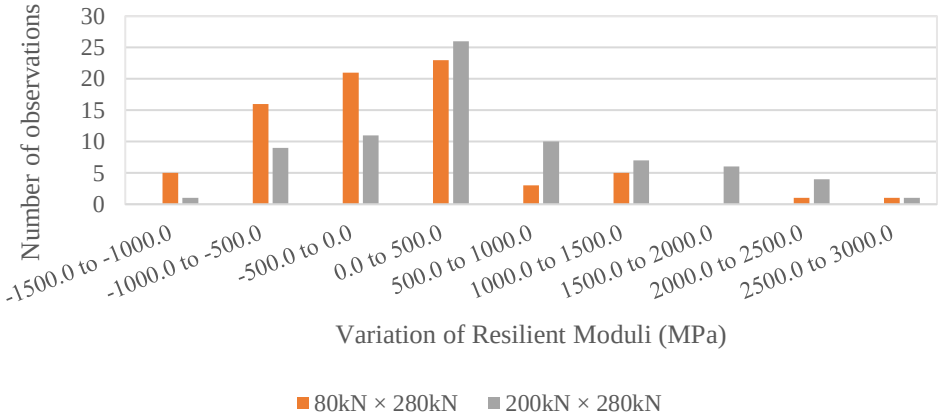

Source: THE AUTHOR.

4.5.2 Impacts of load variation in back-calculated Resilient Modulus for base layer

The distribution of the differences of RM for the base layer is similar for the three airports. As observed for the surface layer, the majority of cases where RM decreases with the load increasing occur for Airport A (Figure 48) and C (Figure 50). For Airport C, as presented in Figure 50, the number of observations in the positive side of the graph remains considerable but less expressive than the observed for the distribution of RM differences for the surface layer.

Figure 48 – Variation of RM for base layer (Airport A)

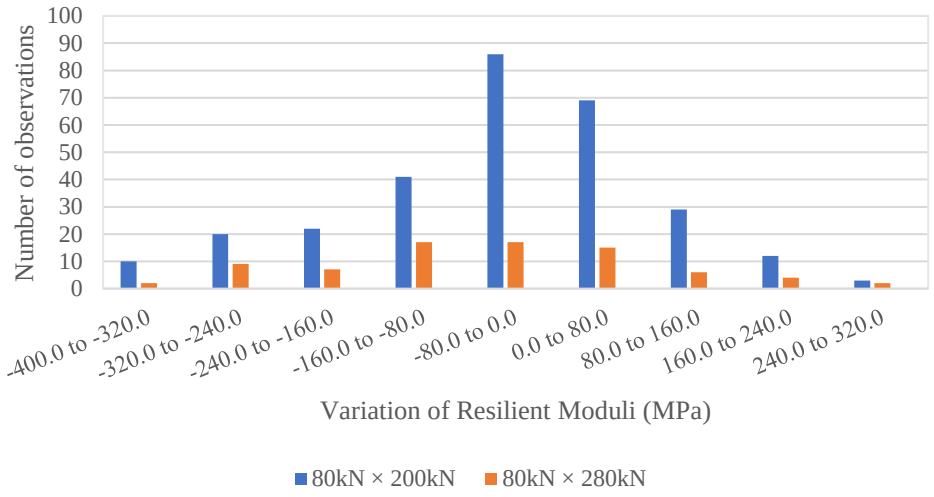

Source: THE AUTHOR.

Figure 49 – Variation of RM for base layer (Airport B)

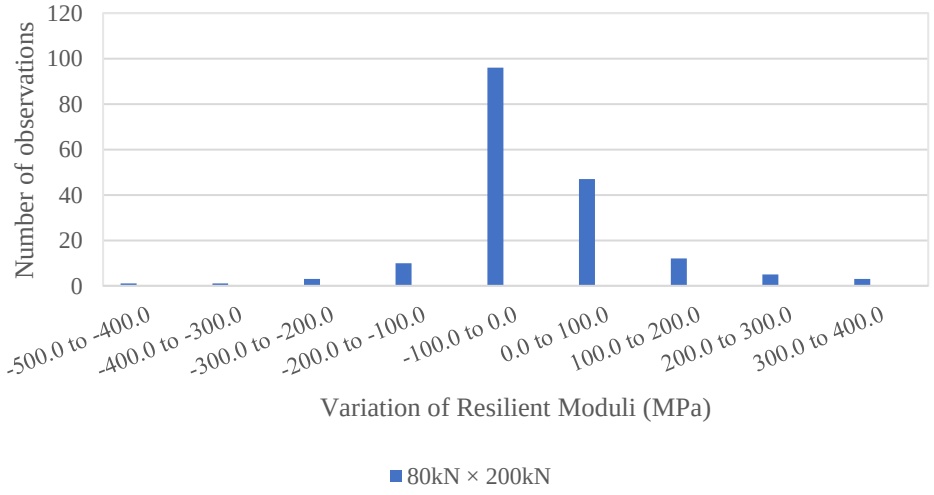

Source: THE AUTHOR.

Figure 50 – Variation of RM for base layer (Airport C)

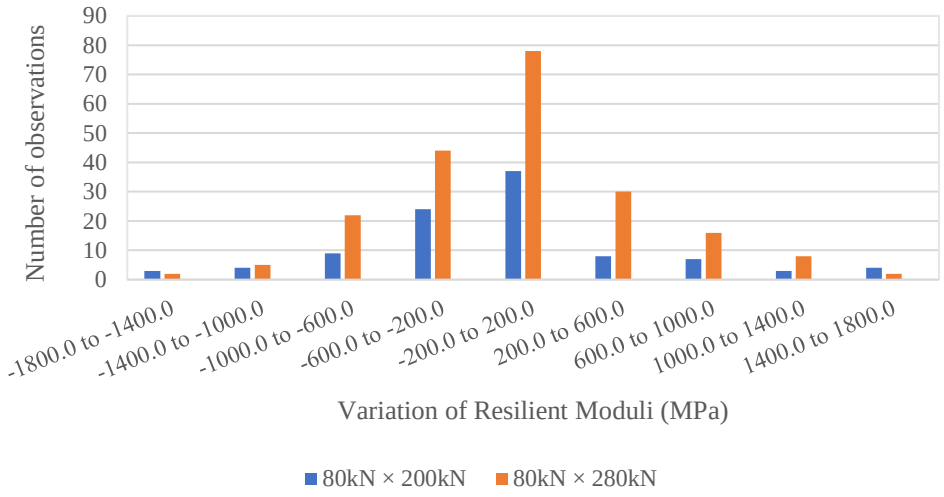

Source: THE AUTHOR.

The results of the comparison of the loads 80kN and 200kN presented in Figure 48, Figure 49, and Figure 50, for the airports A, B, and C can be expressed in median values as decreases of 16.9%, 6.6%, and 6.9%, respectively. If the loads 80kN and 280kN are compared, the median values represent decreases of 30.3% for Airport A and 2.4% for Airport C. Airport B does not have the application of the 280kN-load. These results are also diverging from the affirmed by Kim *et al.* (1995). The authors say that when the FWD loads are increased, the back-calculated moduli for granular bases increase as well. The structures of the runways studied are constructed with granular material (macadam and hydraulic macadam) and decreases in the back-calculated moduli were obtained.

4.5.3 Impacts of load variation in back-calculated Resilient Modulus for subbase layer

The subbase layer presented median decreases for the comparisons of loads of 80kN and 200kN. Respectively for airports A, B, and C the reductions in RM values were of 26.5%, 10.7%, and 7.3%. Figure 51, Figure 52, and Figure 53 present the distributions of RM variation measured in MPa.

Figure 51 Variation of RM for subbase layer (Airport A)

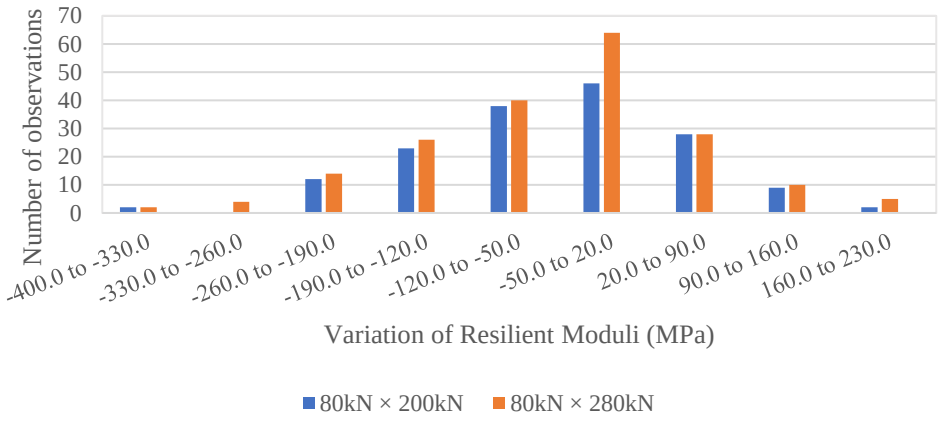

Source: THE AUTHOR.

Figure 52 – Variation of RM for subbase layer (Airport B)

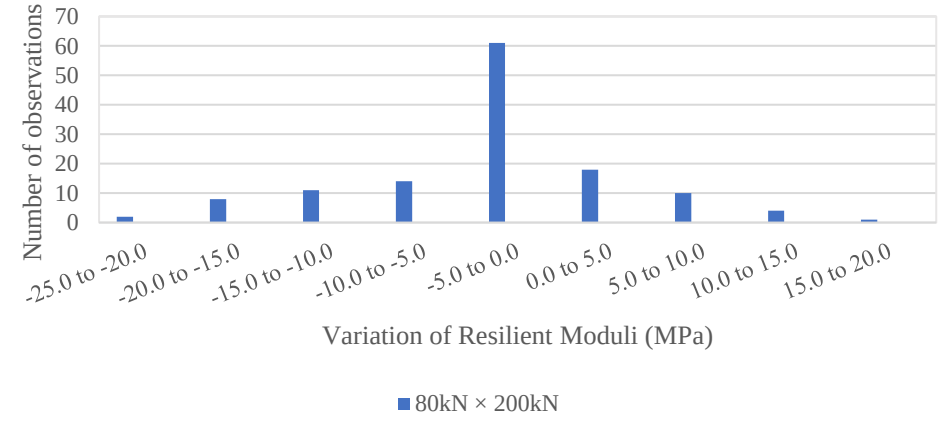

Source: THE AUTHOR.

Figure 53 – Variation of RM for subbase layer (Airport C)

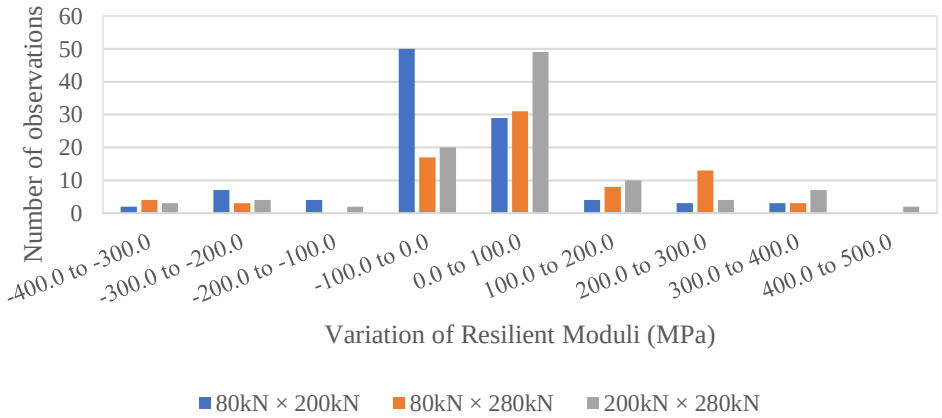

Source: THE AUTHOR.

The subbase is the first layer in which appeared significant data for comparisons with the 280kN-load. For this load, Airport A's subbase presented a median decrease of 25.3% when comparing the 80kN-load to the 280kN-load. For Airport B, increasing the load from 80kN to 200kN led to a median decrease of 10.7% in the subbase RM.

Airport C presented statistical significance in the comparisons between 80kN- and 280kN-load, and between 200kN- and 280kN-load. Respectively for these comparisons, increases of 17.1% and 12.3% were obtained for the back-calculated RM of the sandy clay subbase of Airport C. These results converge to the findings of Kim *et al.* (1995) and White and Beehag (2022).

4.5.4 Impacts of load variation in Resilient Modulus for subgrade

The analysis of the Figure 54, Figure 55, and Figure 56 permits to be visualized that, except for Airport C, the majority of the variations stays in the negative side of the graphs. This confirms the behavior of decreasing that RM presents and that was previously commented. Because Airport C has the results of just one load pair (80kN × 200kN), it is not possible to conclude with reliability the cause of this different behavior since it is not confirmed if the results for other loads also should present the same trend.

A similar distribution of the values of variation in RM for the three airports, however, can be verified by comparing Figure 54, Figure 55, and Figure 56. The majority of increases have values near to the zero of the graphs. It suggests the impacts of the load variation on the RM are not considerably strong, but it cannot be affirmed since it depends on the values of the back-calculated RM that are being compared to generate these differences. For reliable interpretations of RM variation, a percentual analysis of the data would be adequate. Figure 57, Figure 58, and Figure 59 present the percentual distribution of the variations depictured in the graphs of Figure 54, Figure 55, and Figure 56.

Figure 54 – Variation of RM for subgrade layer (Airport A)

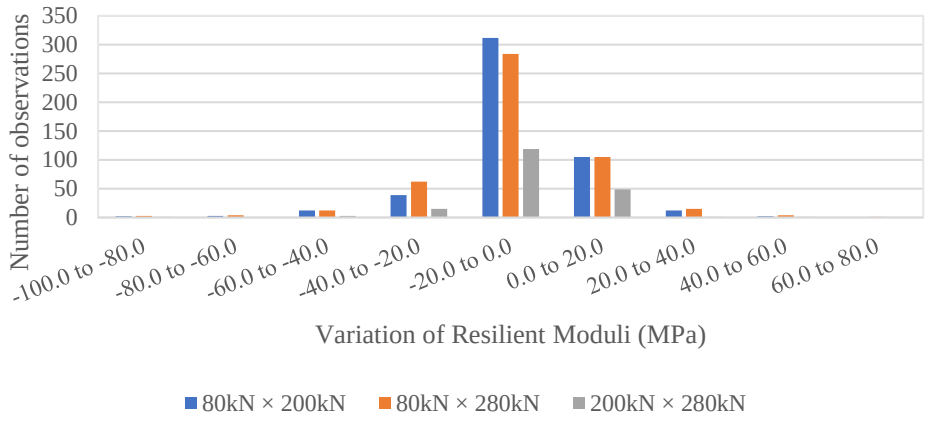

Source: THE AUTHOR.

Figure 55 – Variation of RM for subgrade layer (Airport B)

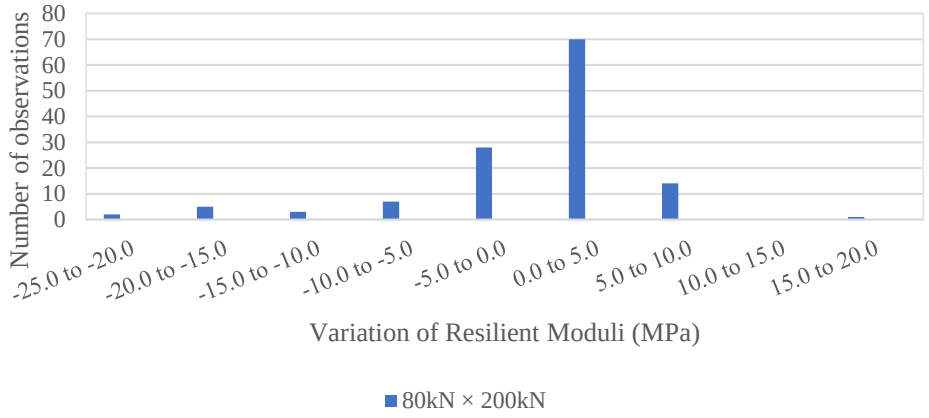

Source: THE AUTHOR.

Figure 56 – Variation of RM for subgrade layer (Airport C)

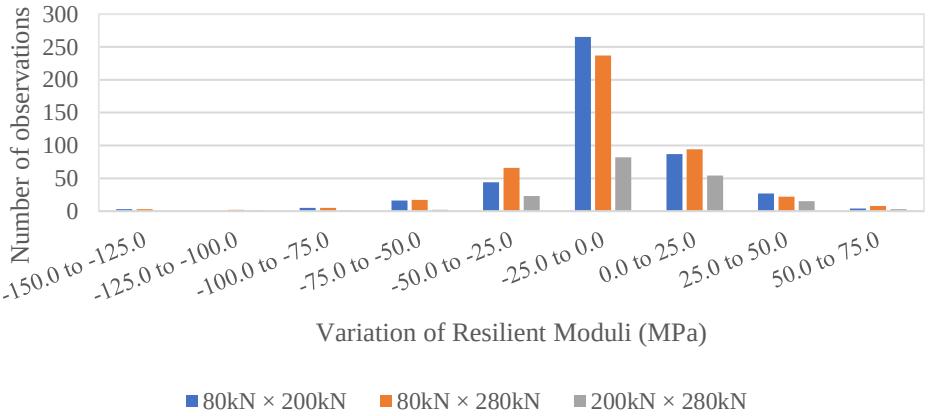

Source: THE AUTHOR.

Figure 57 – Percentual variation of RM for subgrade layer (Airport A)

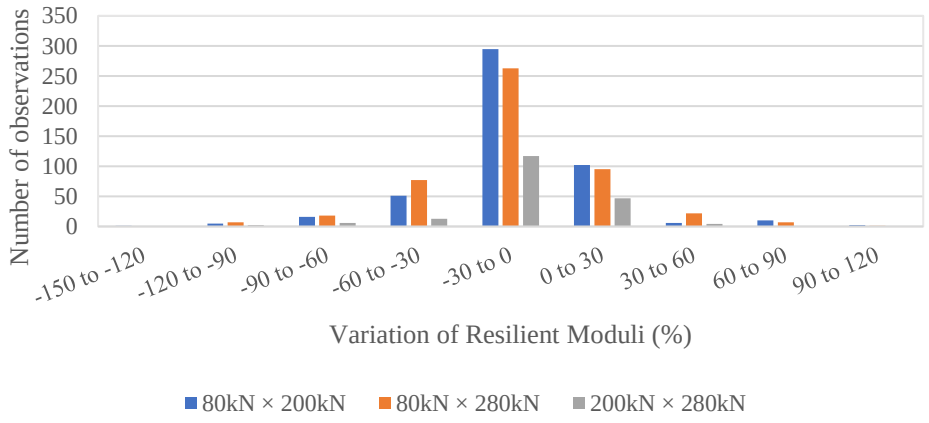

Source: THE AUTHOR.

Figure 58 – Percentual variation of RM for subgrade layer (Airport B)

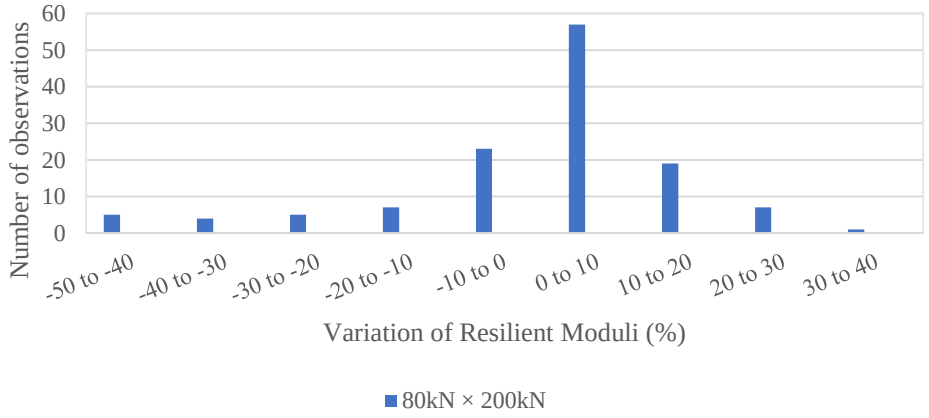

Source: THE AUTHOR.

Figure 59 – Percentual variation of RM for subgrade layer (Airport C)

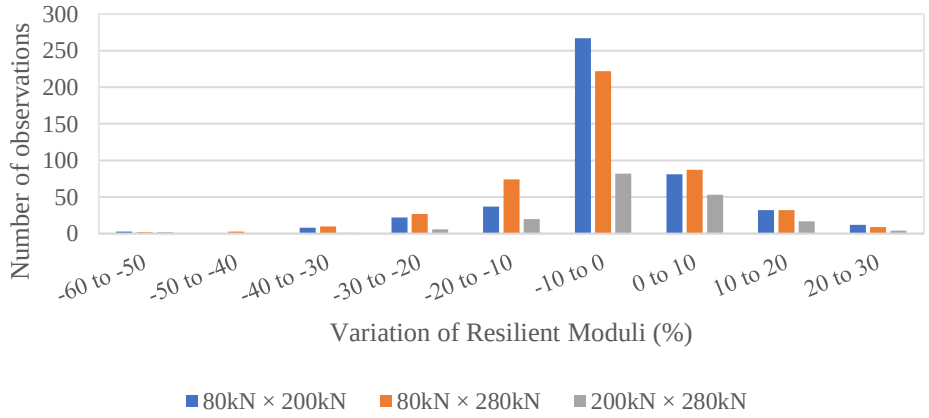

Source: THE AUTHOR.

From Figure 57, Figure 58, and Figure 59 it is possible to conclude that, despite being low values of variation when measured in MPa, as presented in Figure 54, Figure 55, and Figure 56, these changes in RM are not insignificant for the subgrade. Although the values being lower than 50MPa in the majority of the cases, these changes represent variations of about 20% to 30%. Even for Airport C, which presented variations of RM about 5.0MPa to 10.0MPa in its majority, the low variations represent considerable percentual changes of 10% to 20% in the RM. It is an impact that should not be ignored.

These obtained results are divergent from the obtained by McQueen *et al.* (2001), that said that the back-calculated RM for the subgrade is independent of the load intensity of FWD or HWD. The authors obtained their results by computational simulations, which can represent a lack of representativity from the real behavior of the pavement structure in field, where it is subjected to some variables the software could not consider as pavement degradation and various conditions of construction.

5 CONCLUSIONS

This research addressed the investigation of the structural response of airport pavements subjected to variations in the applied load. The flexible pavement structure of three runways' airports from distinct regions of Brazil were analyzed. The offsets -6.0m, -3.0m, axis, +3.0m, and +6.0m of these runways were assessed using Falling Weight Deflectometer (FWD) and Heavy Weight Deflectometer (HWD) loads of 80kN, 200kN, and 280kN. A total of 1692 points were used in the analysis.

Four distinct parameters were investigated aiming to take some conclusions about the structural response of the pavement when subjected to load variation by using the impacts observed in these parameters studied. They were the raw and normalized deflections, the Radius of Curvature, the Impulse Stiffness Modulus, and the Resilient Modulus. From the analysis, it is possible to conclude that the load intensity influences the structural response of the pavement. The statistical tests confirmed that for all the analyzed parameters there are changes in the results when the load intensity is varied.

5.1 Main conclusions

The first investigation was about the influence of the load on the measured deflections. For the raw deflections, it is expected that they would be higher when the load increases, and it was confirmed. The percentual increase in the deflections is similar to the percentual increase in the load. Analyzing the deflections by sensor it was verified that the intermediate sensors are more impacted by the load variations compared to the first sensor (under the load application point) and the two further sensors. This could be due to the spreadability and the size of the pressure bulbs the different loads present, and to the fact, the mentioned sensors (first and further) measure the influence of the deeper layers of the pavement.

To analyze the linearity of the structural response, a normalization of the deflections was performed. The deflections were normalized to a 200kN load. The results suggest there is no linear response of the pavement. When the load is varied the normalized deflections present statistically significant differences of up to 8% on average. These are small variations but that indicates the nonlinear response of the structure.

The second analyzed parameter was the Radius of Curvature (RC). It was expected to the RC present variations under the changes in the applied load because this parameter is calculated using deflections that were confirmed that are impacted by the load variation. It was verified that the RC values change when the loads vary, but an unexpected behavior was

identified. When the lighter loads are compared to heavier loads RC increases instead of the expected behavior of decrease when the load grows up.

This behavior could be observed because of another identified effect. When the same load is repeatedly applied the measured deflections become smaller. It could be due to an instantaneous stiffening the structure can present, leading the following load applications to generate smaller deflections. 73% of all the loads applied repeatedly presented this decrease in the values of the last deflections.

The third parameter studied was the Impulse Stiffness Modulus (ISM), which can be understood as a relative rigidity of the structure. It was verified that ISM decreases when the loads increase. An average decrease of 5% was identified. It is a small variation that does not impact the use of the ISM in practical structural evaluations but supports the conclusion about the nonlinearity of the pavement response to the load variation.

The main use of ISM is the distribution of its values along the full extension of the pavement studied, aiming to be identified segments with distinct variability of ISM in such a way the structure could be divided into homogeneous sections for suitable evaluation and proper maintenance application. The variability ISM data presents when the load varies is not high enough to impact in this process.

Finally, the Resilient Modulus (RM) was studied. The influence of the load on the RM results was not so remarkable as for the other parameters. The amount of statistically significant results for this parameter was considerably lower than for the others. It could be due to the structures analyzed and the load intensities used in this study. However, analyzing just the significant results, some interesting behaviors were identified.

The first of them was that the influence of the load variation increases as the layer is deeper. The subgrade presented a higher amount of statistically significant changes in RM results (50% of the total of the tests with statistically significant differences induced by the load variation), followed by subbase (20% of the total of significant tests), base (17%), and surface course (13%), respectively. Once again, the spreadability and the size of the pressure bulbs can be used to explain this observed behavior.

The second identified pattern in RM response to the load variation is that the values decrease with increasing the load. This behavior is the same presented by the ISM. 77.3% of the significant results for the RM presented a reduction in its values when the load was increased. This effect is remarkable if a lighter load and a heavier load are used, so the bigger the gap between the applied load intensities, more significant is the impact on RM decreasing. If the

results of two heavy loads are compared the RM presents the same proportion of increases or decreases.

Another behavior where RM and ISM present similarities is in the amount of decrease observed when the compared loads are heavier. As the load increases the percentage of points presenting a decrease of RM drops. The same is observed for the ISM.

The magnitude of these decreases depends on the analyzed structure. Depending on the combination of conditions of layers' thicknesses and materials, and on the structural integrity of the pavement the values vary, but in general, they are not high enough to considerably impacts the structural evaluation. If the RM results would be used to design reinforcements or overlays, however, the load chosen must be adequate to avoid misevaluations of the structure.

Considering these discussions, it is possible to conclude that the airport pavements do not present a linear response to the applied loads. The variations observed when the applied load is varied, however, are not high enough to prejudice the structural evaluation of the pavements so FWD and HWD are suitable to be used in evaluating airport pavements. The results generated for the ISM or for normalized deflections when distinct loads are applied do not impact their uses for structural evaluation, and the back-calculated RM variation is not high enough to lead the decision-maker to evaluate the structure with a considerably different level of degradation. Nevertheless, if the results of the structural evaluation will be used to perform the design of reinforcements or overlays, the chosen load must be compatible with the traffic the pavement is subjected to aiming to avoid improper projects.

5.2 Main limitations of the research

It is important to highlight the limitations faced by this study. Despite being used three distinct loads, not all the airports studied received these three different levels of solicitation. The number of points was also not the same. The uniformity in the conditions of the tests is important in producing results that can be compared in their entirety.

The process of analysis included the back-calculation of materials' properties. This back-calculation requires information on seed modulus and layer thicknesses as fundamental inputs. Variations in these inputs leads have a considerable impact on the generated results. The most adequate manner to catch these inputs is by using geotechnical investigation in the pavements studied. It was not possible to be executed in this study. This information was obtained from the literature or by using nondestructive tests. These sources of information can

generate inputs considerably different from the real characteristics of the materials present in the structures studied, which could lead to misevaluations and imprecise results.

Part of the process of analysis required the use of models of prediction and correction of the pavement temperature. These models were identified in the literature but presented a considerable gap of time from their idealization until the present day. The models also were not developed specifically for the regions the pavements studied are located in, which could lead to an accumulation of inaccuracies or generate data disconnected from reality.

5.3 Future research proposals

Considering the limitations commented and the results obtained in the present study, some suggestions for future research must be done to support the development of the national scenario of knowledge in the pavement materials applied to airfield pavement structures. Investigations in this field of research produce material that can be incorporated into the national regulations regarding civil aviation. It collaborates with the Brazilian Civil Aviation Authority to continuously improve the regulation and supervision of Brazilian airports, increasing the safety of landing and take-off operations, and also producing tools to support the airport operators in properly maintaining their structures resulting in a better use of financial resources. Some of these suggestions are following listed:

a) To repeat the investigation about the load influence on the RM results using seed modulus obtained in the laboratory and checking the layer thicknesses by performing geotechnical investigation in the pavements studied;
b) To compare the back-calculation results generated by distinct tools/software aiming to determine the one that produces RM closer to those observed in the national reality of materials;
c) To investigate the loading threshold from which the results become different from light to heavy loads;
d) To develop an updated model of temperature correction of deflections and back-calculated RM;
e) To develop an updated model of temperature prediction that determines the temperature inside the asphaltic layer considering the actual national pavement materials and climate conditions.

REFERENCES

AMERICAN ASSOCIATION OF STATE HIGHWAY AND TRANSPORTATION OFFICIALS. **Guide for Design of Pavement Structures 1993.** Washington, D.C., USA, 1993.

AKBARZADEH, Hossein; BAYAT, Alireza; SOLEYMANI, Hamid R. Analytical review of the HMA temperature correction factors from laboratory and Falling Weight Deflectometer tests. **International Journal of Pavement Research and Technology**, v. 5, n. 1, p. 30-39, 2012. Disponível em: <https://www.springer.com/journal/42947>. Acesso em: 20 abr. 2023.

AGÊNCIA NACIONAL DE AVIAÇÃO CIVIL. **Manual de sistema de gerenciamento de pavimentos aeroportuários – SGPA**. Brasília, DF., BR, 2017.

_____. **Avaliação funcional e estrutural não-destrutiva de capacidade de suporte:** Relatório preliminar. Brasília, DF., BR, 2018.

_____. **Análise e definição de soluções de engenharia:** pavimentação de pista de pouso e decolagem. Brasília, DF., BR, 2020.

_____. **Alerta aos operadores de aeródromo n°003/2021.** Brasília, DF., BR, 2021.

AMERICAN SOCIETY FOR TESTING AND MATERIALS. **D4695 – 03. Standard guide for general pavement deflection measurements**. West Conshohocken, USA, 2008.

_____. **D4602 – 93 Standard guide for nondestructive testing of pavements using cyclic-loading dynamic deflection equipment**. USA, 2020.

ANTUNES, Maria de Lourdes Baptista da Costa. **Avaliação da capacidade de carga de pavimentos utilizando ensaios dinâmicos**. 1993. Thesis (Doctor in Civil Engineering) – Technical University of Lisbon, Lisbon, PT, 1993.

BALBO, José Tadeu. **Pavimentação asfáltica:** materiais, projeto e restauração. São Paulo: Oficina de Textos, 2007.

BRASIL. Ministério dos Transportes. Departamento Nacional de Infraestrutura de Transportes. **DNIT 133/2010-ME Pavimentação asfáltica – Delineamento da linha de influência longitudinal da bacia de deformação por intermédio da Viga Benkelman – Método de ensaio**. Brasília, D.F., BR, 2010.

BROUTIN, Michael; MOUNIER, Damien. Release of the French Technical Guidance for Flexible Airfield Pavement Assessment Using HWD. **Airfield and Highway Pavements 2015**, p.330-341, 2016. Disponível em: <https://ascelibrary.org/doi/book/10.1061/9780784479216>. Acesso em: 20 abr. 2023.

BROUTIN, Michael; DUPREY, A. Towards improved temperature correction for NDT data analyses. **Airfield and Highway Pavements 2017**, p. 244-255, 2017. Disponível em: <https://ascelibrary.org/doi/book/10.1061/9780784480953>. Acesso em: 20 abr. 2023.

CHEN, Dar-Hao; BILYEU, John; LIN, Huang-Hsiung; MURPHY, Mike. Temperature correction of Falling Weight Deflectometer measurements. **Transportation Research**

Record, v. 1716, p. 30-39, 2000. Disponível em: < https://journals.sagepub.com/home/trr>. Acesso em: 20 abr. 2023.

DEPARTAMENTO DE ESTRADAS DE RODAGEM (São Paulo, SP). **IP-DE-P00/003 Avaliação funcional e estrutural de pavimento**. São Paulo, BR, 2006.

DEVORE, Jay L. **Probabilidade e Estatística para Engenharia e Ciências**. 6th ed. São Paulo: Cengage Learning, 2005.

DIRENG. **Levantamento de dados de aeroportos brasileiros**. Brasília, DF: Aeronautics Ministry, 1991.

ENTE NAZIONALE PER L'AVIAZIONE CIVILE (Italy). **LG 3/2015-APT Airport pavement management system:** Linee guida sulla implementazione del sistema di gestione della manutenzione delle pavimentazioni. Roma, IT, 2015.

FEDERAL AVIATION ADMINISTRATION (United States of America). **AC 10/5370-11B Use of nondestructive testing in the evaluation of airport pavements**. Washington, DC., USA, 2011.

_____. **AC 150/5320-6G Airport pavement design and evaluation**. Washington, DC., USA, 2021.

GROGAN, William P.; FREEMAN, Reed B.; ALEXANDER, Don R. Impact of FWD testing variability on pavement evaluations. **Journal of Transportation Engineering**, v. 124, n. 5, p. 437-442, 1998. Disponível em: <https://ascelibrary.org/doi/abs/10.1061/(ASCE)0733-947X(1998)124:5(437)>. Acesso em: 20 abr. 2023.

HACHIYA, Yoshitaka; TAKAHASHI, Osamu; TSUBOKAWA, Yukitomo. Nondestructive structural evaluation system for airport pavements with 200kN-FWD. **Advancing Airfield Pavements**, p. 279-288, 2001. Disponível em: <https://ascelibrary.org/doi/abs/10.1061/40579(271)23>. Acesso em: 20 abr. 2023.

HOFFMAN, M.S.; THOMPSON, M.R. **Nondestructive testing on flexible pavements field testing program summary**. Urbana, USA: University of Illinois, 1981.

HORAK, Emile. **Aspects of deflection basin parameters used in a mechanistic rehabilitation design procedure for flexible pavements in South Africa**. 1987. Thesis (Doctor of Philosophy) – University of Pretoria, Pretoria, ZA, 1987.

HORAK, Emile; EMERY, Stephen. Falling Weight Deflectometer bowl parameters as analysis tool for pavement structural evaluations. *In*: ARRB CONFERENCE: RESEARCH INTO PRACTICE, 22., 2006. Camberra. **Proceedings** [...]. Disponível em: <http://155.212.5.248/Presto/collections/BrowseContentCollection.aspx?ccID=OA==&iCatIi=NTA4>. Acesso em 20 abr. 2023.

HORAK, Emile; HEFER, Arno; EMERY, Steve; MAINA, James. Flexible road pavement structural condition benchmark methodology incorporating structural condition indices derived from Falling Weight Deflectometer deflection bowls. **Journal of Civil Engineering**

and Construction, v. 4, n. 1, p. 1-14, 2015. Disponível em: <http://www.techrev.org.uk/jcec/4.1/jcec.4.1.1.pdf>. Acesso em: 20 abr. 2023.

JOHNSON, Andrew M.; BAUS, Ronald L. Alternative method for temperature correction of backcalculated equivalent pavement moduli. **Transportation Research Record**, v. 1355, p. 75-81, 1992. Disponível em: <https://onlinepubs.trb.org/Onlinepubs/trr/1992/1355/1355-009.pdf>. Acesso em: 20 abr. 2023.

KIM, Y. Richard; HIBBS, Bradley O.; LEE, Yung-Chien. Temperature correction of deflections and backcalculated asphalt concrete moduli. **Transportation Research Record**, v. 1473, p. 55-62, 1995.
Disponível em: <https://onlinepubs.trb.org/Onlinepubs/trr/1995/1473/1473-007.pdf>. Acesso em: 20 abr. 2023.

LYTTON, Robert L.; SMITH, Roger R. Use of nondestructive testing in the design of overlays for flexible pavements. **Transportation Research Board**, v. 1007, p. 11-20, 1985. Disponível em: <https://onlinepubs.trb.org/Onlinepubs/trr/1985/1007/1007-002.pdf>. Acesso em: 20 abr. 2023.

MOROPOULOU, Antonia; KOUI, Maria; AVDELIDIS, Nicolas P.; KAKARAS, Kostas. Inspection of airport runways and asphalt pavements using long wave infrared thermography. *In*: **Thermosense**, 22., 2000. Orlando, United States. **Proceedings** […]. p. 302-309. Disponível em: < https://www.spiedigitallibrary.org/conference-proceedings-of-spie/4020/0000/Inspection-of-airport-runways-and-asphalt-pavements-using-long-wave/10.1117/12.381562.short?SSO=1>. Acesso em: 20 abr. 2023.

MOROPOULOU, Antonia; AVDELIDIS, N. P.; KOUI, M.; KAKARAS, Kostas. An application of thermography for detection of delaminations in airport pavements. **NDT&E International**, v. 34, p. 329-335, 2001. Disponível em: <https://d1wqtxts1xzle7.cloudfront.net/85323192/s0963-8695_2800_2900047-520220502-1-vbjorf-libre.pdf?1651479578=&response-content-disposition=inline%3B+filename%3DAn_application_of_thermography_for_detec.pdf&Expi Exp=1682030160&Signature=gKiO2p9NkyiEUcq~WTzBq-4RM0-EQ8Qacmcj7LuI2qFFncsjeKfc9GXuwKVc~gy22kvWqHt9aduAbVtIAcyQNUAnUgd2qiDRq1FRFZVqFtLqGOHhybe7a7aeBD76v~2An5s2pXvAOxYJbRZKAwXT893Ku5N-pNisTuvJz2Mc8R2LIH4l23N2vqv69CLBxfO6ya3Wo~IofKR7ywsJGzDeC5YJf1jSOkvNajacj9iC8n-0H91e-vKpPDo6KxgtXAbrkJ3TY9S5bn0NhC8ljUuqJnQsBvS5JUUTae6ee6W5~aR6gZpF5GMLtHGMLtHMjhU23ZnLRK9K6DegGJQxFywz7w__&Key-Pair-Id=APKAJLOHF5GGSLRBV4ZA>. Acesso em: 20 abr. 2023.

MCQUEEN, Roy D.; MARSEY, Wayne; ARZE, Jose M. Analysis of nondestructive test data on flexible pavements acquired at the National Airport Pavement Test Facility. **Advancing Airfield Pavements**, p. 267-278, 2001. Disponível em: <https://ascelibrary.org/doi/abs/10.1061/40579(271)22>. Acesso em: 20 abr. 2023.

NAM, Boo Hyun. Transition of the Rolling Dynamic Deflectometer device from a screening tool to an evaluation tool for rigid airfield pavement projects. **Transportation Research Record**, v. 2206, p. 39-51, 2011. Disponível em:

<https://journals.sagepub.com/doi/abs/10.3141/2206-06?journalCode=trra>. Acesso em: 20 abr. 2023.

NAM, Boo Hyun; YEON, Jung Heum; BEHRING, Zachary. Effect of daily temperature variations on the continuous deflection profiles of airfield jointed concrete pavements. **Construction and Building Materials**, v. 73, p. 261-270, 2014. Disponível em: <https://www.sciencedirect.com/science/article/abs/pii/S0950061814010897>. Acesso em: 20 abr. 2023.

OMAR, Hadi Mohamed. **The effect of cracking on the deflection basin of flexible pavements.** 1996. Thesis (Doctor of Philosophy) – Department of Civil Engineering, University of Manitoba, Winnipeg, CA, 1996.

PIGOZZI, Franco; PORTAS, Silvia; MALTINTI, Francesca; CONI. Mauro. Analysis of runway deflectometer campaign for implementation on airport pavement management system. **The International Journal of Pavement Engineering and Asphalt Technology**, v. 15, n. 2, p. 11-26, 2014. Disponível em: <https://iris.unica.it/handle/11584/233537>. Acesso em: 20 abr. 2023.

PINTO, Salomão.; PREUSSLER, Ernesto Simões. **Pavimentação rodoviária:** conceitos fundamentais sobre pavimentos flexíveis. 2. ed. Rio de Janeiro: Synergia: IBP, 2010.

PRIDDY, Lucy P.; BIANCHINI, Alessandra; GONZALEZ, Carlos R.; DOSSETT, Cayce S. **Evaluation of procedures for backcalculation of airfield pavement moduli**. US Army Corps of Engineers, 2015.

ROCHA FILHO, Nelson Rodrigues. **Estudo de técnicas para avaliação estrutural de pavimentos por meio de levantamentos deflectométricos**. 1996. Thesis (Master in Science) – Instituto Tecnológico de Aeronáutica, São José dos Campos, BR, 1996.

SONG, Injun; GAGNON, Jeffrey; LARKIN, Albert. Load pulse width and deflection analysis using HWD and MDD data at National Airport Pavement Test Facility. *In:* 2014 FAA WORLDWIDE AIRPORT TECHNOLOGY TRANSFER CONFERENCE, 2014. Galloway, New Jersey, USA. **Proceedings** […]. Disponível em: <https://trid.trb.org/view/1322626>. Acesso em: 20 abr. 2023.

THOLEN, Olle; SHARMA, Jay; TERREL, Ronald L. Comparison of Falling Weight Deflectometer with other deflection testing devices. **Transportation Research record**, v. 1007, p. 20-26, 1985. Disponível em: <https://onlinepubs.trb.org/Onlinepubs/trr/1985/1007/1007-003.pdf>. Acesso em: 20 abr. 2023.

TRANSPORT CANADA. **ERD n121 Guidelines respecting airport pavement structural condition surveys**. Ottawa: Government of Canada, 2004.

_____. **AC 302-011 Airport pavement bearing strength reporting**. Government of Canada, Ottawa, Canada, 2016.

ULLIDTZ, Per. **Pavement analysis. Developments in civil engineering, 19**. Amsterdam: Elsevier, 1987.

VAN GURP, Christ. **Characterization of seasonal influences on asphalt pavements with the use of Falling Weight Deflectometers**. Thesis (Doctoral Thesis) – Faculteit der Civiele Technik, Technische Universiteit Delft, Delft, NL, 1995.

WHITE, Greg; BARBELER, Andrew. Evaluating Falling Weight Deflectometer back-calculation software for aircraft pavement strength rating. *In:* GEOMEAST INTERNATIONAL CONGRESS AND EXHIBITION ON SUSTAINABLE CIVIL INFRASTRUCTURES, 2., 2018. Cairo, Egypt. **Proceedings** […]. P. 64-83. Disponível em: <https://www.researchgate.net/profile/Greg-White/publication/328640468_Evaluating_Falling_Weight_Deflectometer_Back-Calculation_Software_for_Aircraft_Pavement_Strength_Rating_Proceedings_of_the_2nd_GeGeoMEa_International_Congress_and_Exhibition_on_Sustainable_Civil_Infra/links/5be77458a6fdcc3a8dcd726e/Evaluating-Falling-Weight-Deflectometer-Back-Calculation-Software-for-Aircraft-Pavement-Strength-Rating-Proceedings-of-the-2nd-GeoMEast-International-Congress-and-Exhibition-on-Sustainable-Civil-Infra.pdf >. Acesso em: 20 abr. 2023.

WHITE, Greg; BEEHAG, Josh. Variability and Repeatability of Falling Weight Deflectometer survey results for airport pavement management. *In*: CONFERENCE OF MANAGING PAVEMENT ASSETS, 11., 2022. Chicago, Illinois, USA. **Proceedings** […]. Disponível em: <https://trid.trb.org/view/1322626 >. Acesso em: 20 abr. 23.

APPENDIX A – DEFLECTIONS FOR AIRPORT A (80KN-LOAD, FREE OF OUTLIERS)

Load	D_0	D_1	D_2	D_3	D_4	D_5	D_6	D_7	D_8
78.89	117.3	102.8	94.9	86.8	69.1	58.1	45.2	39.4	31.9
78.09	263.5	131.3	105.7	96.2	76.9	62.4	52.8	43.9	30.5
76.02	174.7	94.8	84.5	80.4	68.4	56.4	50.2	41.1	33.6
73.95	122.3	100.7	85.8	73.8	56.4	47	35.4	32.2	29.9
75.86	141.5	123.8	108.9	93.5	72.4	61.5	46.7	38.2	31.6
75.55	183.6	154.2	130.4	112.5	82.6	54.9	46.4	46.2	16.1
74.91	220.7	162.4	130.4	112.4	82.1	63.5	53.2	43.7	35.4
70.77	191.3	119.6	106.9	90.8	69.1	55.3	43.3	38	32.4
73.95	215.5	117.7	91.4	82.3	64.8	55.3	42.7	35.7	31
73.32	160.1	111.1	92.7	83.7	61.3	45.3	38.3	15.6	13
70.62	204.5	147.6	104.7	89.6	62.5	48.8	37.5	30.1	23.9
75.07	205	117.7	101.3	87	65.2	50.7	41.8	27.2	24.2
74.75	157.3	110.1	88.5	78.9	59.8	47.8	37.1	33	26.1
72.84	153.3	102.4	90.4	78.8	59.4	50.1	38.9	31.1	23.4
73.16	160.2	109.2	93.3	80.2	60.4	46	35.7	35.3	23.9
76.18	143.1	97.4	83.2	70.4	53.8	44.5	37.9	28.6	24.2
73.8	176.2	121.4	93.5	75.7	56.7	44.7	35.9	27.8	24.9
75.86	136.9	89.7	73.2	63.6	50.1	40.9	33.4	27	22.4
76.66	195.1	132.9	103.6	84.1	60.7	46.4	29.6	28.7	22.3
76.98	98.5	77.2	70.1	62.4	48.7	38.9	31.8	27.8	20.9
75.55	199	97.6	79.6	70.4	51.6	44.4	33.2	28.4	23.5
77.77	117.7	90	77.4	67.3	50.6	42	33.9	27.3	23.6
73.95	176.7	114.8	86.7	76.1	54.3	43.3	32.4	26.9	23.6
78.73	96.3	76.7	68.8	59.6	44.6	38	32.8	25.5	22
76.34	152.8	90.9	75.4	67.3	48.9	39.2	32.7	30.6	21.9
75.55	140.7	112.9	93.8	78.2	55.4	44.3	35.2	26.5	23.2
76.34	173.2	112.8	89.4	76.1	55.9	44.2	35.6	31.8	23.1
76.34	141.3	98.6	85.8	73.3	54.2	48.2	36.7	30	25.1
75.55	143.1	103.8	88.4	75.4	56.3	46.4	37.5	33.1	26.4
71.73	187.5	112.3	85.7	76.4	56.8	43.1	37.2	35.2	31.3
75.7	119.2	86.6	76.9	65.6	49.9	42.8	28.1	25.1	23.3
75.07	145.1	105.5	80.6	64.4	46.9	38.7	32.9	26.8	20.8
75.23	140.5	90.5	74.4	61.8	45.3	37.8	31.4	22.3	19.9
71.73	111.3	92.6	67.9	61.9	42.9	35.2	26	18.5	14
73.16	127.6	77.3	61.3	53.4	38.5	31.9	25.5	20.6	16
74.91	116.5	81.9	67	58.9	43	33.1	26.3	22.2	18.2
75.39	184.5	99.2	78.6	68.4	46.7	38.5	29.9	26.8	16.7
76.34	149.2	108.9	87.4	70.9	49.1	33.6	29.8	26.2	19.8
74.11	184.5	113.2	89.4	76.3	52.9	37.3	30.3	27	17.2
76.18	144.7	90.7	72	64.2	43.1	34.4	27.3	21	18.7
74.27	173.8	112.8	88.5	73.8	49.7	42.2	29.4	24.7	19.6
76.02	172.2	102.3	84.5	71.6	51.4	36.6	33	27.5	18.5
75.23	216.1	113.2	87.3	74.6	55.4	37.2	30.9	28.5	17.2

77.61	197.7	103.6	83	71.6	51.2	42.4	32.5	27.5	21.9
77.93	186.5	105.3	77.7	63.8	46.2	37.1	29.2	26.2	21
75.7	115.5	78.4	63.3	52.4	36.2	29.5	24.1	19.4	15.7
76.98	180	103	73.8	61.1	40.5	31.4	26.2	21.4	16.7
74.43	115.4	85.9	71.5	58.6	40.4	30.8	22.5	19	15.2
73.16	109.3	83.5	66	52.8	32.7	25	19.1	16	14.6
75.7	140.8	108.1	84.8	62.8	38.9	28.1	21.6	17.4	13.7
73.48	117.6	93.5	77.4	60.9	39.9	30	21.9	16.9	15.5
77.29	130.3	90.6	74.4	59.5	36.4	27.8	21.8	17.6	14.8
75.39	127.3	91.3	74.7	58.3	37.3	29	21.9	17.8	15.3
75.39	110.6	84.1	69.4	56.2	36.1	28	19.1	16.9	14.9
75.07	102.9	88	71.1	57.3	34.7	23.6	16.4	13.4	11.6
72.52	105	81.1	67.2	52.2	31.8	23.9	16.4	13	10.9
76.18	112.6	87.1	68.5	53.5	34.1	24.6	19	14.7	12.8
74.59	95.5	80.3	65	53.5	34.6	25.6	19.9	16.5	13.3
74.75	93.3	71.4	60.8	51.6	34.8	25.7	19.1	16.6	15.1
76.82	79.1	61	51.1	42.6	32.1	26.6	21.9	19.7	16.7
74.43	59.8	54.8	50.7	46.3	39.1	35.4	29.2	25	20.9
77.61	84.7	60.2	53.9	50.6	41.7	34.9	29.3	25.9	17.8
78.57	121.5	60	53.4	49.2	37.4	31.2	25.7	21.3	17.7
76.66	292.8	195.6	131.7	86.9	45.5	31.8	24.9	22.3	16.7
74.43	359.8	229	158.1	103.9	54	34.9	27.6	22.4	19.4
77.14	351.8	239.4	174.9	122	61.5	38.1	28	23.6	21.7
75.23	390.3	249.5	178.8	120	58.6	37.6	27	25.6	17.2

APPENDIX B – DEFLECTIONS FOR AIRPORT A (200KN-LOAD, FREE OF OUTLIERS)

Load	D_0	D_1	D_2	D_3	D_4	D_5	D_6	D_7	D_8
195.78	301.5	254.3	237.4	217.9	174.7	146.7	121.7	99.2	80.7
193.71	602.7	316.3	261.8	240	192.8	161.6	131.8	108.9	92.6
193.4	470.2	239.9	218.1	204.9	174.9	155.5	129.6	110.4	92.1
189.74	331.5	271	237.8	203.7	152.8	123.9	99.2	80.5	64.3
191.49	385.5	331.9	298.1	259.6	201.9	166.1	131.3	104.1	84.4
190.53	479.2	395.6	353.7	308.2	227.9	180.6	136.4	105.3	81.3
189.58	567.8	431.9	358.5	312.9	230.4	182.6	139.9	110.1	87.9
182.26	520.8	326.3	281	249.6	192.7	157.9	127.9	103.8	85.3
190.69	533.4	325	268.1	239	189.7	158	123.3	102.7	81.8
189.26	445.5	313.1	261	234.8	179.1	146.8	115.8	96.5	79.1
182.58	574.3	416	315.1	271.9	193.4	142.6	113.5	88.8	74
191.96	562.8	332.6	295	255.2	192.4	157.9	120.1	98.9	75.3
190.69	435.2	302.4	260.3	228.7	174	140.2	110.4	86.9	71.5
188.31	427.6	300	264.6	233.2	176.8	141.7	112.9	90.6	72.6
186.08	422.2	301.9	264.4	230.4	171.3	137.3	106.8	84.4	67.3
192.6	412.7	273.7	235.3	207.3	155.7	125.8	99.8	79.1	65
189.1	461.3	331.2	269.9	230	167.3	132.3	102.7	80.9	67.5
192.12	378.1	251.4	208.2	185	144.5	118.4	95	77.7	64.8
192.76	545.7	356.5	290.2	245.7	178.2	138.2	104.4	82.6	66.4
194.35	272.3	223	208.7	181.2	141.5	116	93.2	76.9	62.5
189.74	475.2	267.2	228.9	203.1	152.9	123.6	100.9	77.4	61.7
194.35	341.3	253.7	224.2	196.1	147.5	119.5	94.2	74.6	62.5
187.67	474.3	316.7	245.9	214.1	154.5	121.6	92.3	74.5	63
195.46	275.2	214	192.3	170.2	131.9	112.2	88.7	73.9	59.6
193.71	422.7	265.4	224.2	197.6	147.2	123.4	95.5	75	67.2
190.69	394.7	315.4	268.7	225.5	160.5	125.4	95.2	79.6	65
191.81	461.7	314.4	260.1	221.8	162	130.6	103.5	83.6	68.3
192.76	391.6	280.2	247.6	215.7	162.6	130	105.1	86.7	71.4
191.17	379.7	284.3	245.4	211.9	158.7	128.6	103.2	84.7	69.6
186.88	484.2	308.8	247.7	213.2	158.7	126.2	100.3	91.2	71.5
191.33	312.5	241	210.5	181	134.1	110.1	89	75.4	62
191.01	388.6	279	223.4	186.3	137.1	109.7	89.4	73.4	60.8
191.49	386.5	243	204.6	173	126.5	101.5	80	64.7	54.6
185.44	297.4	238	195.1	169.7	124.3	97.8	73.5	61.3	53.1
189.42	328.9	216.6	179.2	154	111.3	88.2	68.1	56.8	47.3
190.69	330.4	239.8	200.3	170.7	123.8	97.6	77.6	61.4	51
191.81	469.9	285.5	233.3	199.8	141.3	110	85.3	66.8	57.8
192.76	434.8	312	255.6	213	149.3	114.9	88	68.7	55.4
190.53	524	343.2	265.7	226.8	159.6	124.2	94.6	72.8	61.8
193.56	416.3	263.8	217.7	182.9	129.1	99.6	75.7	59.9	48.2
188.47	480.7	325.6	268.3	222.7	153.6	118	88	69.4	54.6
192.12	496.2	314.8	260.4	224.9	161.2	124	93	71.1	58.7
191.65	598.3	327.2	262	228.8	164.9	126	96.6	75	63.6

193.71	402	223.8	173.6	154.6	120.9	102.9	82.6	70	56.9
195.62	519.9	257.8	211	184.6	139.1	110.8	88.2	69.9	58.3
195.46	540.4	262.3	202.7	169.1	123.1	100.1	80.6	64.4	57.1
193.08	341	226.6	186.9	155.2	108	82.7	63.1	50.1	40.5
194.83	557.5	274.2	209.6	176	119.9	91	69.3	55.5	45.7
192.12	340.8	251.2	210.8	175	117.5	88.7	65.5	51.6	40.3
190.06	332.6	248.5	198.2	158	102.3	75.2	55.8	44.4	40.5
193.08	431.3	305.6	242.2	186.6	114.2	81.1	60.4	47.4	37.7
188.47	346.3	272.4	226.9	183.3	118.8	85.4	61.8	48.4	40.4
194.99	370.9	252.1	209.7	169.4	106	80.3	55.1	46.6	38.9
192.6	361.4	264.4	213.6	168.2	108.8	80.3	62.2	49.4	38
193.56	326.3	245.9	202.7	165	106.3	80.2	57.1	45.8	38
191.81	306.7	252.3	208.4	164.3	101.4	67.8	47.7	36.1	29.4
188.94	326.9	251.9	207.9	162.9	98.1	66.6	47.3	35.6	28.7
194.03	322.4	243.1	193.3	151.9	97.6	70.3	53.4	41	35.8
192.92	279.3	224.8	185.9	151.4	101.2	74.9	55.5	43.2	35.7
193.4	264.5	209.4	180	144.6	97	73.2	54.7	44	35.5
195.46	218.4	162	137.6	116.2	86.6	70.4	57	48.2	41.1
192.92	153.6	137.9	129.4	120	99.9	86.8	72.8	61.9	51.4
195.94	238.7	150.2	135.8	126.1	104.3	89.4	74.6	60.8	51.9
196.9	354.3	148	135.9	124.7	95.7	79.9	65.5	53.9	45.8
190.85	864.6	583.5	403.3	268.8	130.4	87.1	66	55.7	47.7
186.56	958.2	611.3	432.5	296.4	149.6	96.2	70.5	58.1	49.8
191.33	947.9	674.7	505.1	360.8	180	108.2	72.1	58.5	51.7

APPENDIX C – DEFLECTIONS FOR AIRPORT A (280KN-LOAD, FREE OF OUTLIERS)

Load	D_0	D_1	D_2	D_3	D_4	D_5	D_6	D_7	D_8
281.67	452	357.2	334.6	306.3	246.1	206.2	173	143	114.1
278.8	798.8	430.8	362.6	331.9	268.2	225.7	183.9	152.6	130.1
279.92	522.3	332.5	309.4	285.8	243.5	218.4	179	153.3	131.6
274.19	453.8	379.4	336.1	288.2	216.5	177.3	141.5	117.9	97.7
276.42	533.4	461.6	417.1	361.3	281.8	236.9	186.3	154.6	115.4
275.94	650.6	543	486.1	425.9	316.7	254.1	195	155.2	122.2
272.76	787.6	585.1	491.8	432.2	322.1	253	200.3	164	130.1
262.42	730.3	453.7	399.9	353	272.9	222.5	180.9	148.1	120.1
271.8	944.4	436.9	374.3	336.3	266.2	220	176.5	145.2	116.2
270.53	608	430.1	371.4	330.1	256.2	204.1	165.6	123.5	100.1
265.76	810.6	570.4	451.2	391.1	282.2	214	169.3	132.6	106.8
276.42	754.5	454.9	409.5	357.6	270.5	219.5	173.1	144.3	110.9
275.14	594.7	424.5	367.1	329	249.7	201.9	160.9	127.6	104.1
271.17	594.7	425.7	375	331.8	255.6	205.9	164.7	131.2	106.8
268.78	588.9	424.3	374.6	327	246.1	198.6	155.2	124.3	100
278.17	556.1	391.9	341.1	303.4	228.4	187.4	147.3	119.7	98.4
272.92	639.7	460.2	384.9	329.2	242.5	193.3	152.2	120.2	99.1
277.21	740.4	358	300.4	269.7	213.5	174.8	140.9	117.7	94
277.85	737.9	490.3	406.3	347.6	256.2	203.5	158.9	122.4	97.9
279.92	389.7	327.8	300.6	268.4	210	173	139.8	116.3	95.5
274.19	652.4	378.5	333.9	295.2	224.7	182.3	143.2	115.8	92.2
281.35	485.3	365	321.8	285.3	216.4	177.7	141.2	114.5	93.1
271.17	649.7	442.7	352	306.3	225.1	177.7	137.7	111.3	91.8
282.94	402.3	314.8	282.9	252.5	198.6	165.8	133.8	110.9	90.1
278.33	688.8	380.3	324.4	287	216.7	177.2	141.8	114.5	98.2
275.46	548.2	445.2	380.6	323.6	234.1	181.8	140.5	115.8	92.6
278.01	650.1	446.1	370.8	321.7	238.6	189.4	150.5	124.5	102.4
278.48	646.8	399.1	353.8	311.7	235.6	190.8	153.1	126.4	101.9
277.21	540.8	398	345.8	299.8	226.3	185	149.3	123	101.1
270.21	679.5	433	355	308.1	228.4	187.3	145	128.3	104.2
275.78	445.9	340	300.8	259.2	192.9	159.2	128.4	107.2	90.7
275.94	541.1	388.4	317.2	267.2	198.3	161.1	128.4	106.9	86.3
277.21	561.4	348	292.4	249.7	185.1	147.1	117.9	99	79
268.46	417	326.6	278.3	238.5	178.1	142.9	108.4	88.3	80.3
273.55	528.8	312.7	260.6	227.3	163.8	128.2	99.7	82.9	67.9
274.83	469	348.9	295.5	252.6	184.3	146.1	116.7	93.6	75.1
276.58	630	404.5	337.3	292	208.6	165.7	127.2	102	79.3
277.37	618.5	443	365.8	311.2	220.7	171.4	130	104.3	83.1
275.46	724.2	473.7	382.4	327.5	238.1	183	141.3	113.5	93.4
279.92	568.1	378.3	316.6	273.1	191.3	149.7	112.8	91.6	72
272.6	670.7	462.1	390.3	322.6	226.3	174.4	131.8	104.3	84
277.85	665.4	456.4	380.2	333	242.4	187.4	143.3	112.7	90.4
277.21	1076.5	463.6	379.7	337.7	242.2	185.4	144.1	114.8	90.8

278.17	930	430.5	326.5	262.9	167.6	115.5	82.6	67.3	51
276.58	651.6	409.1	304.6	253.8	173.4	129.4	98.9	76.1	59.9
278.64	986	458.8	369.4	300.7	193.8	138.2	100.6	75.8	60.9
276.42	763.8	481.4	389.7	326.2	227	169	119.6	95.1	75.2
280.23	496.1	357.9	306.2	257.5	185.1	145.1	109.5	88.6	66.8
277.05	759	503.9	409.5	341.2	232.2	169.1	124.1	93.6	72.6
274.83	802.4	506.3	402.4	329.1	221.8	169.3	128.3	99	75.9
279.44	711.8	512.3	433	359.6	245.9	181.1	131.1	102.4	82
277.85	659.9	468.2	392.5	327.3	231.8	173.8	130.8	99.4	79.2
274.83	631.2	418.9	361.3	307	215.7	166.6	126.4	98.6	75
277.53	760.2	524.5	422.6	351.1	240.3	174.4	123.4	99.8	76.2
280.07	510.2	405.7	355.4	311.6	231	181.5	139.1	107.9	85
282.3	445.2	356.5	314.5	277	210.4	166.2	129.6	103.7	83.8
281.35	578.1	348.3	308.3	263.8	197.8	155.7	120.4	95.2	74.9
279.12	578.1	458.7	388.8	322.6	227.2	175.1	133	104.5	81.7
281.19	521.8	399.4	344.5	298.3	221.3	174.1	133.8	105	82.8
282.46	431.1	347.3	304.5	267.4	200.7	159	122.4	97.7	74.6
280.55	567.7	339.2	301.9	264.4	203.5	166	131.1	105.3	85.6
281.35	395.5	312.9	280.4	250.9	191.6	156.6	124.2	100.6	80.3
283.26	414.3	321.8	283.4	247.7	189.1	155.3	123.1	99.9	81.8
281.98	412	317.1	281.1	252.1	194.7	160	128.1	105.4	83.7
274.51	699.1	304	245.7	221.5	174.1	145.1	122.2	102.3	80.2
280.55	731.1	354.9	295.9	258.7	199.1	163.7	130.5	107	86
281.51	801.3	363.8	283.2	251.6	177	145.2	117.5	97.9	80.4
279.28	519.6	329.2	274.6	229.6	160.6	125	95.2	78.3	62.3
278.64	892.6	391.2	301.9	256.9	177.4	134.1	100.4	82.2	64.9
276.58	496.9	362.6	307.4	254.9	172.5	131.6	98.6	75.9	61.5
275.62	487.9	364.3	292.8	234.5	153.5	113	85	67.9	57.2
277.05	628.3	436.3	345.6	269.7	167.9	121.5	91.3	71.9	58.6
272.6	522.9	398.2	333.7	271.8	177	127.4	93.2	73.3	60.7
282.3	547.9	374.4	307.2	246.9	160.3	118.5	86.9	69.3	57.2
278.33	525	385.4	312.5	247	163.1	121.6	92.6	74.8	62
279.28	489.4	357.3	294.6	242.7	160.1	118	86.8	68.4	56
278.33	452.7	369.4	307.2	244.2	150.6	104.2	72.8	56.2	45.7
273.87	481.5	391.5	310.5	244.7	150.1	108	72.8	55.7	42.5
280.07	472.2	353.6	282.7	223.1	145.1	105.3	78.5	61.2	51.9
279.6	420.1	327.6	270.3	221.8	148.7	110.6	82.4	64.5	53
279.6	390.9	302.3	259	212.7	144.5	107.5	80.2	66.3	55.5
283.89	325.4	237.6	200.6	168.4	128.6	103	82.4	71.6	61.2
277.85	212.4	195	181	168.4	140.4	121.1	102.3	87.9	73
280.71	350.9	210.3	189.7	177.8	146.2	125.2	104.3	86	73.7
283.89	481	210.7	190	176.1	134.4	113	92	77.4	64.5
272.12	1231.9	831.8	579.6	394.9	196.9	131.1	97	81.9	70.6
264.49	1448.2	920.9	653.8	448.4	227.4	143.2	102	83.8	70.2
274.99	1349.9	969.5	735.8	534.2	274.2	164.4	107.1	85.9	75.6

APPENDIX D – DEFLECTIONS FOR AIRPORT B (80KN-LOAD, FREE OF OUTLIERS)

Load	D_0	D_1	D_2	D_3	D_4	D_5	D_6	D_7	D_8
80	185.2	134.7	113.5	96.7	72.8	59.4	48.3	40.5	34.4
81.11	221	118.5	98.5	86.9	67.9	56.7	46.9	39.9	34.8
81.27	189.9	124	98.9	85.2	66.9	55.8	46.5	39.6	36.6
79.84	154.3	109.3	88.9	75	58.1	46.5	39.3	32.1	27.6
80.16	167.2	106.9	86.9	73.7	57.7	47.8	40.2	33.2	28.4
79.68	156.3	112	91.2	78.1	59.9	49.4	41.2	34.7	29.6
78.09	139.4	114.6	87.9	74.6	56	45.8	39.1	33.2	29.5
80.63	208.4	138.3	108.6	85.9	63.1	55.2	43	40	34.9
80.48	172.1	121.1	99.4	85.5	66.9	56.1	47.7	41.3	35.5
80.32	269.6	172.2	133.1	111.3	83.5	71.2	58.2	50.5	42.4
79.84	285.1	163.4	122.6	99.1	74.8	61.5	51.7	43.7	36.3
79.36	278.5	170.1	121.7	95.3	69.9	58.3	49.7	42.2	36.3
80.63	242.8	153.6	112.6	90.5	66.9	55.8	46.7	40.7	34.4
79.84	212.7	149	120	100.9	76.5	62.8	54	44.4	39.4
80.32	227.2	145.8	119.5	98.6	73	59.8	50.3	42.8	38.4
79.84	251.2	169.1	128.7	105.1	77.5	67.6	55.6	46.7	40.6
80	310.8	163.2	127.3	103.8	77.9	64.8	54.4	45.7	39.1
78.89	389	186.3	140.3	118.1	86.5	71.3	59.2	49.8	42.2
80	232	169	139.2	119.8	95.1	80	66.6	56.7	48.1
80.63	216.3	177.2	149.6	129.5	101.9	87.6	75.1	63.4	54
79.84	321.5	178.6	145.8	124.7	100.7	86.1	70.4	60.4	52.5
79.52	309.7	193.6	152.1	127.4	99.2	82.7	72.4	59.6	49.2
79.52	293.8	165.4	135.8	113.3	84.8	69.2	55.6	46.2	38.6
80	228.3	133.8	109.5	92	68.1	55.4	44.9	36.7	31.4
80	139.5	106.7	94.6	80.9	62.6	53.4	43.7	37.3	31.1
79.84	173.6	116.5	100.8	88.3	70.9	59.5	51	42.8	33.8
80	217.6	123.5	98.7	89.1	71.7	59.2	50.5	41.7	34.5
79.84	210.6	113.7	91.2	81.1	67.7	58.1	50.9	42.5	37.9
80.32	161	96.1	82.8	75	62.8	54.7	47.7	41	35.8
80	163.4	105.8	90.4	81.1	66.7	57.5	49.7	43.5	35.9
79.36	194.5	109.9	88.5	81.3	67.8	58.2	52.2	45.6	40.3
80.16	126.3	97	82.5	74.1	62.1	54.6	48.1	42.6	37.4
79.52	135.5	93.8	83.6	76.3	65.1	58.8	51.5	45.3	40.7
78.57	154.4	104.8	90.9	81.7	66.6	57.4	48.5	38	37.5
79.84	210.5	139	108.3	92.4	72.5	59.5	51.2	43.8	36.9
80.63	221.6	137.4	112.8	98.8	78.6	67	57.2	48.3	42.8
79.84	242.5	148.2	121.8	107.5	87.7	72.6	62.1	55.3	47.5
80.48	180.9	126.1	104.1	91.7	70.9	60.7	53	45.2	39.3
79.52	221.5	133.6	108.6	95.9	76.7	65.5	56	47.7	42.2
79.52	164.9	112.9	94.9	82.6	67	57.1	48.9	42.6	37
80.32	127.1	101.8	90.2	79.6	65.6	56.6	49.4	42	36.5
79.68	205.5	132.8	104.6	88.2	72.8	63.3	55.1	47.3	39.7
79.84	255.1	151.6	114	95.2	72.7	59.3	51.7	43.9	39.5

79.36	321	231.8	180.2	151	111.1	86.3	66.9	52.7	40.2
79.36	496.9	329.9	232.5	181.5	116.7	84.5	60.6	46.1	38.3
78.57	348.5	249.5	191.4	157.5	108.9	83.4	63.3	49.6	41.5
80.79	282.7	225.6	188.2	156.8	111.3	90.2	74.4	61.3	52.2
78.25	330.6	260	214.3	173.2	123.4	96.3	76.3	61.7	57.5
79.84	315.3	242.6	195.9	159.4	114.3	92.1	73.4	60.9	52.2
79.2	327.7	248.8	197.5	160.9	114.7	89	71.8	59.1	50.2
80.48	270.7	211.7	174.8	149.5	109.1	87.5	71	57.3	49.6
80.32	275.3	225.3	192.4	159.7	116.8	92.3	76.8	62.4	53.4
79.2	226.8	183	154.7	131.2	101.5	83.8	69.7	58.3	50.2
80	226.4	186.9	166.2	146.8	115.5	96.7	78.7	64.8	54.9
80	234.4	191.8	164.6	141.8	107.9	88.9	72.8	61.3	51.4
80.16	218	177.3	153.7	137.9	109.2	92.7	75.7	64.4	55.2
81.11	234.6	202.3	178.2	154.2	119.6	96.6	78.7	64.9	54.6
80.63	194.2	168.8	152	137.8	117.4	99.5	81.2	64.7	57.2
81.43	136.5	115	107.3	102.7	90.5	80.4	69.5	59	51.3
80.32	152.8	134.8	123.5	114.7	98.4	85.8	71.9	59.5	51.7
80.48	233.7	186.2	159	137.6	106.4	87	68.2	53.9	44.7
79.52	383.5	305.3	251	200.5	131.1	92.8	69.1	54.9	45.5
80.16	368.2	297.8	246.4	199.6	133.1	96.4	73.7	59	50
81.27	365.8	294.6	243.8	196.2	130.2	96.1	74.5	60.4	51.5
80.48	366.3	304.7	255.1	211	145.2	109.4	84.8	68.2	57.6
80.32	391.8	317.6	269.5	219	153.6	115.7	89.4	71.2	59.7
80.16	315.2	275	238.1	202	149.6	116.8	94.3	76.9	65.4
79.2	301.9	257	222.8	186.6	136.2	107.5	83.7	68.2	58.7
79.52	330.8	268.6	216.3	173.3	117.4	89.8	70.3	57.4	50.2
79.84	300.7	264.3	227.8	191.6	138.7	108.7	85.9	69.6	60.6
80.48	334.9	276.9	231.8	182.5	126.9	99.3	79.1	64.9	57.1
79.36	411.1	322.5	257.2	198.9	131.5	103	82.7	69.9	60.9
79.84	327.1	272.8	232	191.4	136.9	105.5	81.1	66	53.5
79.2	321.4	280.8	241	203.4	146.8	112.8	87.9	70.1	59.5
78.89	408.7	324.8	248.4	195	130.1	101.1	84.7	70.9	59.1
77.45	367	310.4	253.9	207.1	150	115	91.4	75	61.8
80.16	308	246.7	199.4	159.3	112.6	90.7	75.2	63.6	56
77.61	290.5	250.8	214.4	182.4	136.7	107.2	87	72.1	63.4
78.41	343.7	279.1	239.9	202.4	143.4	110.7	88.6	70.9	58.8
79.52	330.5	271.1	236	198	142.5	109.1	85	68.1	56.5
81.11	271	238.6	208.5	178.2	134.5	105.4	83.2	67.5	56.5
80.95	239.9	216.5	191.7	168.5	128.7	105.8	85.7	69.2	58
80.16	293.5	248.6	215.1	179.2	132.7	106.7	84.3	68.4	56.7
79.84	389.7	307.7	247.8	198.7	137	104.1	81.4	67.5	57.8
80.48	360.9	291.6	240.6	198.4	142.6	111.4	88.6	73.3	62
80.79	260.7	226.2	197.6	174.9	134.4	109	88.9	73.6	63
79.68	291.7	248.4	211.4	173.2	121.8	95.3	77.9	65.4	55.4
80	405.2	328	256.8	200.1	136.1	105.7	86.3	71.9	62.2
80.63	275.6	234.8	204.2	174.9	133.5	107.5	86.7	73	63.7
78.57	697.6	457.6	309.7	201	111.5	86	71.5	63.9	54.7
77.29	752.1	552.4	385.7	266.7	160.9	121.5	98	82.9	70.4

APPENDIX E – DEFLECTIONS FOR AIRPORT B (200KN-LOAD, FREE OF OUTLIERS)

Load	D_0	D_1	D_2	D_3	D_4	D_5	D_6	D_7	D_8
202.62	480	349.5	300.7	258.4	196.6	157.4	127.2	104.5	87.5
203.58	569.8	323.7	271.5	241.4	188.8	155.9	126.1	104.7	87.7
203.26	494.3	323.9	266.5	232.4	180.1	148.3	122	102	86.4
201.83	411.5	295.3	246.8	209.7	161.5	130.2	106.5	86.6	72.3
202.3	429.6	292.8	243.1	207.2	160.5	131	107.2	87.6	72.9
201.98	402.4	296.1	248.6	212.6	161.7	134.1	107.9	89.7	76.3
197.05	376.7	301.2	241.8	204.1	154.2	123.8	103.4	84.9	73
202.14	562	386.3	312.6	254	183.4	147	117.4	98.2	85.8
202.62	465.8	329.6	276.4	239.2	185.9	151.9	125.7	104.2	89.5
201.03	716.1	476	378.3	314.6	234.7	189	155.5	128.8	107.1
201.03	745.2	434.5	339.3	280.3	204.7	165.5	135.7	112.2	94.7
200.08	735.1	467.8	349.5	277.1	195	156.5	127.9	107.1	93.7
201.67	642.8	424.3	323.7	261.2	191	151.8	123.2	102.8	85
201.19	556.4	410.6	339.8	285.7	213.7	170	138.8	112.2	95.8
202.14	591.6	400.5	332.4	281.7	204.4	163	132	109	90.9
199.6	653.9	456.2	359.9	298.3	219.1	174.9	141	116.7	97.7
200.39	788.3	459.7	364.2	297.4	214.6	171.8	139.8	113.7	95.6
198.49	922.8	491.4	383.5	322.4	232.7	179	143.3	115.7	95.8
200.39	600.4	440.6	370.9	316.7	248.3	201.8	163.7	136	111.6
202.3	545.3	445.5	380.3	330.9	257.6	214.7	178	147.5	123.5
201.03	787.9	456.9	379	327.3	254	206.8	170.2	141.3	117.5
199.28	785.2	500.6	403.7	339	257.2	210.2	170.3	140.4	121.9
200.55	755.7	433.2	368.1	311.4	232.9	183.5	144.8	116.7	94.3
202.3	615	370.3	307.7	260.6	191.3	152	120.4	99.7	78.8
202.14	398.1	288.5	256.5	221.4	169.5	139.6	114.1	95.5	78.6
199.6	460.7	305.2	263.5	234.6	187.8	158.5	131.3	111	91.2
201.51	568.7	327.1	268.5	241.7	193.8	158.7	130	107.5	91.2
203.89	521.8	292.4	245.1	219.6	180.2	154.2	131.5	112.2	94
203.89	405.2	250.6	219.5	198.3	169.3	143.8	123.8	105.7	91.9
203.42	437.4	278.4	245.3	220.3	174	149.9	128.4	109.7	92.4
202.3	515	284.7	232.5	213.9	177.1	150.5	129.9	112.8	95.7
203.1	340.5	253.9	218.3	197.2	164.4	141.8	122.9	107.6	93.2
201.19	333.9	238.7	214.1	195	166.3	146.4	128	112.5	97
199.44	418.5	285.4	246.4	220.2	178.5	151.2	127	104.4	93.1
201.03	553.5	371.2	301.3	259.1	198.1	158.3	129.8	107.2	89.9
202.46	570.6	364.8	304.2	267.8	211.6	173.6	144.3	119.3	100
202.78	599.7	378.6	319.1	282.6	225.4	188	157.2	132.9	113.8
203.58	458.4	323.3	275.9	238.6	190.4	159.5	132.8	112	95.1
201.35	551.6	353.7	291	262.8	208.6	173.8	144.9	122.1	103.8
201.83	445	301	257.4	224.3	177.3	150.7	125.8	105.5	91.3
203.73	333.3	265.9	238.9	211.4	173.2	148.7	126.1	106.3	91.9
201.03	532.5	343.8	283.1	242.8	193.6	164.8	138.1	117.6	100.2
201.67	647.6	403.8	314.8	268.7	203.1	164.1	134.6	111.1	94

199.92	820.6	590.1	473.5	400.7	295.6	230	176.8	134.8	103.8
199.28	1254.2	851.4	628.3	493	321.4	223	158.7	117.9	91.7
198.96	884.2	644	510.6	423	303.4	229.8	170.2	133.5	103.1
202.3	728.7	586.2	497	414.4	308.2	243.4	191.1	157.2	128.8
197.69	880.2	675.3	562.7	464.2	334.7	258.7	204	167.2	137.6
200.71	819.8	648.8	534.3	439.3	317.7	245	197.6	162.5	134.2
200.08	824.2	641.4	523.6	436	310.7	240.7	192.1	151.2	126.1
201.51	715.2	570.9	482.1	408.4	301.2	234	182.6	144.2	118.2
202.62	697.1	568.1	486.9	409.1	300.7	234.7	189.4	150.8	124.1
200.24	581.5	458.3	390	335.3	261	212.2	172.5	141.4	118.4
202.3	572.2	466.7	416.4	367.6	287.6	234.8	191.1	154.1	128.5
201.51	608.9	498.3	431.5	372.9	287.3	230.9	186.6	152.9	128.1
200.87	598.9	484.1	421.1	369.1	290.3	237.4	193.7	157.7	132.2
202.94	606.7	516.4	455.2	395.8	310.2	243.9	194.4	155	125.2
203.42	487.8	428.8	386.8	352.9	298.3	255.7	198.7	154.5	126.7
205.64	328.9	273.2	257.7	244.1	214.8	190.5	164.2	139.5	115.8
205.01	385.1	317.1	292.3	270.2	232.8	201.1	169.7	140.9	116.8
202.3	573.2	459.8	394.6	342	262.7	207.4	155.6	118.9	100.2
199.44	905.1	723.7	600.7	485.2	321.6	223.9	163.4	127.6	106.3
201.35	896.4	723.2	605.5	495.2	334	238.9	177.6	138.8	113.9
204.21	877.1	710	592.6	480.9	323.7	232.1	174.7	137.5	114
201.03	881.9	724.9	612.9	508.9	353.7	261.1	197.4	155.2	127.7
201.67	931.4	754.5	638.7	527.9	373	276.7	208.3	164.4	134.2
202.14	835.4	695.3	606.4	518.8	385.8	299.8	235.8	188.2	154.2
200.08	753.5	636.3	550	468.4	345.7	266.6	207.3	164.4	135
199.76	804.3	659	544.7	442.2	305.3	222.2	168.7	132	111.2
202.14	760.6	654.6	569	482.4	353.1	271.3	213.8	171.9	141.6
201.98	839.2	681.2	568.4	461.7	325.5	247.2	192.6	154.6	129.6
199.28	970.3	760	616.8	490.7	331.3	251.7	199.3	164.9	140.3
201.35	803.7	663.1	563.1	473.3	339.1	254.1	195.5	152.1	124.9
200.71	818.3	684.2	593.8	502.8	365.5	277.3	211.1	166.3	135.2
197.85	961.9	773.6	612.7	488.4	330.6	250.5	201.7	165.4	135.6
195.15	893.1	746.8	620.1	514.7	373.8	284.3	219.9	173.2	141.6
201.98	726.1	574.4	475.8	394	287.6	230.9	188.5	157.5	133.5
196.58	744.6	640.7	551.5	473.2	352.7	278.1	217.9	177.2	147
196.58	865.7	696.2	602.4	512.4	370.8	282.4	217.3	170.9	137.9
200.71	818.3	676.1	586.7	498.1	361.3	275.5	210.2	164.3	132.1
204.05	707	604.1	530.2	457.9	344.6	270.1	209.1	164.6	132
202.78	647.2	550.9	491.9	433.1	335.4	268.7	216	173.3	142.3
202.94	734.3	615.8	531.4	450.7	338.1	268.3	210.7	167.3	134.5
200.24	921.5	741.8	608.8	498.9	354.6	266.3	206.5	163.6	134.1
201.83	887.1	708	593.7	497.7	365.4	285.1	224.6	182.9	151.9
202.94	695.3	600	528.3	460.4	356.6	285.7	228	186.2	154.9
198.8	739.5	620.8	531.9	441.9	314.2	242.3	193.1	158.6	134.1
200.24	987.6	779.3	624.9	490.6	326.6	243.6	195.8	164.3	142.5
202.62	730.8	607.3	525.7	448.7	336.2	265.2	210.5	171.9	144.6
191.01	2180.3	1429.6	970.9	624.7	316.6	226.3	184.9	156.3	134.5
191.96	2319.2	1497.8	1038.8	709.8	411.4	298.6	236.6	197.3	165.2

APPENDIX F – DEFLECTIONS FOR AIRPORT C (80KN-LOAD, FREE OF OUTLIERS)

Load	D_0	D_1	D_2	D_3	D_4	D_5	D_6	D_7	D_8
87.24	112.5	100.7	92	82.5	66.2	51.5	38.6	32.4	25.3
84.29	118.6	110.2	101.8	92.5	73.6	61	45.3	41	32.3
82.99	634.4	377.5	246.7	163	70	45.1	38.9	31.9	22.5
84.69	459.1	277.3	190.6	129.6	67.4	49.7	40	33.7	31.1
85.14	329.3	220.6	157.6	118.7	70.2	56.1	45.8	37.4	33.6
84.26	404.3	283.4	204.6	146.9	86.2	64.8	52.8	44.8	39.3
83.7	541.4	342.8	229	159.1	94.2	72.6	56.9	48.2	41.3
84.5	390.9	271.1	202.6	154.4	100.9	77.8	62.5	53.4	44.5
84.66	349.3	220.6	169.5	127.7	80	63	51.1	45.1	37.9
84.02	427.6	277	200.2	144.4	91.7	67.7	56.5	50.1	40
84.93	445.3	274.9	206.8	151.5	93.9	72.1	53.4	46.8	41.2
85.17	332.6	199.5	148.5	109	64.6	48.8	40.9	37	31.5
83.86	467.8	300.2	203.5	132.3	60.5	33.4	23.6	19.8	16.7
84.85	395.3	258.4	181.5	126	61.6	36.4	21.9	18.5	15.5
83.9	336.1	233.9	174.7	122.3	63	38.5	22.4	18.2	15.6
84.29	268.1	184.2	136.2	96.6	51.4	31.8	19.1	15.6	12.3
85.33	306.7	207.7	153	107.9	52.6	30.5	19.5	19.1	15.3
83.55	285.2	188.6	135	96.6	52.9	36.7	27.9	22.5	18.5
84.74	279.6	194.3	147.2	108.9	62.1	40.2	28.2	25.5	19.7
84.13	317	231	177.5	134.5	77.8	51.1	39.6	32.5	27.5
82.7	307	207.8	152	109.7	64.6	48.2	37.1	33.8	28
84.5	344.6	233.6	181.5	134.5	91.6	64.6	50.6	40.5	38.7
83.15	340.5	249.1	194.9	150	100.4	75.4	59	51.9	44.1
81.64	322.5	239.8	180.8	138.2	92.9	70.3	55.4	47.5	41.5
83.86	389.7	286.9	223.5	172	114.3	79.2	59.7	50	42
82.78	363.6	252.1	191.7	148.3	95.9	72.6	57.7	49.4	41.3
84.66	278.4	220	182.2	147	96.9	68.7	53.9	46.2	41.6
83.31	440.6	333.2	255.9	196	119.2	88.1	64.2	55.5	42.5
83.5	578.9	414.6	310.7	225.5	131.8	86.9	63.6	54	44.5
83.26	411.7	300.3	231	180.4	115.4	82.3	58.6	49.2	40
83.26	536.4	381.6	285.9	208.7	121.4	81.2	59.4	49.1	44.6
83.18	406.3	275	196.9	143.7	93.1	66.7	52.9	41.9	37.5
80.4	487.3	370.7	274.9	208.8	118.2	83.9	65	54.8	51.9
83.66	438.1	315	245.6	188.8	125.1	87.6	64.7	52.2	44.9
82.15	534.8	350.5	250	181.3	106	75.2	56.3	51.4	44.6
82.19	551.5	413.5	300.4	216.8	129.4	92.3	67.7	54.8	49.3
83.26	563	402.2	294.1	212.5	122.6	86.7	66.8	55.8	50.4
83.39	479.2	329.8	253.7	191.9	119.3	83.8	61.9	51.4	42.6
82.67	450.7	311.5	229.3	169.4	111.4	81	60.2	54.7	47.7
83.9	486.6	336.3	256.9	195.5	123.4	90.4	64	54.3	46.2
81.72	580.6	435.6	338.6	254.8	156	102.3	69.2	60.7	49.6
82.94	592.6	424.4	311.8	232.5	143.9	95	71.6	59.9	48
82.15	599.7	415.5	300.4	218.1	135.4	90.2	69.2	58.3	55.1

84.77	453.1	342.4	273.5	208.5	135.1	98.3	71.7	60.2	48.8
83.47	426.7	313.2	244.7	191.1	118.3	97.2	65.9	55.8	45.3
82.7	504.3	345.8	228.6	154.1	90.7	80.6	60.2	48.3	46.1
82.51	504.6	338.6	250.3	189.2	125.7	92.3	73.2	58.2	51.7
82.7	540.7	352	277.8	222.6	150.6	112.4	83.3	67.9	56.2
83.5	590	375.9	285.5	219.1	139.7	107.8	79.1	67.7	57.1
84.13	458.8	369.5	291.4	231.1	153.6	112.2	82	66.4	56.3
82.23	383.1	295.8	236.9	190.7	131.7	97.9	74	60.1	48
81.75	432.3	318.2	255	203.7	134.2	96.8	76.8	61.4	52.5
83.55	562.7	371.3	279.3	212.8	137.9	104.1	78.6	63.2	49.7
82.54	701.3	406	302.6	225.4	142.2	103.8	77.8	63.7	52.6
83.94	532	388.4	298.6	234.1	149.1	108.9	80.2	66.4	49.7
81.03	435	320	245.4	194.7	130.3	96.8	72.2	59.4	49.9
84.26	564	397.2	297.9	232.9	154.6	109.1	81.8	66.1	64.1
84.69	415.1	308.9	247	196.9	128.1	95.8	69.2	59.3	49.8
83.82	486.9	339.8	248.2	182.8	114.6	87	69.7	55.4	49.8
82.38	617.9	445.6	354.9	273.4	167.2	120.7	80.6	71.7	54.5
83.5	614.7	446.1	327.7	246.2	161.5	115.5	84	68	60.7
84.1	698.7	395.8	315.6	245	169.5	116.9	90.3	72.9	64.4
82.43	590.4	460.4	362.5	288.7	187.1	136.8	98.3	78	64.1
78.3	650.1	452.8	347.1	268.1	175.8	123.8	90.7	77.8	61.7
83.1	542	376.5	300.9	236.5	154.2	115.2	87.4	74.9	63.4
80.6	510.8	384	297.2	231.6	150.4	114.9	83.6	76.8	59.9
81.03	524.8	381.1	291.1	222.1	143.9	101.5	81.4	72.5	57.5
82.46	638.9	415.7	309.2	221.9	140.5	102.8	76.7	64	56.7
83.42	729.1	365.7	250.9	188.8	117.6	88.6	69.5	61.5	53.8
82.23	526.5	360.4	265.4	194.5	123.6	91.3	72.9	61.8	50.7
80.95	536.9	357.5	264.1	177.2	101.6	79.2	64.2	54.7	44.6
79.04	392	279.2	215	162	106.8	76.2	61.5	47.8	40.5
82.19	543	358.8	254.7	182.9	105.8	75	61.8	52.6	44.5
82.38	450.8	308.2	212.7	148	90.2	69.6	58.1	50.3	41.9
84.53	357.4	260.8	199.6	151.3	96.8	69.9	56	47.5	46.5
79.81	511.6	338.5	249.4	183.4	107.6	77.4	64.6	56.1	46.7
85.33	370.3	264.2	200.5	155.3	105.1	78.9	64.3	54.4	44.7
83.02	316.3	240.2	184.2	147.2	97.6	79.2	61	53.8	45
79.97	360.7	257.8	212.5	167.3	110.7	82.1	65.4	54.2	47.7
78.17	378.7	280.4	216.6	172.5	110.1	84.4	69.2	61	49.2
81.83	557.8	378.1	278.7	201.6	121.5	97.8	75.1	58.9	49.7
80.63	414	289.6	233.2	182.6	121.1	92.4	66	59.1	51.1
78.89	433.1	290.7	219.1	172.6	117.5	90.4	71.5	61.6	51.9
78.41	481.8	331.9	251.9	199.8	129	100.5	76.2	64.7	53
84.5	474	385.8	300.4	226.3	142.9	103.3	77.6	65.9	51.4
81.19	438.5	307.5	241.5	195.7	136.5	99.5	77.5	65.6	59.8
82.59	656.5	481.6	374.3	295.2	190.1	137.2	99.2	79.6	66.6
81	526.3	361.9	285.4	227.1	153.8	117.1	89.9	73	57.9
79.92	356.1	268.1	214.2	172.9	123.1	95.3	74.6	64.5	50.8

APPENDIX G – DEFLECTIONS FOR AIRPORT C (200KN-LOAD, FREE OF OUTLIERS)

Load	D_0	D_1	D_2	D_3	D_4	D_5	D_6	D_7	D_8
206.76	273.5	245.6	221.3	200.8	158.5	124.5	87.1	70.7	60.9
203.07	298.2	274.2	251.9	228	184.2	144.4	102	84.9	74
195.46	1543.8	911.7	609	400.8	178.4	88.4	73.6	70.9	63.6
197.58	1133.9	674.7	469.5	326.6	164.1	106.9	86.1	77.6	69.7
200.55	807.6	548.1	397.5	293.6	175.7	128.5	102.7	89	81.3
198.01	1014.1	710.2	519.7	379.4	219.7	159.2	123.9	107	93.3
196.23	1363.1	863	595.5	419.8	238.1	174.3	134.7	116.1	99.1
198.29	1014.9	688.2	519.2	397.9	253.7	191.5	147.3	121.9	106.6
199.09	892.6	566.5	425.7	325.1	203.7	150.1	115.7	100.2	87.2
197.85	1078.1	707.2	514.4	377.9	228.5	164.2	128.4	107.8	101.3
197.26	1119.8	680.2	504.3	375.4	236.4	167	125.3	108	88.6
200.79	838.8	489.6	368.8	271.2	162.1	115.1	89.6	75.9	68.2
197.66	1238.9	739.8	516.5	348.5	155.8	79.8	52.9	46.5	42.7
198.69	1030.1	661.5	476.6	333.7	168.2	85.1	53.7	44.1	40.7
198.45	869.9	609.8	460.2	332.4	175.2	94	57.9	47.1	44.5
201.11	711	485.9	360	261.5	135	78	49.1	40.4	33.8
199.81	842.8	551.1	410.6	295.3	142.9	76.9	47.5	39	38.1
200.08	691.4	475.9	348.6	251.9	138.3	82.8	61.2	52.8	49.8
201.67	671.2	475.2	365.9	274.5	158.2	99.1	70.9	60.9	56.3
199.65	816.3	594.1	454.8	350.8	200.1	126	86.4	74.6	66.6
199.73	925.2	522	385	281.1	157.1	109.6	85.3	76	67.5
199.09	826.3	558.8	431.3	328.2	206.7	148.4	116.2	98.8	88.7
199.89	828.7	585.1	466.4	370.5	249.3	186	142.6	120.8	101.3
198.17	775.9	588.1	457.3	361.2	242.6	177.7	137.4	115.8	101
197.82	913.4	670.6	528.5	411.6	276.4	194.8	141.8	120	107
198.06	909.9	598	457	354.7	234.5	173.7	133.1	113.8	98.2
199.2	649.6	517.4	428.9	347	227.8	166.6	125.4	107.8	96.1
196.47	1070.1	804.6	627.1	485.9	300.7	204.5	149.6	127.5	110.7
194.56	1334.8	948.9	723.8	540.9	327.7	215	154.4	132.4	116.3
197.02	969.7	704.7	557.2	441.1	285.8	199.8	143.8	119.2	99
195.3	1200.8	856.7	653.1	488.8	283.2	185.7	137	117.7	105.9
198.06	957.2	645	475.2	359.1	225.5	166.2	127.9	103.4	87.6
193.95	1592	871.7	668.5	515.3	308.4	207.5	149.9	127.2	113
197.66	1073.4	765.5	612.3	483	315.9	221.9	158.8	129.2	109.3
194.88	1290.9	820.4	608.7	448.9	269.2	182.3	139.2	121.7	107.5
193.92	1298.6	962.3	724.4	548	334	233.6	168.8	139	120.8
195.78	1245.7	896	673.2	506.1	303.6	209.1	158.3	137.1	120.6
197.02	1080.7	742.5	582.9	459.6	298	206.5	149.9	124.4	107.2
196.23	1030.9	710.7	539.6	414.5	268	195.3	151.2	130.6	112.1
197.85	1142.4	771.8	599.1	468.5	303.5	215.9	160.3	135.8	117.7
194.64	1313	973.7	769	594.8	371.3	247	170.2	142.5	127.2
194.72	1349	961.8	732.5	563.3	355.3	242.9	173.8	146	124.8
194.8	1317.1	909.4	678.5	510.3	313.9	218.3	163.5	138.9	119.3

196.47	1175.1	786.3	542.4	376.3	233.1	179.1	140.7	118.7	102.5
194.95	1430.8	803.5	605.5	471	310.7	227.5	172.3	140.7	121.9
194.88	1467.7	896.9	716.3	576.1	387.6	283.5	202.6	163.9	142.4
193.84	1455.4	921.3	709.6	554.4	361.9	263	188.1	157.3	133.7
193.76	1129.3	880.2	699.3	562.6	374.4	269.1	192.6	159	132.9
195.23	948.2	728.1	593.5	484.3	336.4	247.7	178.4	146.9	123.9
195.35	1091.6	795.4	632.7	512.3	344.4	245.5	180	149.5	130.4
191.38	1328.3	871.4	670.6	523.7	341.7	249.2	183.2	150.2	124
190.37	1733	980.6	751.3	570.4	361.8	251.5	184.1	153.2	136.3
196.34	1268.2	910.5	718.5	569.2	371.2	264.4	188.2	156.8	128.4
197.29	1096.4	793.2	623.3	497.9	336.9	247.3	180.4	148.2	125
194.64	1409.1	947.6	728	582.6	405	273.8	191.8	156.2	146.7
196.82	997.8	735.9	589.5	469.9	314.6	230.8	167.2	139.6	117.2
195.75	1158.2	809.9	605.2	457	289.7	212.2	157.3	133.4	111.6
190.93	1435	1038	830	650.2	405.3	274.5	194.4	165.3	141.8
193.87	1504.5	1070.6	816	630.3	402.3	283.4	203.1	172.9	144.9
190.69	1680.8	931	741.1	594.5	402.5	288.4	205.8	173.3	144.2
192.01	1492.7	1125.2	898	728.2	473.5	324.2	228.6	188.6	159
189.79	1692.5	1189.7	923.2	719.8	468	321.6	220.2	181.2	151
195.38	1356.6	954.1	774.5	614.3	398.8	285.2	205.2	170.2	145.6
193.4	1212.3	961.8	761.2	585.3	380.5	278.7	207.7	175.3	150.5
191.33	1283.6	928.1	726.5	566.4	361.2	255	189.4	162.6	142.3
190.9	1467.3	928	703.8	535.5	345.8	245.2	183.4	151.6	134.2
193.32	1753.2	834.9	597	459.8	296.5	218	165.2	141.4	126.5
194.43	1183.6	821.8	619.7	467.2	296.5	219.1	167.5	142.6	124.5
195.07	1239.8	814.8	594.5	424.1	261.7	192.7	153.5	128.7	115.5
197.34	972.3	683	535.1	411.3	265.7	190.1	146.6	127.1	110.8
194.4	1194	791.5	579.9	418.5	247	169.8	133.9	122.2	109.6
196.97	1036.4	705.6	498.3	359	216.2	161	131.7	116.8	102.8
197.93	933.9	602.6	466	362	231.3	167.2	125.7	110.6	101
193.71	1336.4	807.6	597.2	450.1	271	193.4	151.5	133.1	115.4
196.58	871.9	611.6	472.9	367.4	243.8	183.3	140.8	121.4	108.4
197.53	753.8	560.8	445	349.9	242.4	182.1	143.1	123.9	106.9
196.7	918.5	677.7	549.4	433.9	290.9	207.6	159.5	135.1	118
191.09	963.7	723	571.8	457.1	297.4	223.1	165.5	142.8	121.4
192.6	1367.6	919.1	681.8	507.7	304.3	218.4	168.4	146.1	123.2
194.48	1132.4	753.8	608.7	480.9	317.6	229.3	170.6	147.9	121.6
194.19	1112.1	749.3	579.8	461.4	312.7	230.9	173.6	150.2	127.5
194.19	1222.9	854.2	666.7	527.5	352.1	250.1	182.6	154.3	132.6
194.95	1143	917.6	710.6	552.7	348.8	247.9	182.5	153.9	132.5
196.18	1093.5	791.7	639.2	520.9	353.1	259.8	191.3	159.8	139.1
192.6	1698.4	1234.5	970.8	774	501.7	345.8	239.6	195.9	166.7
191.96	1301.7	899.8	724.8	585.5	397.3	290.7	213.5	180.6	143.7
196.42	886.8	664.4	535.5	432.7	299.1	227.6	172.7	146	126.4

APPENDIX H – DEFLECTIONS FOR AIRPORT C (280KN-LOAD, FREE OF OUTLIERS)

Load	D_0	D_1	D_2	D_3	D_4	D_5	D_6	D_7	D_8
295.42	396	358.9	319.5	289	228.7	178.9	121.3	94.3	86.1
288.9	427.1	384.1	350.7	319.8	254.5	198.4	137.4	114.8	98.6
276.62	2153.2	1259.4	835.8	550.2	243.2	124.2	103.9	101.4	92.1
280.71	1702.4	924.1	635.4	447	227.5	148.5	119.9	109.5	100.1
283.78	1127.9	747	545.2	406.7	246.5	181.2	142.3	127.3	112.6
280.6	1406.9	976.1	706.5	521.1	316.4	228.9	176.1	153.2	130.5
276.1	1817.7	1182.1	816	588.2	343.2	249.6	191.6	167.4	136
280.15	1364.2	965.9	730.8	565.7	369.4	277.5	207.2	175.3	152.9
281.51	1243.1	791.9	598.2	459.3	293.9	215.2	165.3	142.1	121.5
278.64	1531.2	976.8	715.5	533.6	326.2	236.8	179.5	155.2	135
278.09	1545.1	933	699.9	529.4	337.9	239.1	178.9	153.7	128.7
284.61	1153.7	678.6	512.8	378.6	227.9	160	124.3	107.9	96.8
279.09	1632.5	1010.5	709	486.4	222.3	112.7	74.7	66.6	57.4
280.95	1381.9	921.9	660.4	472.6	235.6	123.1	75.1	61.5	56.9
281.71	1234.3	857	639.2	470.8	252	139.3	83.4	68.7	59.7
285.64	1039.4	696.4	511.6	375	202	117.3	70.1	57.6	49.6
283.22	1275.9	797.2	603.5	426.9	210.8	115	68.1	56.1	46.2
284.61	1006.9	647	478.5	347.7	195	119.6	82.9	77	70.5
285.48	963.9	651	505.4	379.3	222.6	140.1	99.6	86.2	77.3
283.41	1140.7	853.7	634.7	492.6	283.2	176.6	123.1	107.5	93.9
284.05	1120.6	711.7	525.9	388	218.5	150.8	118.4	103.6	93.7
283.26	1113.3	753.8	585	451	284	209.6	163	141.2	125.9
284.58	1151.4	797.6	635.5	515.4	354.7	265.9	203.9	167	136.4
281.55	1087.2	801.2	633.1	507.2	341.7	254.5	195.1	163.2	140.7
281.35	1208	918.2	724.8	576.5	382.4	276.8	205.6	174.5	148.9
280.87	1279.5	819	625.9	501.7	331.2	247.1	190.8	163.8	142.2
283.62	908	715.8	596.8	482.1	324	235.7	178.7	151.2	131.7
277.69	1627.3	1115	868.1	682.5	435.1	299	218.7	185.9	160.7
274.35	1754.2	1304.1	992.1	751.9	463.6	314.5	225.7	193	166.6
279.12	1359.1	980.4	769.5	614.1	404.7	288.5	208.2	171.9	142.3
277.61	1608.5	1139.5	874.5	666.2	402.2	272.5	199.3	169.4	148.2
282.99	1326.7	868.2	651.2	495.8	320.9	239.2	181.4	149.9	128.5
274.91	1595	1163.9	908.9	713	437.5	299.5	215.1	181.1	159.3
280.31	1448.1	1070.3	865.9	692.3	459.1	324.3	229.3	188.9	163.4
276.26	1608.6	1101.7	835.3	630.9	387.3	266.8	203.1	175.1	152
274.27	1767.2	1311.8	998	772.1	480.1	341.4	243.6	199.9	171.1
277.74	1672.7	1195.6	905.3	695.4	429.3	302.9	226.2	199.2	174.8
279.52	1449.4	1020.5	801	638.2	425	297.9	217	179.3	153
279.52	1392.6	964.6	744.2	577.1	381.9	281.6	216.2	185.9	162
280.04	1519	1068.3	827.5	657	433.2	311.6	230.1	193.5	165.9
276.5	1677.8	1323.6	1033.3	816.6	520.3	353.5	244.1	203.4	181.6
274.64	1712.5	1307.9	1005.4	790.7	510.2	353.1	250.8	207.5	176.8
276.31	1809.6	1229.4	931.6	707.1	447.7	315.2	233.7	195.9	167.8

278.72	1452.5	1001.1	794.7	640.6	435.4	314.4	226.7	188.9	157.8
278.29	1495.3	1048.9	722.9	513.9	323.7	253.3	195.6	167.1	150.4
273.84	1636.4	1110.7	836.8	658.2	443.6	325.4	242.4	198.5	173.9
270.02	2028.7	1285.2	1024.6	825.7	558.4	404.3	288.5	233.8	198.5
269.1	2212.6	1296.9	1004.3	793.2	532.6	378.7	267.7	219.5	186.3
272.6	1617.9	1239.6	990.6	799.3	540.6	391.9	276.6	226.1	197.9
274.87	1371.1	1032.4	842.3	690.5	485.2	357.4	254.5	207.9	178
272.68	1537.5	1118.2	884	721.5	492.1	354.7	254.5	209.3	178.6
268.31	1920.4	1221.8	952.5	756.4	506	364.1	265.4	218.1	183
261.04	2252.5	1386	1050.5	812	518.9	356	259.6	215.8	190.3
267.35	1761.9	1216.7	972.6	777.6	514.7	366.7	256.6	215.3	176.3
277.58	1694.9	1110.4	873.1	708.1	483.1	355.8	257.7	214.9	181.8
271.85	1979.7	1324.9	1031.4	833.7	566	401	276.4	226.3	189.2
279.04	1411.6	1064.3	819.6	662.6	451.1	337.8	241.5	197.7	168.7
276.81	1601	1123.2	854.8	657.6	428.9	311.2	231.2	195	165.9
268.15	1990.8	1473	1158	917.3	584.3	400.6	282.1	235.7	202.9
271.69	2071.5	1516	1221.7	909.3	588.1	411.5	294.3	241.5	205.8
262.23	2317.9	1291.9	1032.7	839	562.5	404.1	283.9	232.9	196.8
269.1	2314.5	1602.4	1277.6	1045	688	472.6	329.6	271.3	228.9
264.01	2246.6	1702.1	1305.6	1030.1	675	463.4	314.2	252.2	208
271.22	1955.3	1373	1117.9	876.4	573.8	411.9	290.6	243.1	207.3
271.25	1810.9	1338.1	1085.2	846.9	551.6	397.2	292	243.7	208.7
271.61	1716.5	1293.9	1016.2	800	521.6	369.9	273.6	233.8	202
266.24	1994.5	1232.7	940.8	742.8	481.1	347.8	258.2	216.8	185.6
271.61	2365.1	1114.2	808.9	634.5	417.8	309.2	233.1	198.9	172.8
277.34	1710.7	1122.4	837.1	641.3	418.4	313	236.1	199.3	174.1
273.76	2923.1	1110.3	801.7	584	364.5	267.3	209.9	184.1	152.5
279.2	1357	926.6	719	557.4	364.5	268.6	206.4	177.2	156.4
277.66	1724.5	1063.5	773.8	569	345.7	244.7	196.1	175.2	152.1
281.11	1411.9	947.8	673.6	493.6	304.4	227	181.6	160	138.2
283.65	1169.4	824.2	635.1	494.1	321.5	234.4	179.2	155.9	140
274.03	1971.8	1074.3	796.6	603.4	372.6	271.3	210	179.7	157
281.19	1215.7	826.1	644.6	511.2	340.7	259.4	199.1	171.9	151.9
282.54	1077.8	774.9	613.9	489.3	340.7	263.1	203.1	174.2	150.8
280.39	1336.6	932.5	754.3	602.4	411.2	300	226.1	191.7	164.8
267.8	1324.9	998.7	784.5	636.4	427.2	318.5	232.2	192.1	168.7
271.61	2682.4	1275.9	949.6	715.7	440.4	315.5	239.5	205.6	182.1
276.46	1622.7	1073.7	857.4	685.3	464.6	331.3	246.2	206.8	178.2
276.38	1466.8	1055.1	815.5	653.3	451.9	334.8	249.4	210.8	181.2
275.83	1667.5	1192.4	942.4	757.7	505.2	363.9	261.8	219.4	186
277.1	1596.7	1310.7	1018.7	792.1	513.5	364.6	262.8	220.1	190.3
278.17	1631.4	1173	932.3	761.1	519.9	382.9	276.7	228.4	193.8
269.26	2270.6	1744.9	1380.3	1106.4	722.8	498	340.1	275	232.3
274.87	1739.9	1314.4	1047.7	851	581	424.8	306.6	251.6	214.5
282.3	1265.1	934.1	749.2	608.6	426.1	326	244.1	206.6	181.2
266.92	2732.1	1850.7	1321.6	1003	620.1	431.9	335	267.9	234.1